

DETERMINATION OF THE STRUCTURAL FEATURES OF
A-BAND LIPOPOLYSACCHARIDE FROM A ROUGH MUTANT OF
PSEUDOMONAS AERUGINOSA

BY

TODD L. ARSENAULT, B.Sc.

A thesis

Submitted to the School of Graduate Studies
in Partial Fulfillment of the Requirements

of the Degree

Doctor of Philosophy

McMaster University

1992

**STRUCTURE OF A-BAND LIPOPOLYSACCHARIDE
FROM PSEUDOMONAS AERUGINOSA**

DOCTOR OF PHILOSOPHY (1992)
(Chemistry)

McMaster University
Hamilton, Ontario

TITLE: Determination of the Structural Features of A-Band
Lipopolysaccharide from a Rough Mutant of Pseudomonas Aeruginosa

AUTHOR: Todd Lawrence Arsenault, B.Sc. (University of New Brunswick)

SUPERVISOR: Professor D.B. MacLean

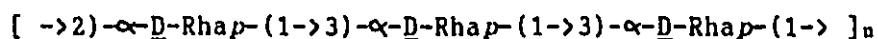
NUMBER OF PAGES: xiii, 174

ABSTRACT

"A-band" lipopolysaccharide (LPS) is believed to be widely distributed among serotypes of the bacterium *Pseudomonas aeruginosa*. The present work is a study of the structural features of the polysaccharide portion of A-band LPS ("A-PS") from strain AK1401.

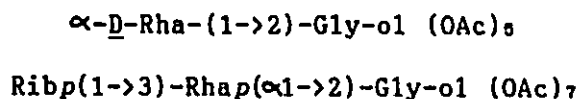
The A-PS was found to consist principally of D-rhamnose, with lesser amounts of 3-*O*-methylrhamnose, ribose, mannose, and glucose. These monosaccharides were found to exist as 1,3-linked rhamnopyranose, 1,2-linked rhamnopyranose (2:1 ratio), 1,4-linked 3-*O*-methylrhamnopyranose, and 1,4-linked manno- and gluco-pyranoses; the ring form and linkage positions of ribose could not be determined directly, but could be inferred to be 1,3-linked ribopyranose.

¹H- and ¹³C-NMR of the intact A-PS showed the presence of three principal monosaccharides, all of which were α -D-rhamnosides, suggesting a trisaccharide repeating unit structure composed of two α -(1,3)-linked rhamnopyranosides and one α -(1,2)-linked rhamnopyranoside. The ¹H-NMR spectrum of this repeating unit was assigned by use of homonuclear correlation spectroscopy (COSY) and relayed coherence transfer (RELAY) experiments. Nuclear Overhauser enhancement experiments allowed the assignment of the sequence of monosaccharides. The deduced structure of the repeating unit of AK1401 A-PS is:

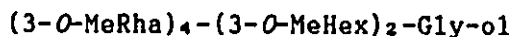


This work represents the first assignment of the $^1\text{H-NMR}$ spectrum of this repeating unit structure.

The A-PS was subjected to sodium periodate oxidation, reduction, and mild acid hydrolysis (Smith degradation), which yielded an oligosaccharide of predictable structure as the major product. The peracetate derivatives of the minor oligosaccharide products were studied in an attempt to learn more about the role of the monosaccharides that are not included in the repeating unit. Gas chromatography-mass spectrometry (GC-MS) revealed the presence of at least five oligosaccharides in addition to the major product. The structures of two of these could be inferred from the mass spectra as:



A fraction containing oligosaccharides which were too involatile to be analyzed by GC-MS was isolated by liquid chromatography and analyzed by direct chemical ionization (DCI) mass spectrometry. This revealed the presence of at least two components, one of which was inferred to be the peracetate of:



These components provide some insight into the structure of the non-repeating portion of the A-PS.

Acknowledgements

I would like to thank Professor David B. MacLean for his teaching, guidance, and seemingly endless patience throughout the course of this project. Thanks are also due to Dr. Richard Smith, Faj Ramelan, Jim Kapron and Jack Chan for getting me started in mass spectrometry. I am also grateful to Drs. Thomas Hemscheidt and Zbigniew Czarnocki for helping me to learn the ins and outs of chemistry. The assistance of Dr. Don Hughes in running the NMR spectra is greatly appreciated.

Thanks to my coworkers in room 465 for making my stay at McMaster an enjoyable one. In no particular order, they are Bob Gerard, Jahangir, John Peltier, Lynn Cameron, Monica Fischer, Jian Wang and Dennis Suh. Thanks also to the Bell Boys (Dave, Howard, Rob, Fred and Chuck) for some good laughs. Likewise to Mo, Scotty and anyone else I may have overlooked. May you all live as long as you want, and never want as long as you live.

Finally, I would like to acknowledge the financial assistance of the Province of Ontario and the Canadian Cystic Fibrosis Foundation.

Dedication

This work is dedicated to my family:

To my dear wife, Tracy, without whom I would have given up years ago. Thank you for helping me to remember that there is more to life than chemistry.

To my Mum and Dad, who always wanted me to do my best; here, at last, is that book I was always going to write.

To my little sister Denise, whom I will always remember as being six years old, since that was the only year we were in school together.

To my grandfather, Walter Burns, who sat me on his knee and taught me to read my first words: "The Evening Times-Globe".

To my grandmothers, Marie and Evangeline, and my grandfather Alphonse, all of whom passed away while I was thousands of miles away in pursuit of my studies.

TABLE OF CONTENTS

Chapter 1	<u>Page</u>
<u>Introduction</u>	
1.1 General introduction	1
1.2 <i>Pseudomonas</i> species and their lipopolysaccharides	2
1.2.1 Lipopolysaccharides (LPS)	4
1.2.2 Lipopolysaccharides of <i>P.aeruginosa</i>	4
1.2.3 A-band LPS and related polysaccharides	5
1.3 <i>P. aeruginosa</i> and Cystic Fibrosis: significance of A-band LPS	7
1.3.1 Derivation of A-band LPS used in this study	8
1.4 Methods used in carbohydrate structure determination	9
1.4.1 Alditol acetate analysis: identification of monosaccharides	10
1.4.2 Chiral glycoside method: assignment of absolute configuration of monosaccharides	10
1.4.3 Assignment of anomeric configuration	12
1.4.4 Assignment of ring size	14
1.4.5 Methylation analysis: assignment of linkage positions	15
1.4.6 Sequencing of monosaccharides	16
1.5 Nuclear magnetic resonance spectroscopy	17
1.5.1 Single pulse (1-Dimensional) NMR spectra	17
1.5.2 Other one-dimensional experiments	19
1.5.2.1 Proton-coupled ^{13}C -NMR	19
1.5.2.2 Nuclear Overhauser enhancement difference spectroscopy	20
1.5.3 Two-dimensional NMR methods: general	21
1.5.3.1 Homonuclear Correlation Spectroscopy (COSY)	22
1.5.3.2 Relayed coherence transfer (RELAY)	24

	<u>Page</u>
Chapter 2	
<u>Experimental</u>	
2.1 Materials	26
2.2 Sample isolation	26
2.2.1 NMR sample preparation	27
2.3 Analytical methods	28
2.3.1 Instrumentation	28
2.3.2 Composition analysis: alditol acetate method	29
2.3.3 Absolute configuration	32
2.3.4 Methylation analysis	32
2.3.5 Smith degradation	35
2.3.6 Analysis for RNA contamination in the AK1401 A-PS	37
2.4 Nuclear magnetic resonance spectroscopy	39
Chapter 3	
<u>Results and Discussion</u>	
3.1 Introduction	41
3.2 Degradative analyses of the AK1401 A-PS	42
3.2.1 Composition analysis	42
3.2.2 Absolute configuration of the monosaccharides	45
3.2.3 Methylation Analysis of the AK1401 A-PS	47
3.2.4 Summary of the degradative analyses	52
3.3 NMR Analyses of the AK1401 A-PS	53
3.3.1 ¹ H- and ¹³ C-NMR of the underivatized AK1401 A-PS	53
3.3.2 Homonuclear Correlation Spectroscopy (COSY) of the A-PS	55

	<u>Page</u>
3.3.3 Relayed Coherence Transfer Spectroscopy (RELAY)	60
3.3.4 Unassigned resonances	62
3.3.5 Determination of linkage stereochemistry	64
3.3.6 Nuclear Overhauser enhancement experiments and structure of the repeating unit	67
3.3.7 Significance of the repeating unit structure	72
3.4 Studies on the minor monosaccharide components of AK1401 A-PS	73
3.4.1 Rationale for the Smith degradation	73
3.4.2 Liquid chromatography of the oligosaccharide Acetates resulting from Smith degradation of the A-PS	79
3.4.3 Gas chromatography and GC-MS of the oligosaccharide acetates resulting from Smith degradation of the A-PS	80
3.4.4 Alditol acetate analysis of the product of periodate oxidation and borohydride reduction of the A-PS	95
3.4.5 Methylation analysis of the polymer remaining after periodate oxidation and borohydride reduction of the A-PS	100
3.4.6 Summary of the experiments on Smith degradation	105
3.4.7 Attempts to analyse the involatile oligosaccharide acetates resulting from Smith degradation of AK1401 A-PS	106
3.5 Assessing the possibility of RNA contamination of the A-PS preparation	117

	<u>Page</u>
Chapter 4	
<u>Conclusions</u>	120
Appendix 1 Additional Mass Spectra	126
Appendix 2 Additional NMR Spectra	150
Appendix 3 Computer programs	165
References	168

LIST OF TABLES

	<u>Page</u>
Table 1 Composition of the A-PS from <i>P. aeruginosa</i> AK1401	44
Table 2 Partially methylated alditol acetates from AK1401 A-PS.	49
Table 3 ¹ H-NMR data for A-PS from AK1401 in D ₂ O	63
Table 4 Determination of Linkage Stereochemistry	66
Table 5 Observed nuclear Overhauser enhancements	69
Table 6 Structures of Oligosaccharide Acetates Resulting from Smith Degradation of the AK1401 A-PS	97
Table 7 Alditol Acetates from the Polymer Remaining after Periodate Oxidation and Borohydride Reduction of the AK1401 A-PS	99
Table 8 Partially Methylated Alditol Acetates from the Polymer Remaining after Periodate Oxidation and Borohydride Reduction of the A-PS	101
Table 9 Calculated Masses of (M + NH ₄) ⁺ Pseudomolecular Ions of Malto-oligosaccharide Acetates	109

LIST OF FIGURES

	<u>Page</u>
Figure 1: Generalized cell wall structures of bacteria	3
Figure 2: Alditol acetates from AK1401 A-PS	43
Figure 3: Determination of the absolute configuration of rhamnose	46
Figure 4: Major partially methylated alditol acetates (PMAA's) resulting from methylation analysis of the AK1401 A-PS	50
Figure 5: NMR spectra of the AK1401 A-PS	54
Figure 6: Portion of the ^1H - ^1H -COSY spectrum of AK1401 A-PS showing assignments of H1 to H5 of the A residue	56
Figure 7: Portion of the ^1H - ^1H -COSY spectrum of AK1401 A-PS showing assignments of H1 to H3 of the B residue.	57
Figure 8: Portion of the ^1H - ^1H -COSY Spectrum of AK1401 A-PS showing assignments of H1 to H5 of the C residue	58
Figure 9: Portion of the ^1H - ^1H -COSY spectrum of AK1401 A-PS showing assignments of H5 and H6's for each residue	59
Figure 10: Portion of the RELAY spectrum of AK1401 A-PS showing B2-B4 correlation	61
Figure 11: Anomeric carbon region of the ^1H - ^{13}C -coupled ^{13}C -NMR spectrum of the AK1401 A-PS	65
Figure 12: A representative nOe difference experiment	68
Figure 13: Structure of the repeating unit portion of AK1401 A-PS	71
Figure 14: Gas chromatography of oligosaccharide acetates resulting from Smith degradation of the AK1401 A-PS	81

	<u>Page</u>
Figure 15: Total ion current chromatograms of oligosaccharide acetates from Smith-degraded AK1401 A-PS	82
Figure 16: EI mass spectrum of Peak X (molecular weight= 448)	83
Figure 17: EI mass spectrum of Peak B (molecular weight= 678)	87
Figure 18: EI mass spectrum of Peak D (molecular weight= 664)	89
Figure 19: EI mass spectrum of Peak A (molecular weight= 664)	92
Figure 20: EI mass spectrum of Peak C (molecular weight= 664)	94
Figure 21: EI mass spectrum of Peak E (molecular weight= 692)	96
Figure 22: PMAA derivatives from AK1401 A-PS and periodate oxidized/ borohydride reduced A-PS	104
Figure 23: NH ₃ -DCI mass spectrum (non-centroided) of the involatile oligosaccharide acetates from Smith-degraded A-PS	108
Figure 24: 1200 to 1700 amu region of the NH ₃ -DCI mass spectrum of the involatile oligosaccharide acetates from Smith-degraded AK1401 A-PS.	110
Figure 25: NH ₃ -DCI mass spectrum of the involatile oligosaccharide acetates from Smith-degraded AK1401 A-PS.	112
Figure 26: Schematic representation of possible components of the involatile oligosaccharide acetates from the Smith-degraded AK1401 A-PS.	114
Figure 27: HPLC chromatograms of the products of Nuclease P1 and Alkaline phosphatase digestion of AK1401 A-PS, yeast transfer RNA, and a standard test mix of ribonucleosides	118

CHAPTER 1

Introduction

1.1 General introduction

The objective of this research was to determine the structural features of the polysaccharide portion of A-band lipopolysaccharide, which is a cell surface molecule common to most strains of *Pseudomonas aeruginosa*. This study involved the use of a variety of spectroscopic and degradative methods. The composition and some of the structural details of the polysaccharide (PS) were determined by various controlled degradations, followed by analysis by gas chromatography (GC) and combined gas chromatography/ mass spectrometry (GC-MS). Nuclear magnetic resonance spectroscopy (NMR) was used to provide information about the linkage positions and sequence of monosaccharide residues in the undegraded PS.

This chapter deals with the clinical significance of *Pseudomonas aeruginosa*, and of A-band lipopolysaccharide. The general structural features of lipopolysaccharides are presented, along with a summary of methods that have been used to determine polysaccharide structures. In Chapter 2, the experimental details of the degradative procedures and spectroscopic techniques are described. Chapter 3 contains the results of these experiments, as well as a discussion of the interpretation of the data and the structural features which could be determined from them. Finally, Chapter 4 presents a concise summary of the results obtained. Mass spectra and NMR spectra that are not directly discussed in the text are presented in the Appendices.

1.2 Pseudomonas species and their lipopolysaccharides

The genus *Pseudomonas* consists of bacteria which are straight or slightly curved rods 0.5 to 1.0 μm in diameter by 1.5 to 4 μm in length that have one or more flagella.¹ The species belongs to the Gram-negative class of bacteria, the general membrane structure of which is shown in Figure 1. Pseudomonas species are strict aerobes, meaning that their metabolism requires oxygen.

P. aeruginosa (Latin "aeruginosus", "full of verdigris", hence green) is a pigmented species by virtue of the synthesis of the pigments pyocyanin and pyoverdine.^{1,3} This species has minimal nutritional requirements, and can utilize a wide variety of compounds as the sole source of carbon and energy.¹ It commonly occurs in water and soil, and has become common in hospitals within the last century. *P. aeruginosa* is harmless to normally healthy individuals, but persons with weakened immune systems such as burn victims, cancer patients, and organ transplant recipients taking anti-rejection drugs can suffer infections of the urinary tract, wounds, lungs and blood. The organism can spread from the original site of infection, so an infected burn or wound may lead to blood-poisoning (sepsis) or lung infection (*Pseudomonas* pneumonia), both of which may be fatal.

These infections may be chronic, but they can also progress rapidly; because of its lethality and selectivity for compromised persons, *P. aeruginosa* is one of the most feared pathogens in critical care units.

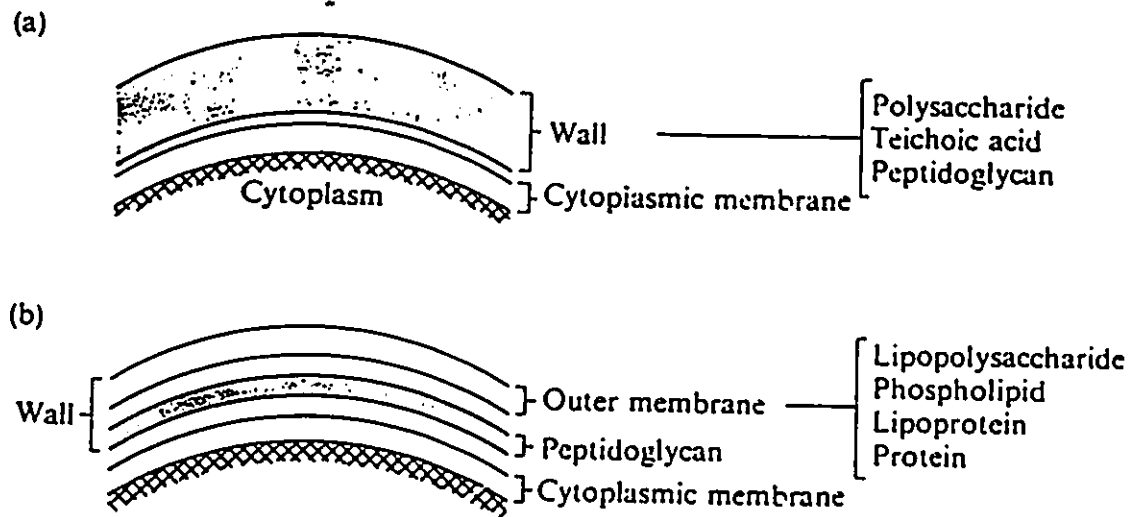


Figure 1: Generalized cell wall structures of a) Gram-positive, and b) Gram-negative bacteria. (From reference 2).

1.2.1 Lipopolysaccharides (LPS)

All Gram-negative bacteria express lipopolysaccharides (LPS) on their cell surfaces. These molecules are anchored in the outer membrane of the cell by a hydrophobic region called "Lipid A", which consists of an amino-sugar disaccharide acylated with fatty acids and/or hydroxy-fatty acids. The Lipid A is substituted by a heavily phosphorylated carbohydrate region called the "core oligosaccharide", and this may be further substituted by a long "side chain polysaccharide" (sometimes called the "O-antigen") consisting of a repeating oligosaccharide.^{4,5} There is little variation in Lipid A and core oligosaccharide structures within a species, but the side chains have diverse structures; it is the variation of these polysaccharides which determines the immunological differences ("serotypes") of bacteria. The serotypes of a given species are usually determined by reaction with a set of typing antisera against standard strains. It should be noted that the side chain polysaccharides may be completely absent in some strains, in which case the bacterium is said to be "rough"; if side chains are present, the bacterium is called a "smooth" strain. As a consequence, LPS's which contain side chains are often called "smooth LPS", while those which do not have side chains are called "rough LPS". Both types are present in smooth strains, but only rough LPS is present in rough strains.

1.2.2 Lipopolysaccharides of *P.aeruginosa*

There are seventeen serotypes of *P. aeruginosa* described by the International Antigenic Typing System (IATS)⁶, which supercedes previous typing schemes described by Homma⁷, Fisher⁸, Habs⁹, Lanyi¹⁰, and others.

About 95% of all isolates may be typed into one of the IATS serogroups; the remaining isolates are called "non-typable". The structures of the side chain polysaccharides from the LPS of the reference strains have been determined.¹¹ In general, the side chain polysaccharides consist of a repeating unit of three to six monosaccharides, are not phosphorylated, and contain mainly aminosugars and uronic acids, as well as some unusual sugars.

1.2.3 A-band LPS and related polysaccharides

The type of LPS described above was originally thought to account for all of the smooth LPS's of *P. aeruginosa*, until the discovery of a minor type of LPS in strain PA01 which was of lower molecular weight and contained no phosphate or aminosugars.¹² This new type of LPS was named A-band LPS, and the major type of LPS was called B-band LPS to reflect their relative migration upon electrophoresis. Preliminary structural investigations^{12,13} showed that the A-band LPS had a similar fatty acid composition to that of the B-band LPS, but lacked amino sugars and phosphate, and contained stoichiometric amounts of sulfate. Thin layer chromatography of a hydrolysate of A-band LPS showed that rhamnose (6-deoxymannose) was the principal sugar constituent. Thus, the polysaccharide portion of the A-band LPS (hereafter called "A-PS") may be considered a *rhamnan*, that is, a polymer consisting principally of rhamnose.

Rhamnans have been previously reported to be present in lipopolysaccharide preparations from *Pseudomonas aeruginosa*^{14,15}, as well as *P. syringae*^{16,17} and *P. cepacia*¹⁸. Those from *P. aeruginosa*

were found as minor components of the LPS that remained intact after destruction of the side chains of acid- or base-sensitive LPS (Lanyi serotype O7¹⁵ and Homma serotype G¹⁴ respectively) under mild hydrolytic conditions. The rhamnans found in the other species are in fact the side chains of the principal LPS's. The two known rhamnans from *P. aeruginosa* (and that from *P. syringae*) have the same repeating unit, comprised of two α -(1 \rightarrow 3)- linked D-rhamnoses and one α -(1 \rightarrow 2)- linked D-rhamnose (note that L-rhamnose is the common enantiomer in Nature). A polymer of this repeating unit was synthesized by Tsvetkov *et al.*¹⁹, and its ¹³C nmr spectrum was reported to be identical with that of the natural material described by Kocharova *et al.*¹⁸

Yokota *et al.*¹⁴ postulated that the rhamnan which they isolated was in fact a *common antigen* (*i.e.*, it is present in several serotypes) since it inhibited the binding of a monoclonal antibody (MAB E87) which is specific for a rhamnose-rich PS in another strain.²⁰ The observation of Kocharova *et al.*¹⁸, that a rhamnan of the same repeating unit structure is present in another serotype, seems to confirm this hypothesis. Rivera and McGroarty¹⁹ found that MAB E87 also bound to their A-band LPS in immunoblots. This information, together with the observation that rhamnose is the principal sugar component, led them to propose that A-band LPS has a similar rhamnan structure to the "common antigen".

However, Kocharova *et al.*²¹ have isolated and determined the structure of a polysaccharide from *P. aeruginosa* culture supernatants that contains L-rhamnose, ribose, and glucose, and which inhibits the binding of MAB E87 to LPS preparations. These workers suggest that MAB

E87 is specific for the polysaccharide that they isolated rather than for the rhamnan structure, so the relationship, if any, between the A-band LPS described by McGroarty¹² and the common antigen proposed by Yokota *et al.*¹⁴, is not clear. Thus, a detailed structural analysis of the polysaccharide portion of A-band LPS is needed.

1.3 *P. aeruginosa* and Cystic Fibrosis: significance of A-band LPS

Cystic Fibrosis (CF) is an inherited dysfunction of chloride ion transport in epithelial cells.²² The disease is characterized by high electrolyte concentrations in sweat, improper pancreas function, viscous bronchial secretions, and progressive pulmonary disease leading to death. The lung condition may be exacerbated by infection by *Pseudomonas*, *Haemophilus*, and *Staphylococcus* species, amongst others. Of these, *Pseudomonas aeruginosa* is the most significant, since it is the most common direct cause of death of CF patients. It is interesting to note that the species of infecting organism is often related to the age of the patient; infants and young patients are usually colonized by *Haemophilus* or *Staphylococcus* species, whereas infection by *P. aeruginosa* is common only in adolescents.²²

P. aeruginosa infections are difficult to eradicate because this bacterium has remarkable resistance to antibiotics, and also has mechanisms for eluding the immune system. In the case of CF patients, an unusually high percentage of isolates are non-typable^{23, 24}, a fact that can be correlated to a lack of O-antigenic side chains on the LPS.

It was subsequently found that side chains were originally present in the infecting strains, but that they were lost over time as

the infection progressed.²⁵ However, it was found that expression of A-band LPS not only occurs in the infecting strain, but also continues in a high percentage of the non-typable strains isolated from CF patients.²⁵ Because expression of B-band LPS can stop during infection (a mechanism for eluding the immune system), immunization with B-band antigens (O-antigens) can be ineffective.²⁶ However, since A-band LPS expression is conserved during the course of infection, a vaccine based on A-band LPS could immunize against the majority of wild type bacteria, and the immunization might still be effective on many non-typable strains that result from prolonged infections of CF lungs.

The detailed structure of A-band LPS is thus of considerable interest, since it may be a common antigen among many strains, and since portions of its structure might prove useful in vaccination against *Pseudomonas aeruginosa*.

1.3.1 Derivation of A-band LPS used in this study

The present work was carried out on a sample of the polysaccharide portion of the smooth LPS derived from strain AK1401, which is a rough mutant of strain PA01.²⁷ Even though it produces no O-antigens, AK1401 expresses a high molecular weight LPS which reacts with several A-band specific monoclonal antibodies.²⁵ Thus, AK1401 is an attractive source of A-band LPS because the LPS can be obtained free from contaminating O-antigen; rough B-band LPS is still produced, however, this is easily removed by size-exclusion chromatography. Because AK1401 is derived from PA01 (the strain in which A-band LPS was first detected), the structure of the AK1401 A-band LPS is relevant to

studies on the common antigen of *P. aeruginosa*.

1.4 Methods used in carbohydrate structure determination

The process of determining the structure of a polysaccharide may be summarized as a series of fact-finding steps, each of which sheds light on a particular aspect of the structure. These are as follows:

1. Composition: what monosaccharides are constituents, and in what proportions?
2. Absolute configurations: which enantiomer of each monosaccharide is present?
3. Anomeric configurations: what is the stereochemistry of the anomeric carbons?
4. Ring forms: do the monosaccharides exist as furanosides or pyranosides?
5. Linkage positions: how are the component monosaccharides joined to one another?
6. Sequence of residues in the polysaccharide?

In addition to these criteria, one may also wish to know the average chain length, whether the polysaccharide is linear or branched, and if there is any non-stoichiometric substitution of the residues (microheterogeneity).

Some of the methods used to determine these criteria will be discussed in the following pages.

1.4.1 Alditol acetate analysis: identification of monosaccharides

In the past, there have been several analytical methods which combine degradation and mass spectrometric analysis for the elucidation of carbohydrate structures. Perhaps the simplest of these is complete acid hydrolysis of the polysaccharide followed by reduction and peracetylation of the resulting monosaccharides to yield a volatile mixture which is then analyzed by coupled gas chromatography/ mass spectrometry.²⁸ It should be noted that reduction of the monosaccharides to alditols is a necessary intermediate step, otherwise the mixture would be complicated by the presence of four isomers of each monosaccharide, namely, the α - and β -anomers of each of the pyranoside and furanoside forms (this results from the hydrolysis step, which leaves an equilibrium mixture of all of the mutarotatory forms). However, upon reduction, all of the mutarotatory forms of a given monosaccharide yield the same alditol. With a suitable set of standards for retention time comparison, the alditol acetate method can be used effectively to identify the constituent monosaccharides: however, it does not give any information about linkage positions nor linkage order.

1.4.2 Chiral glycoside method: assignment of absolute configuration of monosaccharides

This method relies on the principle that derivatization of a mixture of enantiomers with an optically pure reagent results in a mixture of diastereomers that is resolvable by chromatography. With an optically pure standard (either enantiomer), the absolute configuration of a monosaccharide may be determined by forming glycosides with an

optically pure alcohol and analyzing the products by GC.²⁹

To illustrate how the method works, consider the following example. A standard sample of D-glucose is reacted with (\pm)-2-octanol and in a separate experiment with (-)-2-octanol. The first standard reaction gives the following products:

1. (-)-2-octyl- α -D-glucopyranoside
2. (-)-2-octyl- β -D-glucopyranoside
3. (+)-2-octyl- α -D-glucopyranoside
4. (+)-2-octyl- β -D-glucopyranoside,

as well as the corresponding furanosides, which, in the general case, may or may not be formed in significant amounts (they will be ignored here for simplicity). When the standard D-glucose is reacted with the optically pure (-)-2-octanol, only products 1 and 2 are present, thus establishing components 3 and 4 in the previous experiment as being (+)-2-octyl glycosides. Now, if glucose of an unknown configuration is reacted with (-)-2-octanol, components 1 and 2 above will result if the sugar had the D-configuration, whereas the L-configuration would have produced the following:

- (-)-2-octyl- α -L-glucopyranoside, and
 (-)-2-octyl- β -L-glucopyranoside,

which are the *enantiomers* of components 3 and 4 in the standard experiment, and thus have the same retention times as 3 and 4. Thus, one can positively identify the absolute configuration of a monosaccharide with only one of the pure enantiomers as a standard. A further advantage of this method is that it may be used when optical rotation is inappropriate, such as in the analysis of monosaccharide

mixtures, or when only very small amounts of sample are available.

1.4.3 Assignment of anomeric configuration

Upon formation of a hemi-acetal, the ring closure in a free monosaccharide may result in a mixture of ring sizes (see next section) and results in two possible stereochemistries at the anomeric carbon, depending on which face of the aldehydic carbon was attacked by the intramolecular hydroxyl group. The two epimers are often called *anomers*, and are distinguished by the labels α - (alpha) and β - (beta). The definition of α - and β - forms has changed considerably over the years (see reference 30). Initially, the terms referred to the order of isolation of the anomers of glucose; later, the definition was based on optical rotation, the anomer having the greater rotation being called α -; and finally, the definition was standardized in terms of relative stereochemistry, the α -anomer being the one in which the anomeric group is drawn in the Fischer projection in the same direction as the group on the configurational carbon atom (*i.e.*, to the left in the L-series, and to the right in the D-series).

Determination of the stereochemistry of the anomeric carbon was not straightforward once it was realized that the anomer having the greatest rotation was not always the α -anomer under the relative stereochemistry definition (however, it is almost always true). One way to overcome this has been shown for aldohexopyranosides. If any aldohexopyranoside is oxidized by periodate, C-3 is lost as formic acid, and C-2 and C-4 become aldehydes: the only remaining asymmetric centres are C-1 and C-5. Thus, all of the diastereomeric α -D-hexopyranosides

give the same oxidation product, and all of the possible β -D-hexopyranosides give another unique product, so the readily available α - and β -D-glucopyranosides may be used as standards.³¹

The anomeric configurations of the constituent monosaccharides in polysaccharides are most conveniently determined by NMR spectroscopy. The magnitudes of the coupling constants of the ring protons are useful in determining the relative stereochemistry of two adjacent carbons, since trans-diaxial hydrogens (dihedral angle = 180°) have larger coupling constants than trans-diequatorial (60°) or cis-(axial-equatorial) hydrogens (60°) (Karplus relation³²). In the case of sugars with the C-2 *gluco*-configuration (H2 axial), the anomers are easily distinguished by the large difference in coupling constants, since H1 and H2 of α -glucopyranosides are in an equatorial-axial relationship, whereas they are in an axial-axial relationship in β -glucopyranosides (e.g., the average value of J_{H1-H2} for alkyl α -D-glucopyranosides is 3.8 Hz, while alkyl β -D-glucopyranosides have an average J_{H1-H2} of 7.8 Hz, data from ref. 33). In the case of sugars with the C-2 *manno*-configuration (H2 equatorial), the difference in coupling constants is not so clear, since both anomers have an H1-H2 dihedral angle of approximately 60° . Nevertheless, there is a small, but consistent difference (e.g., J_{H1-H2} is 1.9 Hz for α -D-mannopyranose, and 1.1 Hz for β -D-mannopyranose, data from reference 33).

However, there are some cases where this method is not useful, such as when the peak widths of the proton resonances are wide, thus obscuring the coupling information. An alternate method has been devised³⁴ which is based on variations in the anomeric proton- anomeric

carbon coupling constant (J_{C1-H1}). This will be discussed further in a later section.

1.4.4 Assignment of ring size

The determination of ring size of monosaccharide methyl glycosides was first accomplished by permethylation, hydrolysis of the glycoside and vigorous oxidation to give the methylated aldaric acid (4-carbon from furanosides, 5-carbon from pyranosides). Determination of the the number of carbons in the aldaric acid allowed the inference of the ring form in the glycoside.³⁵ Ring sizes of monosaccharide glycosides can also be determined by periodate oxidation and subsequent quantitation of the mole equivalents of periodate consumed, and of formaldehyde and formic acid released: each possible size of cyclic acetal (from 3- to 7-membered) gives a unique combination of mole equivalents of oxidant consumed and products formed.³⁶

These methods are not easily applied to determination of ring sizes in polysaccharides (unless they are *homopolysaccharides*, that is, they have only one type of constituent monosaccharide and a uniform linkage, such as amylose). For heteropolysaccharides, a useful degradative method is *methylation analysis*³⁷, which will be discussed in detail in the next section. This method also provides information about the linkage positions (see below).

One may also determine ring sizes in a non-destructive manner. X-ray crystallography is useful for small molecules, but the complexity, size, and difficulty of crystallizing polysaccharides limits the use of this method. However, it has been used to investigate the structures of

several polysaccharides.³⁶

1.4.5 Methylation analysis: assignment of linkage positions

This method is an extension of the alditol acetate method discussed previously. If the polysaccharide is permethylated prior to alditol acetate analysis, the linkage positions may be determined since all free hydroxyls in the original polysaccharide are methylated, whereas only those which arise from the substituted positions as a result of hydrolysis or reduction are acetylated. The partially methylated alditol acetates (PMAA's) can be identified by GC-MS, and the positions of acetates and methyl ethers may be found by analysis of the mass spectrum, since the most intense fragments are those that result from carbon-carbon bond cleavage between adjacent methoxyls, or if no methoxyls are adjacent, then the charge remains on the methoxylated carbon rather than on the acetoxyated carbon. Thus, the positions of acetates in the PMAA's can be used to deduce the substitution patterns and ring sizes of the constituent monosaccharides. A comprehensive survey of GC and MS data for synthetic samples representing most of the possible PMAA's which could result from aldohexoses, aldopentoses and 6-deoxy-aldohexoses has been published.³⁷ This method, too, has its drawbacks, the principal one of which is that both a 4-linked hexopyranose and a 5-linked hexofuranose give the same partially methylated alditol acetate (namely 2,3,6-tri-O-methyl-1,4,5-tri-O-acetyl-hexitol). This occurs because the method does not distinguish between hydroxyls formed during hydrolysis and those formed from reduction (*i.e.*, both are acetylated).

A method which removes this ambiguity has been devised.³⁹ Instead of hydrolyzing the methylated polysaccharide, the acetals (anomeric carbons) are reduced with triethyl silane and either (trimethylsilyl)-trifluoromethane sulphonate or boron trifluoride-etherate to yield anhydroalditols which are subsequently acetylated and identified by GCMS. Since the ring structures are retained, the method easily distinguishes between furanose and pyranose forms. It also gives an indication of linkage positions because the glycosidic oxygen remains as part of an acetate on the portion of the glycoside which is not reduced. This procedure has not been widely used, so it suffers from a lack of published standard mass spectra and retention times for the various products which could result from the degradation of a polysaccharide.

1.4.6 Sequencing of monosaccharides

All of the methods outlined above cannot give insight into the sequence of monosaccharides in the native polysaccharide (unless the rare case occurs where there is only one way that the monosaccharides could possibly have been arranged). In order to gain sequence information by use of these methods, one must first partially hydrolyze the polysaccharide, isolate the oligomers, and characterize each of these separately. This does not guarantee that an unambiguous sequence can be found, but it can be effective, especially when the polysaccharide contains repeating units (i.e., "overlapping" oligomers will occur more frequently).

Periodate oxidation, borohydride reduction, and mild acid

hydrolysis ("Smith degradation") of polysaccharides has also been used to degrade repeating units into oligosaccharides whose structures can provide sequence information.⁴⁰

Nuclear Magnetic Resonance spectroscopy may be used to assign sequences if the spectrum of the oligo- or polysaccharide can be assigned. This will be discussed in more detail in the following sections.

1.5 Nuclear magnetic resonance spectroscopy

Nuclear magnetic resonance (NMR) spectroscopy is a powerful and well-established tool for structure elucidation in virtually all fields of chemistry. The present discussion will be limited to those experiments which are of particular interest in carbohydrate structure elucidation.

1.5.1 Single pulse (1-Dimensional) NMR spectra

Fourier transform NMR (FT-NMR) is now the most common method of acquiring NMR data. FT-NMR provides spectra which are identical with continuous wave (CW) NMR spectra, except that the FT-NMR method has the following advantages: speed of acquisition, since the entire spectral range is irradiated at once; sensitivity, since the rapid acquisition of a single spectrum allows the addition of many spectra in a relatively short time to increase the signal to noise (S/N) ratio, and finally, the possibility of performing new experiments which were not possible by CW-NMR.

A single pulse NMR experiment consists simply of placing the

sample in a strong magnetic field, perturbing the system with a radio frequency pulse, turning off the pulse, acquiring the decay of magnetization as the system relaxes, and repeating the process to increase the signal to noise ratio. The instrument computer then Fourier transforms the resultant free induction decay (FID) to give the chemical shift spectrum (after internal or external standardization).

In the case of ^{13}C -NMR spectra, the single pulse experiment is usually (but not always) modified by broad-band saturation of the proton frequency range to remove signals due to ^{13}C - ^1H couplings, so that each carbon atom appears as a single line. This method also has the added bonus of increasing the sensitivity of the ^{13}C -NMR experiment by way of nuclear Overhauser enhancement of the carbon signals.

Chemical shift spectra are of great value in carbohydrate structure determination all on their own, since they can indicate the number of residues in oligosaccharides and repeating unit polysaccharides, the existence of deoxy-sugars, amino-sugars, uronic and aldonic acids, and non-carbohydrate components such as lipids and protein in the carbohydrate preparation. Some limited assignments of the structure of an unknown complex carbohydrate may be made from one-dimensional ^1H - and ^{13}C -NMR alone; when information about the sample is available from other methods, such as composition and methylation analysis, the assignment may become much more complete. One may assign certain structural features, such as anomeric configuration, based on chemical shift. Coupling information (discussed in section 1.4.3) can reveal both linkage and ring stereochemistry.³³ Furthermore, the linkage positions can sometimes be assigned based on the downfield

shifts of protons at the site of substitution and vicinal to the site of substitution.⁴¹ Comparison of the spectra to those of well defined oligosaccharides (see, for example, reference 42) may give the complete structure. This approach is being furthered by the development of computer-assisted spectral matching^{43,44}, but this method is not yet generally applicable.

In the general case of dealing with a previously-unknown or incompletely characterized complex carbohydrate, more elaborate NMR methods may prove useful.

1.5.2 Other one-dimensional experiments

There are several other 1-D methods which can give valuable information about complex carbohydrates, and they will be discussed prior to the introduction of two-dimensional (2-D) methods.

1.5.2.1 Proton-coupled ¹³C-NMR

This method is seldom used, since proton-decoupled ¹³C-NMR has the advantages of a simplified spectrum and greater sensitivity due to the nOe caused by saturation of the protons, but the ¹³C-¹H coupling constants can be very useful information in certain circumstances. Bock and co-workers³⁴ (see also references 45-47) have found that the carbon-proton coupling constants (J_{C-H}) depend only slightly on the stereochemistry and degree of oxygenation of all of the carbons in monosaccharides except for the anomeric carbons, which displayed a systematic variation in J_{C1-H1} with stereochemistry. Thus, J_{C1-H1} was found to be approximately 160 Hz for all β -hexopyranosides investigated,

and about 170 Hz for α -hexopyranosides. This relationship has great diagnostic value for carbohydrates whose anomeric configurations cannot be determined by other means.

In practice, the J_{C1-H1} 's are usually determined by a gated decoupling technique⁴⁸ in which the protons are decoupled in the period between the end of acquisition and the ^{13}C sampling pulse, thus providing the coupling information along with some nuclear Overhauser enhancement. However, they may also be determined by ^{13}C two-dimensional J-spectroscopy⁴⁹, or if sufficient spectral dispersion is available, by the observation of ^{13}C satellites in 1H -NMR spectra⁵⁰.

1.5.2.2 Nuclear Overhauser enhancement difference spectroscopy

Saturation of a given nucleus in a molecule will result in population changes in neighbouring nuclei, thereby changing the intensity of the NMR signals for these nuclei. The magnitude of this effect is related to the distance of the affected nucleus from the irradiated nucleus, so nuclear Overhauser enhancement (NOE) measurements are useful in describing the three-dimensional structure and conformation of molecules. NOE's are usually measured as the difference between the spectrum with and without saturation (difference spectroscopy).

It should be noted that the maximum possible enhancement depends upon the magnitudes of the spectrometer angular frequency (ω_0) and the rotational correlation time (τ_c , which is related to the size and mobility of the molecule). If $\tau_c \omega_0 \ll 1$ (small molecules), the NOE is maximized and positive; if $\tau_c \omega_0 \gg 1$ (large molecules), the NOE is

maximized and negative; if $\tau_{cwo} = 1$, the magnitude of the nOe is zero, so one must be aware that nOe 's may not be observed within a certain size range at a given field strength.³¹

NOE difference spectroscopy can yield a wide variety of information about carbohydrate structure, but the experiment must be supported by an assignment of the spectrum obtained by other means, such as the two-dimensional NMR methods which will be discussed later. Since the anomeric protons are the most easily recognized in the NMR spectrum of a complex carbohydrate, they are the usual targets for saturation in nOe experiments; this will result in both intra- and inter-residue enhancements. The intra-residue enhancements allow the determination of the conformation and anomeric configuration of the monosaccharide unit containing the irradiated nucleus. The inter-residue enhancements allow the assignment of sequence and the position of substitution of the neighbouring monosaccharide. It should be noted that the proton on the substituted carbon does not always show the most intense nOe : equatorial protons on carbons vicinal to the site of substitution also show intense nOe 's.⁴¹ This problem can often be clarified by examining the glycosylation-induced shifts (see reference 41) to determine the site of substitution, but this method may be ineffective if the monosaccharide is a branch point (*i.e.*, has more than one site of substitution). Thus, determination of sequence by nOe is unambiguous, but the determination of linkage positions may not be.

1.5.3 Two-dimensional NMR methods: general

In general, two-dimensional NMR methods are those in which the

spectrum is usually presented as a contour plot with two frequency axes (f_1 and f_2) in which the contour lines represent signal intensity, with the 1-D spectrum plotted along each axis. Any given proton signal appears at the same frequency (ν_a) on both the f_1 and f_2 axes ($f_1=f_2=\nu_a$), so the diagonal of the contour plot contains the same information as the 1-D spectrum. However, two coupled nuclei (with resonance frequencies ν_1 not equal to ν_2) will show off-diagonal signals in the COSY contour plot at ($f_1=\nu_1, f_2=\nu_2$) and at ($f_1=\nu_2, f_2=\nu_1$). These signals arise because the signal intensity of one spin is modulated as a function of t_1 by the spin coupled to it.

Since proton spectra are dominated by vicinal and geminal couplings, all of the proton resonances can be assigned by finding the neighbouring protons from the COSY spectrum, providing that one resonance in the 1-D spectrum can be assigned. In the case of simple carbohydrates, this is particularly easy, since the anomeric proton, being deshielded by two oxygen atoms, is always at lower field than the other protons. Thus, knowing the identity of the resonance due to the anomeric proton (H1), H2 may be assigned because it will be coupled to H1, indicated by an off-diagonal peak ("crosspeak") in the COSY spectrum. Since long range couplings are unimportant in most cases, this should be the only proton coupled to H1 unless the carbohydrate is a 2-deoxy-monosaccharide. Now, knowing the assignment of H2, H3 may be determined in a similar manner, and so on until all of the protons have been assigned. Examples of this technique may be found in reference 53.

The application of COSY to oligo- and poly-saccharides is a natural extension of the utility of the technique in assigning the

spectra of monosaccharides. Since ^1H - ^1H couplings across glycosidic linkages are usually absent, each monosaccharide appears as an isolated spin system; thus, the COSY spectrum consists of several connectivity networks, each of which is due to a single monosaccharide. This is a great advantage in assigning the spectrum, since most of the proton resonances are invariably found in a crowded region between 3.0 and 4.5 ppm. The COSY spectrum allows one to examine the spectrum of each monosaccharide as though it were present alone.

There are, however, cases in which the spectrum becomes so complex that two resonances belonging to different spin systems have the same chemical shift, and an unambiguous assignment of the spectrum is not possible because two connectivity networks have a common point. One may circumvent this either by way of additional NMR experiments (see next section) or by preparation of derivatives whose spectra are less crowded. For example, the peracetyl derivative of an oligosaccharide⁵³ shows deshielding (by about 1 ppm) of the protons at the positions whose hydroxyl groups were not substituted, and thus became acetylated in the derivatization reaction. This method has the disadvantage that these protons may be deshielded all the way into the anomeric region, thus making assignment of the anomeric protons more difficult.

1.5.3.2 Relayed coherence transfer (RELAY)^{54,55}

A generally applicable method for resolving ambiguities in the COSY spectrum is to utilize a different pulse sequence which reveals connectivities that are more distant than nearest-neighbours. Since coupling constants to remote protons are essentially zero, this method

relies on intervening protons to "relay" magnetization. The details of the pulse sequence will not be discussed here, but the general phenomenon will be outlined.

Consider a three spin example: A - B - C, where $J_{AC}=0$. The experiment consists of a COSY-like pulse sequence that is followed by additional pulses and fixed time delays. The COSY portion of the sequence produces coherence between coupled spins, so spin B is "labelled" with chemical shift information about A. The latter part of the sequence transfers magnetization from spin B (which contains information about A) to spin C. Thus, the chemical shift information about A will be relayed to C, even though A and C are not coupled.

The Relay spectrum contains the same information as the homonuclear COSY spectrum, except that it also shows connectivities to next-to-nearest neighbour spins (in the above example, a crosspeak would be observed that correlates A to C, in addition to the COSY crosspeaks correlating A to B and B to C). This information provides unequivocal evidence that remote spins are part of the same spin system. This approach has been extended to even more remote spins in the spectra of oligosaccharides⁵⁶, but only the simple one step Relay experiment described here was used in the present work.

CHAPTER 2

Experimental

2.1 Materials

Polysaccharide samples were provided by Dr. A.M.B. Kropinski, Department of Microbiology and Immunology, Queen's University, Kingston, Ontario; Dr. J.S. Lam, Department of Microbiology, University of Guelph, Guelph, Ontario; and by Dr. A. Sen., Department of Chemistry, Queen's University, Kingston, Ontario. Various carbohydrate standards were provided by Dr. W.A. Szarek, Department of Chemistry, Queen's University, Kingston, Ontario. 3-*O*-methylrhamnose was the kind gift of Dr. G.O. Aspinall, Department of Chemistry, York University, Downsview, Ontario. Yeast transfer-RNA was kindly provided by Dr. R.G. Lea, formerly of the Department of Medicine, McMaster University, Hamilton, Ontario.

2.2 Sample isolation

A-band PS was isolated for us by other workers, but the methods used are recounted here for clarity. AK 1401 cells were grown overnight at 37°C in 500 mL of tryptic soy broth (Difco) and then used to inoculate 4.5 L of tryptic soy broth in an SLS fermentor (Labline). The temperature was maintained at 37°C, the rotation rate was 200 rpm, and the aeration rate was 10 L min⁻¹. The cells were harvested, at late logarithmic or early stationary phase, by centrifugation. LPS was isolated by the method of Darveau and Hancock³⁷, and hydrolyzed in 1 %

acetic acid at 100°C for 90 min. The lipid A was removed by centrifugation, and the supernatant was lyophilized to dryness. The residue was dissolved in 0.05 M pyridinium acetate buffer (pH 5.3) and chromatographed on Bio-Gel P-4 (minus 400 mesh). The component of highest molecular weight was used in this study.

Alternatively, AK1401 cells were extracted with phenol/ chloroform/ petroleum ether by the method of Galanos *et al.*²⁸, and the PS prepared as above.

2.2.1 NMR sample preparation

Prior to ¹H and ¹³C NMR analysis, the A-PS sample was chromatographed on Sephadex G-50 in 0.05 M pyridinium acetate buffer. The void-volume fraction was collected and lyophilized. The sample (7 mg) was exchanged three times with 99.9% D₂O (MSD Isotopes) and lyophilized after each exchange. Finally, the sample was dissolved in 0.8 mL of 99.996% D₂O ("D₂O PLUS", MSD Isotopes) and transferred to a 5 mm thin-walled NMR tube.

2.3 Analytical methods

2.3.1 Instrumentation

Gas chromatography was performed on a Hewlett-Packard 5890 instrument equipped with an on-column injector, a flame ionization detector, and an HP3390A integrator. The columns used were all wide bore (0.32 mm inside diameter), bonded phase (0.25 μm film thickness), fused silica capillary columns (J&W Scientific). The carrier gas was helium, which was passed through an oxygen trap and a water trap

(Chromatographic Specialties). Nitrogen at a pressure of 30 psi was used as a make-up gas.

Combined gas chromatography-mass spectrometry (GC-MS) was performed on a variety of instruments:

1. VG Micromass 7070F sector mass spectrometer equipped with a Varian model 3700 gas chromatograph and an on-column injector (J&W Scientific).
2. VG MassLab TRI0-2 quadrupole mass spectrometer equipped with a Hewlett-Packard 5890 gas chromatograph and an on-column injector.
3. Hewlett-Packard 5971A quadrupole mass selective detector equipped with a Hewlett-Packard 5890 Series II gas chromatograph and a split/ splitless injector (operated in the splitless mode). This instrument required the use of narrow bore (0.25 μ m inside diameter) capillary columns, whereas the others used wide bore columns.

Instrument conditions are specified along with the experiments outlined in the following sections. The instruments were calibrated with either perfluorokerosene (PFK) or perfluorotributylamine (PFTBA).

Chemical ionization mass spectrometry was performed on either a VG Micromass 7070F or a VG Analytical ZAB-E mass spectrometer. Samples were introduced either by gas chromatography, solids probe, or direct insertion probe (DCI). The ion source was kept at 200°C, and ammonia was introduced into the source at such a pressure that the ratio of m/z 18 (NH_4^+) to m/z 35 (N_2H_7^+) was approximately 20:1 (electron energy 70 eV). The instrument was calibrated in the absence of reagent gas using

PFK (mass range up to 700 amu) or Fomblin-Y (mass range 600 to 1600 amu, ZAB-E only). The Fomblin-Y was introduced via a solids probe heated to >250°C. Since the calibration was performed in the absence of the reagent gas, a calibration check was performed by acquiring the NH₃-DCI spectrum of a mixture of malto-oligosaccharide peracetates. Further considerations for obtaining an accurate calibration using Fomblin-Y are elaborated in Chapter 3.

High performance liquid chromatography (HPLC) was performed on a DuPont model 8800 HPLC equipped with a variable wavelength DuPont UV spectrophotometer and a Varian RI-3 refractive index detector. All columns were 4.6 x 250 mm stainless steel (Supelco). HPLC grade solvents were from either Caledon Laboratories Ltd. or J.T. Baker Inc., and were degassed with a continuous stream of helium. A flow rate of 1.0 mL/min was used for all experiments. Instrument conditions are specified along with the experiments outlined in the following sections.

Ultraviolet spectra were recorded using a Hewlett-Packard 8451A diode array spectrophotometer.

2.3.2 Composition analysis: alditol acetate method²⁰

Hydrolysis of PS samples (<1 mg) was performed at 120°C in 2 M trifluoroacetic acid (1 mL) in a sealed glass tube for 1.5 h; the water and acid then were removed under reduced pressure.

In an alternate method, a sample of A-PS (<1 mg) was dissolved in 2 M HCl (1 mL) in a thick-walled teflon, screw-cap vial (capacity = 8 mL), which was fabricated from a 1-inch diameter teflon rod; the minimum wall thickness was 6 mm, and the thread depth was 1 cm. The solution

was kept for 3 min in a Panasonic 700-watt microwave oven at medium-high power (these conditions are similar to those described for the rapid total hydrolysis of proteins⁵⁹). The sample was cooled at least 15 min before opening the reaction vial. The sample was evaporated to near dryness under reduced pressure, and residual water and acid were removed by evaporating with 3 portions of 1-propanol.

The dry residue was dissolved in water (1 mL), and the solution was treated with sodium borohydride or sodium borodeuteride (5 mg) at ambient temperature for 2-4 h (or overnight for NaBD₄). The reaction mixture was quenched by the addition of 5% acetic acid in methanol, and evaporated. Further portions of 5% acetic acid in methanol were added, and the solution was distilled until the presence of boron could no longer be detected (flame test). The residue was dried under vacuum and treated with acetic anhydride (1 mL) at 110°C for 2 h. The reaction mixture was cooled, poured into water, and extracted with chloroform. The chloroform extract was washed extensively with 5% aqueous sodium hydrogencarbonate, dried over anhydrous sodium sulfate, and concentrated.

A series of alditol acetate standards (arabinitol, xylitol, 2-deoxyglucitol, 6-deoxygalactitol, and 3-O-methylrhamnitol peracetates) was prepared from the corresponding aldoses as described above for derivatization of sample hydrolyzates. Rhamnitol, ribitol, glucitol, galactitol, and mannitol peracetates were prepared on a larger scale as follows. The sugar (0.5 g) was reduced with sodium borohydride (0.5 g) in water (10 mL) as previously described. The alditols were acetylated under the same conditions using acetic anhydride (10 mL); in the cases

of glucitol, mannitol, and galactitol peracetates, the products were obtained by pouring the reaction mixture into methanol and collecting the crystalline materials. Overall yields were \approx 50%. The identity of all products was confirmed by GC and CI-MS using ammonia as the reagent gas.

Gas chromatography was performed on a 30 m x 0.5 mm DB1701 wide-bore capillary column. The oven temperature was 200°C, and the detector was kept at 280°C. The carrier gas pressure was 8 psi.

GC-MS was performed on a VG Micromass 7070F mass spectrometer. The column described above was used, except that the oven temperature was reduced to 180°C and the helium backing pressure was only 2 psig. The interface temperature was kept at 250°C, the ion source at 200°C, the electron energy at 70 eV, and the accelerating potential at 4 kV. The mass spectrometer was scanned from either 350 or 300 to 40 amu at 2 s per decade, with a 1-s interscan delay. The data were acquired and processed on a Digital Electronics Corporation PDP 11/24 computer using VG 11/250 software.

Alternatively, GC-MS was performed on a Hewlett-Packard 5971A instrument using a 30 m x 0.4 mm DB-1701 narrow bore column. The oven temperature was programmed as follows: 1 min at 40°C, 20°C per min to 280°C, hold. The injector and transfer line temperatures were 250°C and 280°C, respectively. The carrier gas backing pressure was 6 psi, and the instrument was scanned from m/z 40 to m/z 550.

2.3.3 Absolute configuration²⁹

A sample of A-PS hydrolysate was treated with (-)-2-octanol (0.5 mL) and 1 drop of trifluoroacetic acid in a sealed tube at 140°C for 20 h. The mixture was evaporated under reduced pressure, and the residue was treated with fused sodium acetate (10 mg) and acetic anhydride (1 mL) at 110°C for 1 h. The reaction mixture was poured into water and extracted with chloroform. The extract was washed extensively with 5% aqueous sodium hydrogencarbonate, dried, and concentrated. Standard samples for retention-time comparison were prepared similarly, using L-rhamnose with either (-)-2-octanol or (±)-2-octanol. GC and GC-MS analyses were performed as above.

2.3.4 Methylation analysis^{43, 60}

For the methylation reaction, all glassware and syringes were oven-dried overnight at >100°C. Sodium hydride (100 mg of a 60% oil dispersion) was placed in a dry round bottomed flask along with a magnetic stirring bar. The NaH was washed twice with light petroleum ether, the flask was capped with a rubber septum, and residual petroleum ether was removed in a stream of argon. The argon stream was discontinued, but the pressure relief line was left in place as dimethyl sulfoxide (1.5 mL, freshly distilled under vacuum from calcium hydride) was injected. The reaction mixture was immersed in an oil bath at 80°C, and stirred for 20 min. The flask was removed from the bath and allowed to cool before use. The resulting concentration of sodium methyl sulfinyl carbanion ("dimsyl sodium") was about 1.6 M.

A sample of PS (≤ 1 mg, dried overnight in a vacuum desiccator)

was placed in a dry round bottomed flask along with a magnetic stirring bar, and capped with a rubber septum. The sample was dissolved in freshly distilled DMSO (0.2-0.5 mL, as required for dissolution) under an argon or dry nitrogen atmosphere. Dimethyl sodium solution (0.2 mL) was added and stirred for 15 min, followed by iodomethane (0.2 mL), and the reaction mixture was stirred a further 15 min. This sequence was repeated with an additional 0.5 mL of each of dimethyl sodium solution and iodomethane. Finally, the reaction was quenched by the addition of water (2 mL), and the resulting mixture was stirred for 15 min. The methylated PS was isolated by extraction with CHCl_3 (3x 5 mL), and the combined extract was washed with water (3x 10 mL), dried over anhydrous sodium sulfate, filtered and evaporated under reduced pressure. The sample was then placed under vacuum (0.005 Torr) to remove traces of DMSO. Alternatively, the methylated PS could be purified by dialysis (12,000-14,000 molecular weight cutoff membranes) against three portions of 4 L of water (12 h for each portion), but this method is tedious and has no apparent advantages.

The methylated PS samples were hydrolysed in 90% formic acid (1 mL) at 100-110°C for 1.5 h. Formic acid was removed by evaporation under reduced pressure.

The hydrolysate was dissolved in water (1 mL), and the pH of the solution was checked to ensure complete removal of acid in the previous step. Sodium borohydride or sodium borodeuteride (10 mg) was added and the mixture was stirred for 2-4 h at room temperature (16 h for NaBD_4). The reaction was quenched by adding 2 M HCl until the pH was 2. The solution was then passed through a 1 mL column of Dowex 50x8 cation

exchange resin to remove sodium (the column was previously conditioned with 2 M HCl (3x 1 mL), and washed with water until the eluate was neutral). The sample was eluted from the column with 2 mL of water, and concentrated under reduced pressure (rotary evaporator, bath temperature <40°C). Methanol (three portions of 3 mL) was added and the boric acid was removed by distillation at ambient pressure. Residual solvent was removed under vacuum, and the sample was desiccated over P₂O₅.

The mixture of partially methylated alditols was then acetylated with acetic-trifluoroacetic anhydride as follows: trifluoroacetic anhydride (1.00 mL, 0.0071 moles) and glacial acetic acid (0.50 mL, 0.0087 moles) were mixed and allowed to stand 5 min with occasional agitation. This reagent (1.0 mL) was added to the sample and the mixture was stirred at ambient temperature for 20 min. The reagent was removed in a stream of nitrogen in the fume hood, and the residue was placed under vacuum (0.005 Torr) for 5 min to remove traces of the reagent.

For GC-MS analysis, the partially methylated alditol acetates (PMAA's) samples were dissolved in CH₂Cl₂. GC-MS was performed on a Hewlett-Packard 5971A instrument using a 30 m x 0.4 mm DB-1701 narrow bore column. The oven temperature was programmed as follows: 1 min at 50°C, 10°C per min to 200°C, hold. A DB-1 column programmed from 50°C (5 min), 10°C per min to 200°C was also used, but gave inferior resolution of the components. The injector and transfer line temperatures were 210°C (higher temperatures were found to decompose the sample). The carrier gas backing pressure was 6 psi, which gave a linear velocity of 25 cm sec⁻¹ (checked by injecting 0.5 µL of air and

finding the retention time of N₂ by selected ion recording of m/z 28). The instrument was scanned from m/z 40 to m/z 300 at a rate of 2 scans per second.

2.3.5 Smith degradation

AK1401 A-PS (26 mg) was dissolved in distilled water (25 mL) with warming and sonication. The solution was cooled to 4°C, and treated with sodium periodate (268 mg, 0.00125 moles) to afford a solution that was 0.05 M in periodate. The flask was swirled to dissolve the NaIO₄, and kept in the dark at 4°C for 75 h. A few drops of ethylene glycol was added to destroy excess sodium periodate, and the reaction mixture was allowed to warm to ambient temperature. Sodium borohydride (40 mg, ≈0.001 moles) was added and the mixture was stirred at ambient temperature. After 0.5 h, an aliquot of the reaction mixture was dropped into 2 M HCl, but no gas (H₂) was observed, thus indicating the complete consumption of the sodium borohydride. A further 40 mg of sodium borohydride was then added and the mixture was stirred an additional 1.5 h. The reaction was quenched by the addition of 2 M HCl (H₂ gas was evolved), and the pH was adjusted to neutral with 5% sodium hydrogencarbonate. The sample was concentrated to ≈1 mL (rotary evaporator, bath temperature <50°C), and transferred to dialysis bags (12,000-14,000 molecular weight cutoff). The bags were dialysed against two portions of 4 L of distilled water (first portion 6 h, second portion 10 h), and the contents of the bags were freeze-dried to yield 21 mg of a white solid. Portions of this sample (oxidized/ reduced A-PS) were reserved for alditol-d₁ acetate and methylation analyses as

described above.

The bulk of the polymer remaining after periodate oxidation and borohydride reduction was hydrolysed by dissolving it in aqueous HCl (10 mL, 0.5 M) and allowing it to stand at ambient temperature for 52 h with occasional shaking (these very mild conditions allow the selective hydrolysis of the glycosidic linkages of the oxidized residues). The reaction was neutralized with 5% sodium hydrogencarbonate, and NaBH₄ (50 mg) was added and the mixture allowed to stir at ambient temperature for 18 h. The reaction was quenched by the addition of 5% acetic acid in methanol, and the sample was distilled to remove boric acid as described previously. The residue (which contained sodium acetate from the previous step) was dried under vacuum (0.005 Torr), treated with acetic anhydride (5 mL) and the mixture stirred in an oil bath at 115°C for 2 h. The reaction mixture was quenched by the addition of saturated aqueous NaHCO₃ (20 mL) and the mixture stirred for 1 h. The solution was extracted with CHCl₃ (3x 20 mL), and the combined extract was washed with saturated NaHCO₃ (2x 50 mL), then with water (2x 25 mL). The extract was dried over anhydrous sodium sulfate, filtered and evaporated to yield 20 mg of a yellow oil.

The mixture of oligosaccharide acetates resulting from the Smith degradation of the AK1401 A-PS was analyzed by TLC on silica (developed in CH₂Cl₂-CH₃OH, 19:1 v/v, and visualized by spraying with 1% orcinol in 50% sulfuric acid). Analytical HPLC was performed using a Supelco LC-Sil silica column, an eluting solvent of CH₂Cl₂-CH₃OH (99:1, v/v), and differential refractive index detection. Preparative column chromatography was performed on a 20 cm x 2 cm diameter packed column of

Merck Kieselgel 60 (230-400 mesh). Elution was carried out first with $\text{CH}_2\text{Cl}_2\text{-CH}_3\text{OH}$ (99:1, v/v) and then with $\text{CH}_2\text{Cl}_2\text{-CH}_3\text{OH}$ (97:3, v/v).

Fraction were monitored by TLC as described.

Gas chromatography was performed on a 30 m wide bore DB-1701 column held isothermally at 280°C. The carrier gas pressure was 8 psi, and the detector temperature was 280°C. GC-MS was performed on a VG MassLab TRIO-2 instrument using the same column and oven temperature. The helium pressure was 2 psi, the transfer line was held at 280°C, and the ion source temperature was 200°C. The sample was analysed by electron impact and chemical ionization (NH_3) in separate experiments.

2.3.6 Analysis for RNA contamination in the AK1401 A-PS

The following procedure was used to analyze for nucleosides, which are more specific markers than ribose for the presence of RNA. The method used here is adapted from reference 62.

A sample of AK1401 A-PS (0.1 to 0.2 mg, representing 14 to 28 μg of putative RNA) was dissolved in water (25 μL) in a 1.5 mL plastic Eppendorf tube. A positive control was prepared by diluting 5 μL of yeast transfer-RNA (5.6 $\mu\text{g } \mu\text{L}^{-1}$, thus 28 μg) with water (20 μL); water (25 μL) was used as a blank.

Enzyme solutions were prepared as follows: Nuclease P1 (0.15 mg, Pharmacia, 800 units mg^{-1}) was dissolved in 600 μL of 0.03 M sodium acetate (final concentration =200 units mL^{-1}). Calf Intestinal Alkaline Phosphatase (1 μL , Bethesda Research Laboratories, 24 units μL^{-1}) was diluted with water (23 μL); this solution (1 μL) was further diluted with water (500 μL , final concentration =2 units mL^{-1}).

The samples were placed in an oven at 110°C for 2 min, then shock-cooled in an ice water bath. Each sample was treated with 0.02 *M* ZnSO₄ (2 μL), the Nuclease P1 solution (10 μL), and the Calf Intestinal Alkaline Phosphatase solution (10 μL). The samples were placed in a water bath at 37°C for 1 h, after which time 0.5 *M* tris-(hydroxymethyl)-aminomethane (15 μL, pH adjusted to 7.9 with HCl) was added to each. The samples were mixed and placed in the water bath a further 1 h.

A portion of each sample (10 μL) was diluted with water (290 μL), and 100 μL of these solutions were analysed by HPLC (positive control now represents products from ≈1.5 μg of RNA). The diluted samples, and a standard solution containing 0.3 to 0.4 μg of each nucleoside (cytidine, uridine, guanosine, adenosine, all from Sigma) per 100 μL were analyzed by HPLC on a Supelcosil LC-18 reverse phase column using an eluting solvent of 0.01 *M* NH₄H₂PO₄ in 6% methanol (aqueous). Detection was by way of absorbance at 254 nm.

The above experiment was repeated with additional controls as follows: a sample containing 28 μg of t-RNA and 0.1 mg of AK1401 A-PS was diluted to 25 μL and treated exactly as described (this experiment controlled for the possibility that AK1401 A-PS could be an inhibitor of either enzyme). A sample of t-RNA at the same concentration as the positive control was treated as above, except that water (10 μL) was added instead of the Nuclease P1 solution (this experiment controlled for the possibility that the standard t-RNA sample contained mononucleotides). The significance of these experiments is elaborated in Chapter 3.

2.4 Nuclear magnetic resonance spectroscopy

All NMR spectra were recorded on a Bruker AM-500 spectrometer. ^1H Spectra were acquired at 500.137 MHz using a 5-mm dual frequency $^1\text{H}/^{13}\text{C}$ probe. Spectra were acquired over 2.45 KHz in 8K data points (1.671 s acquisition time). Sample temperature was maintained at 30°C by a Bruker BVT-1000 variable temperature unit. The residual H₂O signal was suppressed by saturation for 1.0 s prior to acquisition. The free induction decays (FID's) were processed using Gaussian multiplication for resolution enhancement, and before Fourier transformation were zero-filled to 16K.

Nuclear Overhauser enhancement (nOe) difference spectra were obtained by subtraction of the off-resonance control free induction decay (FID) from the on-resonance FID. The proton of interest was selectively irradiated for 0.2 s, and the decoupler was gated off during acquisition. A 2.0-s relaxation delay was used. For each irradiation 8 scans were acquired with the cycle of irradiations repeated 20 times. FID's were processed using exponential multiplication (line-broadening 4.0 Hz) and were zero-filled to 32K before Fourier transformation. The sample was not degassed, so the enhancements were not quantitated. All of the observed nOe's were negative.

COSY and RELAY 2D NMR spectra were acquired in the absolute-value mode using the standard pulse sequences $90^\circ--t_1--90^\circ--\text{ACQ}$ and $90^\circ--t_1--90^\circ--\tau--180^\circ--\tau--90^\circ--\text{ACQ}$, respectively. Spectra in F2 were acquired over a 2.45-KHz spectral width in 1K data points. The COSY data were acquired in 96 scans for each of the 256 FID's, whereas the RELAY data were acquired in 128 scans. The 90° ^1H pulse width was 19.2 μs . A 1.0-

s relaxation delay was used, during which the HDO signal was suppressed by presaturation. The RELAY experiments used the phase cycling scheme given in ref. 55, and used a fixed delay τ of 0.040 s. Zero-filling in F1 produced a 512 X 512 data matrix with a digital resolution of 4.787 Hz/point in both dimensions. During 2D Fourier transformation a sine-bell squared window function was applied to both dimensions. The transformed data were then symmetrized.

^{13}C Spectra were recorded at 125.759 MHz using the 5-mm dual frequency probe. The spectra were acquired in 105,000 scans over 29.4 KHz spectral width in 32K data points. A 30° pulse width of 2.0 μs was used. The data were processed using exponential multiplication (line broadening 4.0 Hz). The values of the ^1H -- ^{13}C one-bond coupling constants were obtained using the gated decoupling technique¹⁸. A 0.5-s relaxation delay was used. The FID was processed using exponential multiplication (line broadening 3.0 Hz) and was zero-filled to 64K before Fourier transformation.

Chemical shifts for the ^1H NMR spectra are reported in ppm relative to TMS using the HDO signal at 4.60 ppm as internal reference. The ^{13}C chemical shifts were referenced relative to 1,4-dioxane in D_2O at 67.4 ppm as an external reference.

CHAPTER 3

Results and Discussion

3.1 Introduction

The objective of this research was to determine the structural features of the polysaccharide portion of A-band LPS obtained from a rough mutant of *P. aeruginosa* (AK1401).

In the present work the structure of the polysaccharide portion of A-band LPS (A-PS) from AK1401 was examined by a combination of spectroscopic and degradative techniques. The monosaccharide composition was found by gas chromatography (GC) and gas chromatography-mass spectrometry (GC-MS) of the alditol acetates derived from a hydrolysate of the A-PS. The linkage positions and ring sizes of the constituent monosaccharides were determined by methylation analysis. The absolute configuration of the principal monosaccharide was found by GC and GC-MS of its (-)-2-octyl glycoside peracetates. The anomeric configurations were found by determination of the C-1-H-1 coupling constants. The $^1\text{H-NMR}$ spectrum was assigned for the principal monosaccharides with the aid of $^1\text{H-}^1\text{H}$ shift-correlated (COSY) and relayed coherence transfer (RELAY) experiments, and this assignment was used to infer the linkage positions and sequence of residues in the polysaccharide by observation of inter-residue nuclear Overhauser enhancements (nOe's). The polysaccharide was selectively degraded (Smith degradation) to give a mixture of oligosaccharides, one of which had a predictable structure, while the other components were used to study the distribution of minor sugars in the A-PS.

3.2 Degradative analyses of the AK1401 A-PS

3.2.1 Composition analysis

The monosaccharide composition of the AK1401 A-PS was determined by hydrolysis, reduction, and acetylation to give a mixture of alditol acetates that were analysed by GC and GC-MS. The total ion current chromatogram of one such analysis is shown in Figure 2, along with the identities of the components. The mass spectra of all of the components are presented in Appendix 1. The results of the composition analysis are presented, and compared to data obtained for A-PS extracted by a different method (data from A. Sen) in Table 1.

Identities of the alditol acetates are based on electron-impact mass spectra and coelution on GC with authentic standards. The relative intensities were determined by normalizing the integrated areas from the chromatogram obtained by GC with a flame-ionization detector (referenced to rhamnitol pentaacetate= 100) and averaging several runs.

This analysis shows that the principal monosaccharide unit of the A-PS is rhamnose (6-deoxymannose). Minor amounts of 3-O-methyl-rhamnose, ribose, mannose, glucose, and an indeterminate 3-O-methyl-hexose were also present. A 2-O-methyl-6-deoxy-hexose and a 2-O-methyl-hexose were also found in vanishingly small amounts (J. Peltier and A. Sen, unpublished data). Note that the alditol acetates have been assumed to be derived from aldoses rather than ketoses, but this was later verified for rhamnose by methylation analysis and NMR spectroscopy, and for 3-O-methylrhamnose, mannose and glucose by

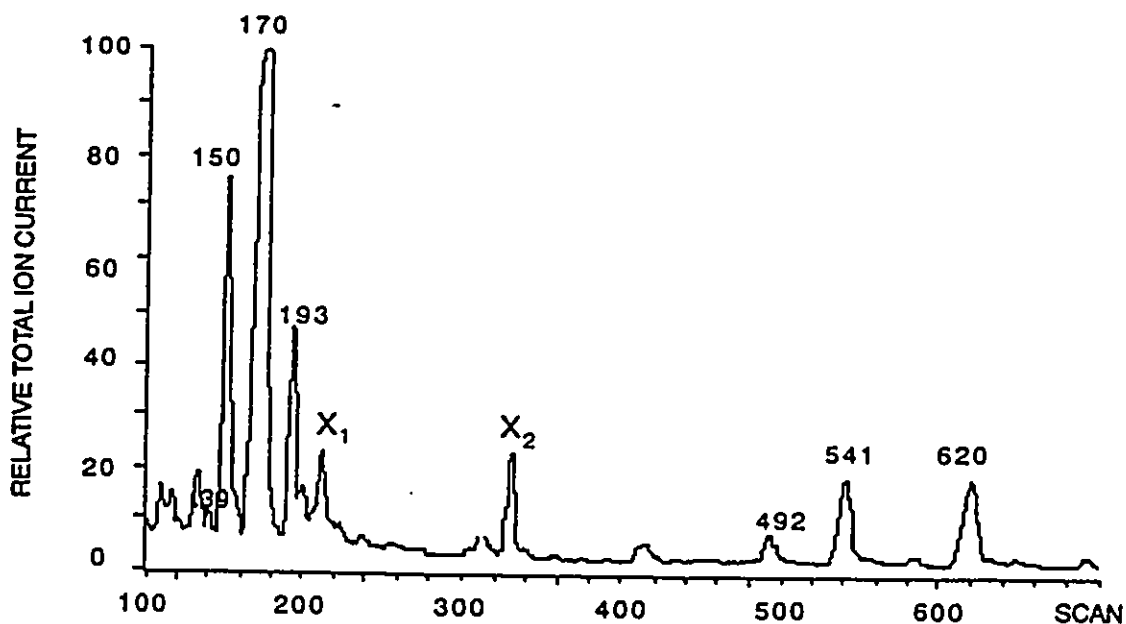


Figure 2: Alditol acetates from AK1401 A-PS, total ion current chromatogram and peak identities.

<u>Scan number</u>	<u>Identity</u>
150	3-O-methyl rhamnitol tetraacetate and ethyl palmitate (coelution of impurity)
170	rhamnitol pentaacetate
193	ribitol pentaacetate
492	3-O-methyl hexitol pentaacetate
541	mannitol hexaacetate
620	glucitol hexaacetate

Impurities

X1	an indeterminate phthalate ester
X2	ethyl stearate (ethyl octadecanoate)

Table 1: Composition of the A-PS from *P. aeruginosa* AK1401

Retention time (min)	Component	Relative intensity ⁽¹⁾		
		A	B	C
7.9	3- <i>O</i> -methyl rhamnitol tetraacetate	26 (1)	9 (0.5)	-
8.5	rhamnitol pentaacetate	100	100	100
9.2	ribitol pentaacetate	11 (0.5)	13 (0.8)	7.7
19.1	3- <i>O</i> -methyl hexitol pentaacetate	3	-	-
20.6	mannitol hexaacetate	9 (0.5)	13 (3)	11
22.9	glucitol hexaacetate	8 (0.6)	20 (4)	6.6

- A. Values obtained from hydrolysis with 2 *M* HCl in a Teflon vial. In this determination ethyl stearate and ethyl palmitate were detected also; ethyl palmitate coelutes with 3-*O*-methylrhamnitol tetraacetate under the GC conditions used, an aspect which accounts for the elevated relative intensity of 3-*O*-methylrhamnitol.
- B. Values obtained from hydrolysis with 2 *M* trifluoroacetic acid in a sealed glass tube.
- C. Values obtained by Dr. Asish Sen (Queen's University, Kingston, Ont.), personal communication. Sen's sample differed from those analysed by us in that the A-band LPS was isolated by phenol-chloroform-petroleum ether extraction, and that a different GC method was used (3 % SP-2340 packed column at 195°C). Values were normalized to Rha=100 for comparison; standard deviations were not provided.
- (1) The values in parentheses are the standard deviations for each average intensity.

methylation analysis. The presence of ribose in the aldopentose form could not be proved directly, but it is a reasonable assumption that the ribitol pentaacetate does not represent a ketose, since reduction of ribulose would yield both ribitol and arabinitol, and the latter was not detected. Furthermore, the ribitol pentaacetate is not derived from ribitol itself (which is a known constituent of some bacterial PS's, notably from *Streptococcus pneumoniae*^{63,64}), since ribitol-d₁ pentaacetate was found when the mixture of monosaccharides from the A-PS was reduced with sodium borodeuteride.

3.2.2 Absolute configuration of the monosaccharides

The absolute configuration of a monosaccharide may be determined without isolation of the sugar by preparing the glycoside of an optically pure alcohol²⁹. The enantiomers are derivatized to yield diastereomers, which are separable by chromatographic methods. In practice, the method does not yield a single diastereomer, but rather four isomers, the α - and β -pyranosides and the α - and β -furanosides, which are present in varying amounts depending on the nature of the sugar being examined. However, for this analysis, it is unimportant to know which isomer is which, as long as the product mixture resulting from the (*R*)-alcohol is separable from the mixture of the glycosides of the (*S*)-alcohol.

When (*R*)-(-)-2-octanol was reacted with a standard sample of L-rhamnose and subsequently acetylated, GC analysis gave the chromatogram shown in Figure 3A, each component being an isomeric (*R*)-2-octyl-L-rhamnoside triacetate (analysis of the bulk sample by NH₃-CIMS showed

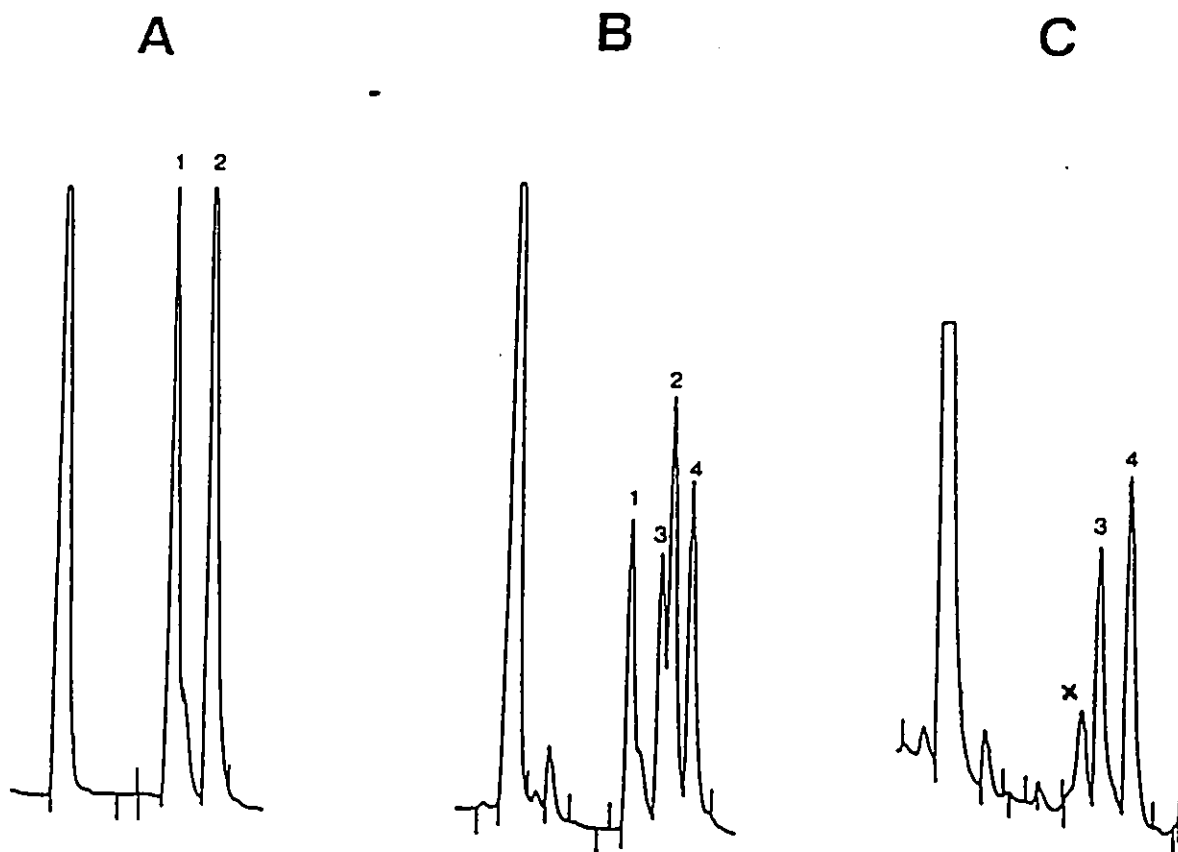


Figure 3: Determination of the absolute configuration of rhamnose from an A-PS hydrolysate.

- A) (*R*)-2-octyl-L-rhamnosides standard
- B) (*R,S*)-2-octyl-L-rhamnosides standard
- C) (*R*)-2-octyl-D-rhamnosides from AK1401 A-PS

that it contained only octyl rhamnoside triacetates, see spectrum in Appendix 1). When the standard L-rhamnose was reacted with racemic 2-octanol, the chromatogram shown in Figure 3B resulted. This was a composite of the (*R*)-2-octyl-L-rhamnosides found previously (peaks 1 and 2) and the (*S*)-2-octyl-L-rhamnosides (peaks 3 and 4). When the mixture of monosaccharides resulting from hydrolysis of the A-PS was reacted with (*R*)-2-octanol, the resulting rhamnosides (Figure 3C) had the same retention times as the (*S*)-2-octyl-L-rhamnosides, so they must have been the enantiomeric (*R*)-2-octyl-D-rhamnosides. The identities of the components in Figure 3C were verified by GC-MS, which showed that the major peak and peak 3 were both rhamnopyranosides, while peak 4 was a rhamnofuranoside (see spectra in Appendix 1). Furthermore, coinjection of the putative (*R*)-2-octyl-D-rhamnosides from the A-PS with the (*R*)-2-octyl-L-rhamnoside standard resulted in a chromatogram similar to Figure 3B. This proved conclusively that rhamnose was present only as the unusual D-enantiomer.

The absolute configurations of the other sugars could not be determined from this analysis, since they were present in very small amounts and thus could not be identified by GC-MS. GC-MS with selected ion recording (GC-MS-SIR) might increase the sensitivity enough to allow identification of the other components, but this experiment was not attempted.

3.2.3 Methylation Analysis of the AK1401 A-PS

The A-PS was per-methylated, hydrolysed, reduced, and acetylated to give a mixture of partially methylated alditol acetates (PMAA's),

each of which bears a methyl substituent at sites which were unsubstituted in the original PS, and acetates at the sites which were originally substituted. In this way, one can determine the linkage positions and ring sizes (not always unambiguously) for each of the monosaccharides present in the PS through separation and identification of the PMAA's by GC-MS. Note that reduction of the partially methylated monosaccharides may be accomplished with either sodium borohydride or borodeuteride, but the latter is advantageous because all even-electron fragment ions which contain C-1 (the former anomeric carbon) have even mass, whereas those fragments from the other end of the molecule all have odd mass. This simplifies the determination of the substitution pattern of the PMAA in a case where computerized spectral matching is limited or unavailable. The alditol-d₁'s can also resolve ambiguities in substitution arising from certain cases of symmetry of the undeuterated PMAA's.

The PMAA's found by methylation analysis of the A-PS are shown in Table 2, along with the monosaccharide linkage isomers which they represent. The mass spectra of all of the components found in the methylation analysis are in Appendix 1. The principal PMAA's are derived from 1,2-, 1,4-, and 1,3-linked rhamnopyranosides (peaks A, B, and C, respectively, in Figure 4) in the approximate ratio 5:2:10. It should be noted that a less polar column (DB-1, same temperature program) was unable to resolve isomers A and B.

The mass spectra of the positional isomers shown in Figure 4 provide a nice example of isomer differentiation by EI mass spectrometry. The major fragmentation pathway is cleavage between

Table 2: Partially methylated alditol acetates from AK1401 A-PS.

R.T. (min.) ⁽¹⁾	Component	Origin
17.95 (---)	1,5-di- <i>O</i> -acetyl-2,3,4-tri- <i>O</i> -methyl rhamnitol-d ₁	term. Rhap
20.25 (21.5)	1,2,5-tri- <i>O</i> -acetyl-3,4-di- <i>O</i> -methyl rhamnitol-d ₁	1,2- Rhap
20.37 (21.5)	1,4,5-tri- <i>O</i> -acetyl-2,3-di- <i>O</i> -methyl rhamnitol-d ₁	1,4- Rhap ⁽²⁾
20.53 (21.65)	1,3,5-tri- <i>O</i> -acetyl-2,4-di- <i>O</i> -methyl rhamnitol-d ₁	1,3- Rhap
21.06 (22.09)	1,5-di- <i>O</i> -acetyl-2,3,4,6-tetra- <i>O</i> -methyl hexitol-d ₁	term. Hexp
24.45 (23.52)	rhamnitol-d ₁ pentaacetate	?
24.80 (23.72)	1,4,5-tri- <i>O</i> -acetyl-2,3,6-tri- <i>O</i> -methyl hexitol-d ₁	1,4- Manp ⁽³⁾
25.49 (23.86)	1,4,5-tri- <i>O</i> -acetyl-2,3,6-tri- <i>O</i> -methyl hexitol-d ₁	1,4- Glcp ⁽³⁾
45.08 (30.10, 30.52)	hexitol-d ₁ hexaacetate	?

(1) Retention times not in parentheses were obtained by GC-MS using a DB-1701 30 metre narrow bore column (conditions: 1 min. at 50°C, 10°C per min. to 200°C, hold). Retention times in parentheses were obtained using a DB-1 30 metre narrow bore column (conditions: 5 min. at 50°C, 10°C per min. to 200°C, hold). The injector and interface temperatures were 210°C in both cases.

(2) Subsequent experiments showed that this component resulted mainly (if not entirely) from 1,4-linked 3-*O*-methyl rhamnopyranose.

(3) Assignments may be reversed.

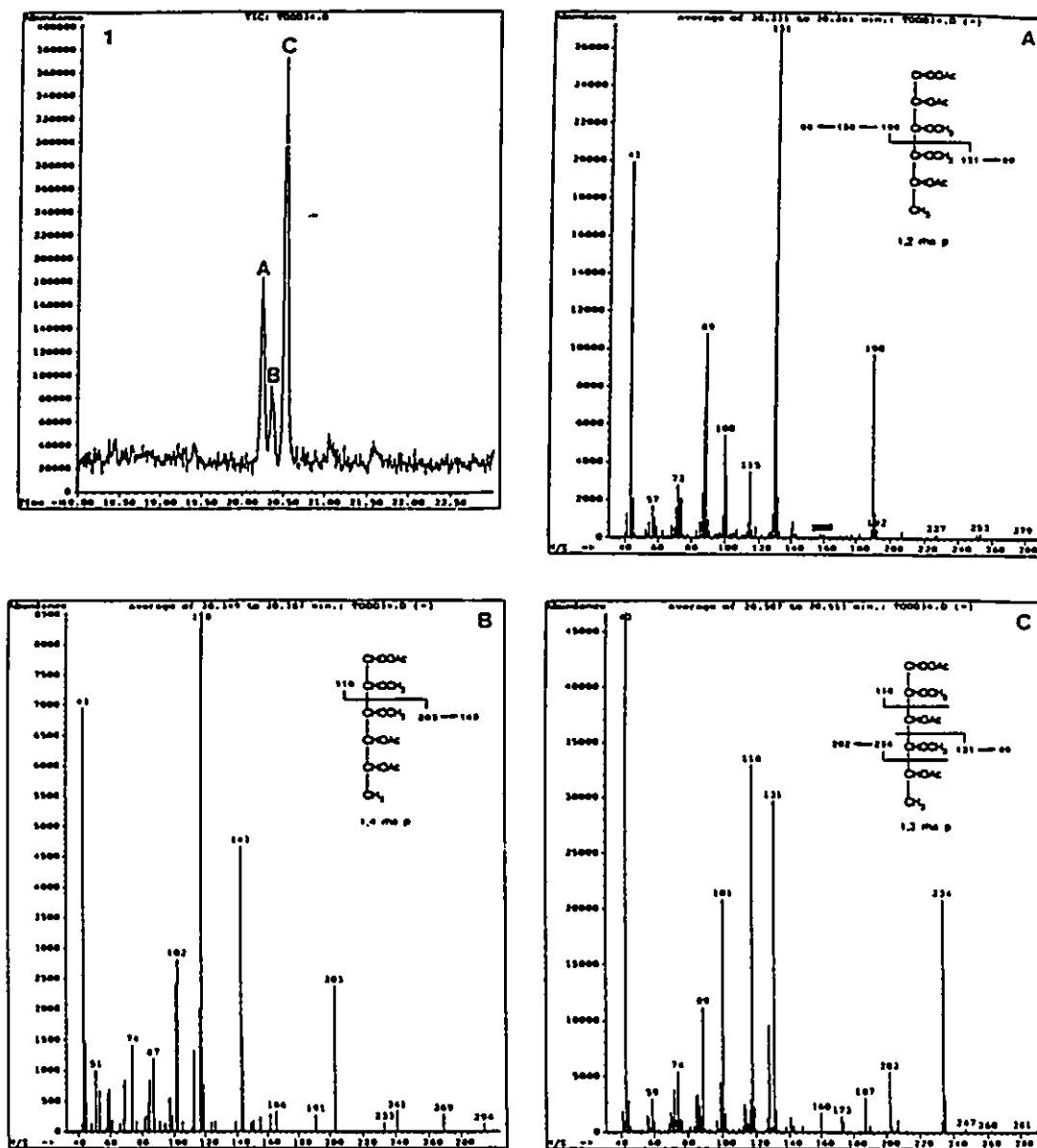


Figure 4: Major partially methylated alditol acetates (PMAA's) resulting from methylation analysis of the AK1401 A-PS

adjacent methoxylated carbons. However, if there are no adjacent methoxylated carbons, then cleavage occurs preferentially to leave the positive charge on a methoxylated carbon rather than an acetoxyated carbon. The major fragments then undergo β -elimination of methanol (32 amu) or acetic acid (60 amu), or loss of ketene (42 amu), depending on the substitution pattern.³⁷

Other PMAA's which were found in lesser amounts represented two diastereomeric 1,4-linked hexopyranoses or 1,5-linked hexofuranoses (presumably derived from mannose and glucose). The determination of the ring size is ambiguous in this case because both carbon 4 and carbon 5 of the alditol bear acetate substituents; one cannot discern whether the C-4 oxygen formed the ring and C-5 was substituted (1,5-linked hexofuranoside) or if the opposite was true (1,4-linked hexopyranoside), because both possibilities yield the same PMAA. However, glucose and mannose are almost invariably encountered in the pyranoside form, so one may assume that the PMAA's found represent 1,4-linked mannopyranoside and 1,4-linked glucopyranoside, although this is not proven by this experiment. Similarly, the PMAA representing 1,4-linked rhamnopyranoside discussed above is unlikely to be derived from the furanoside, but this possibility cannot be proven directly by methylation analysis. Note, however, that the 1,2- and 1,3-linked rhamnose residues are unambiguously defined as pyranosides by this experiment.

In addition, rhamnopyranose and hexopyranose were also found in very small amounts as non-reducing terminal sugars. The fact that two different non-reducing termini are present implies that a branch point

must exist, but PMAA derivatives of branching sugars were not found in this analysis, presumably because any such monosaccharide would be present in very low abundance.

There are two monosaccharides that are known to be minor components of the A-PS which are not easily detected in the methylation analysis. 3-O-methyl rhamnopyranoside would appear as part of the PMAA's representing either 1,2- or 1,4-linked rhamnopyranose, depending on it's linkage positions, so no conclusions about the linkage to 3-O-methyl rhamnopyranose can be drawn from this experiment alone: this problem will be discussed further in section 3.4.5. A second, more pressing problem is that no derivatives of ribose were found in this analysis. One can speculate that this could be due to a variety of reasons, for example, the ribose is preferentially destroyed by this treatment; or that the ribose bears a substituent which is not removed during methylation analysis, and thus forms a substituted PMAA derivative whose retention time and mass spectrum are not similar to other, more common derivatives.

3.2.4 Summary of the degradative analyses

Before proceeding to spectroscopic analysis of the intact A-PS, it is worth reiterating the gross structural features determined by the above degradative analyses. The AK1401 A-PS was found to consist principally of D-rhamnose, which is present as a 1,3-linked rhamnopyranoside, a 1,2-linked rhamnopyranoside, and a 1,4-linked

rhamnopyranoside in the approximate ratio 10:5:2. One of the minor sugar constituents, 3-*O*-methyl rhamnose, accounts for at least some of the 1,2- or 1,4-linked rhamnopyranoside, since the natural methyl group cannot be distinguished from those added in the methylation step. Of the other minor sugars, mannose and glucose were found to be 1,4-linked hexopyranosides (or 1,5-linked hexofuranosides, but these are unlikely), while ribose derivatives were not detected in the methylation analysis.

3.3 NMR Analyses of the AK1401 A-PS

3.3.1 ^1H - and ^{13}C -NMR of the underivatized AK1401 A-PS

The one-dimensional 500 MHz ^1H - and 125 MHz ^{13}C -NMR spectra of the AK1401 A-PS in D_2O are presented in Figure 5. The anomeric regions of both spectra contain only three principal resonances, which is somewhat surprising considering the level of complexity indicated by the degradative analyses of the A-PS. One can account for the simplicity of the anomeric region if the principal structural feature of the A-PS is a trisaccharide repeating unit, *i.e.*, the same three monosaccharides appear over and over again in the same environment, while the other monosaccharide constituents are present in lesser amounts, and possibly in varied environments, thus having little effect on the overall spectrum. Since methylation analysis indicated that the principal monosaccharide types are 1,3-linked rhamnopyranose and 1,2-linked rhamnopyranose in the approximate ratio of 2:1, these may be the constituents of the repeating unit. This is corroborated by the appearance of the anomeric proton resonances as singlets with a linewidth of approximately 3 Hz, indicating that the value of the H-1-

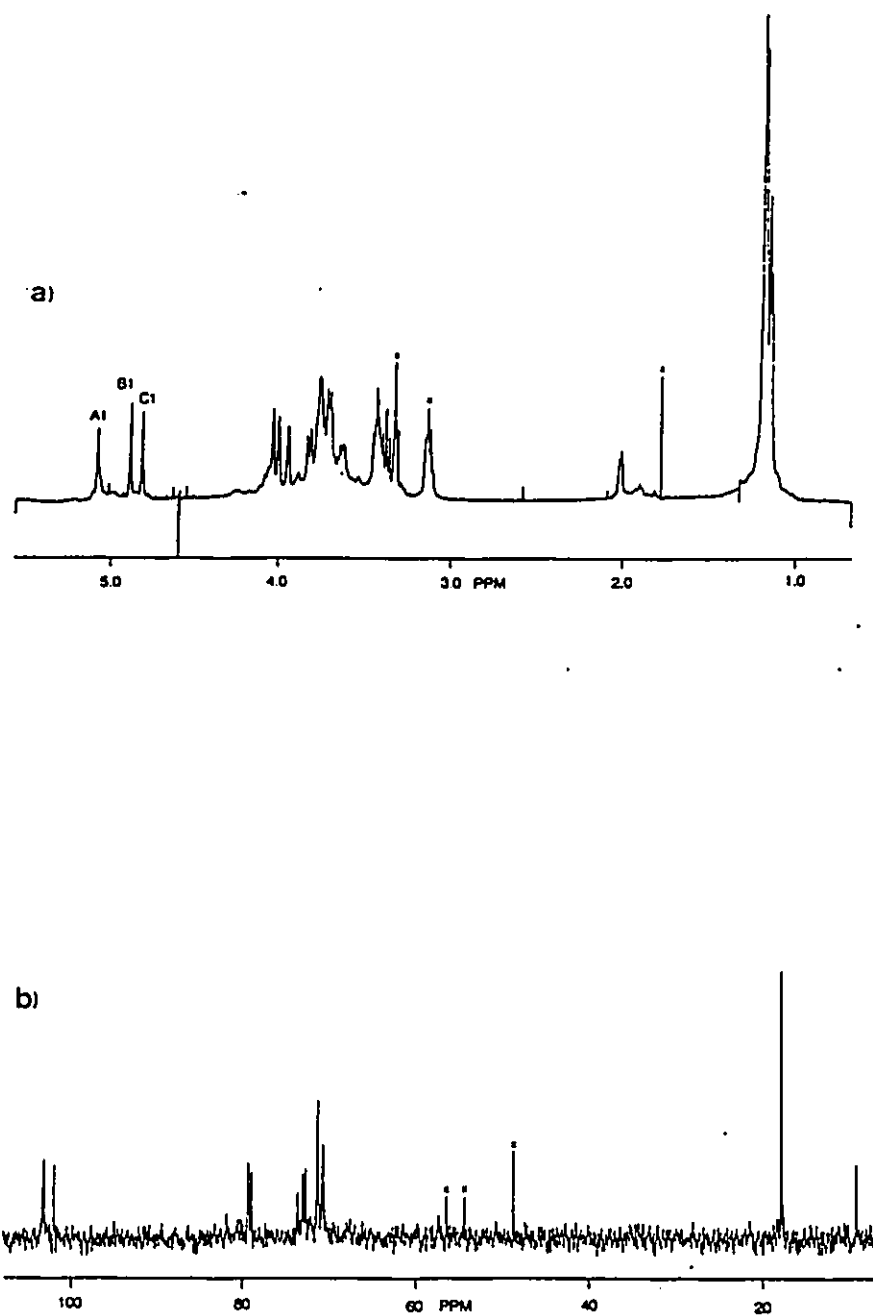


Figure 5: a) 500 MHz $^1\text{H-NMR}$, and b) 125 MHz $^{13}\text{C-NMR}$ spectra of the AK1401 A-PS in D_2O

H-2 coupling constant is of this magnitude; this result is consistent with all of the three monosaccharides having the *manno*-configuration. Also, integration shows that the resonances around 1.2 ppm (CH₂'s of rhamnose) have a total intensity of more than three times the sum of the intensities of the anomeric protons, thus indicating that there is sufficient 6-deoxysugar to account for all three anomeric protons. To verify the hypothesis that the A-PS consists principally of a trisaccharide repeating unit of rhamnoses, the ¹H-NMR spectrum was further investigated by two-dimensional methods.

3.3.2 Homonuclear Correlation Spectroscopy (COSY) of the A-PS

The signals for each of the three principal monosaccharides in the 500-MHz ¹H-NMR spectrum of the intact A-PS could be assigned, in spite of several overlapping signals, through the use of 2D shift-correlated (COSY) and relayed coherence transfer (RELAY) experiments. The signals of the three anomeric protons were labelled A1, B1, and C1 (where A1 refers to the signal of H-1 of residue A, and so on) starting with the resonance at lowest field (see Figure 5a). The COSY spectrum was interpreted by starting from the signal of the anomeric proton of each residue, and locating the signal of H-2 of that residue by finding the coupled resonance (by observation of an off-diagonal peak in the COSY spectrum). This process is illustrated in Figures 6, 7, and 8 for each of the residues A, B, and C. As an example, proton A1 at 5.079 ppm (Figure 6) is coupled to the proton at 3.946 ppm, since there is an off-diagonal peak in the COSY spectrum which correlates them; therefore, the signal at 3.946 ppm is assigned to proton A2, and its neighbour (A3) may

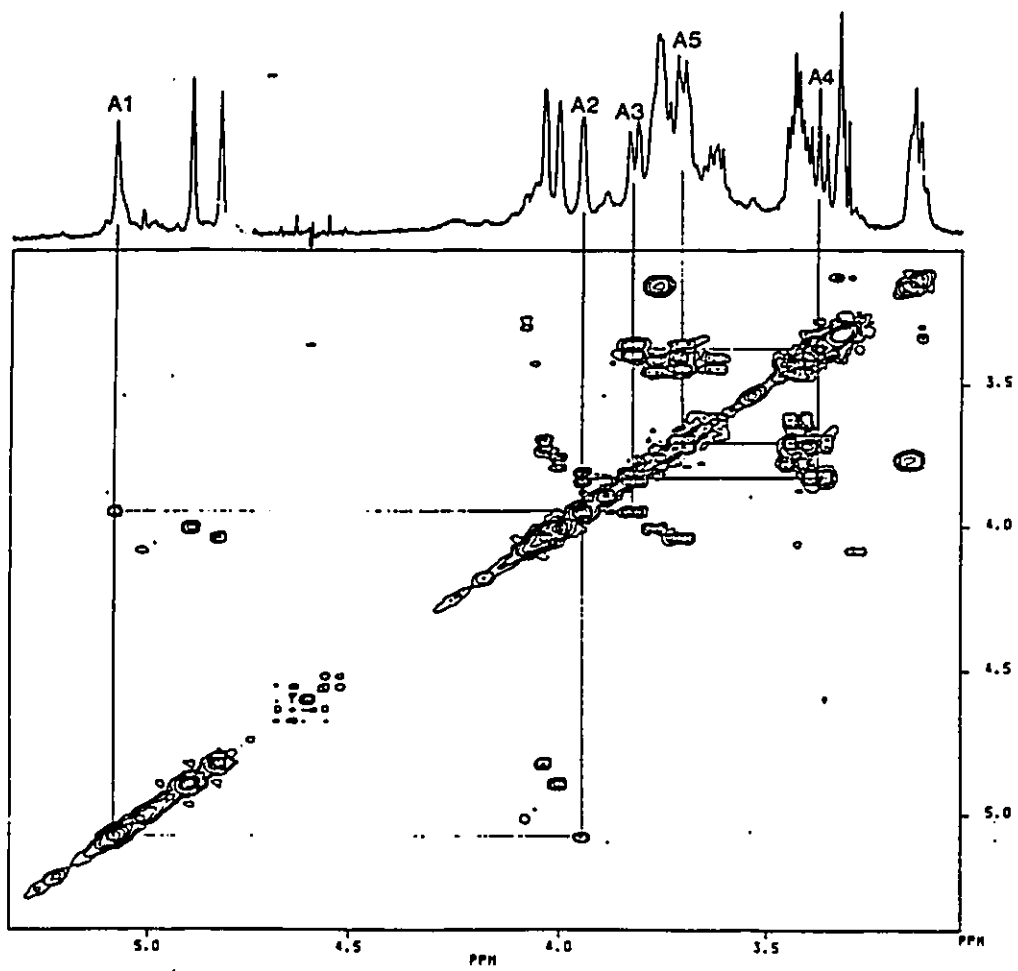


Figure 6: Portion of the ^1H - ^1H -COSY spectrum of AKI401 A-PS showing assignments of H1 to H5 of the A residue

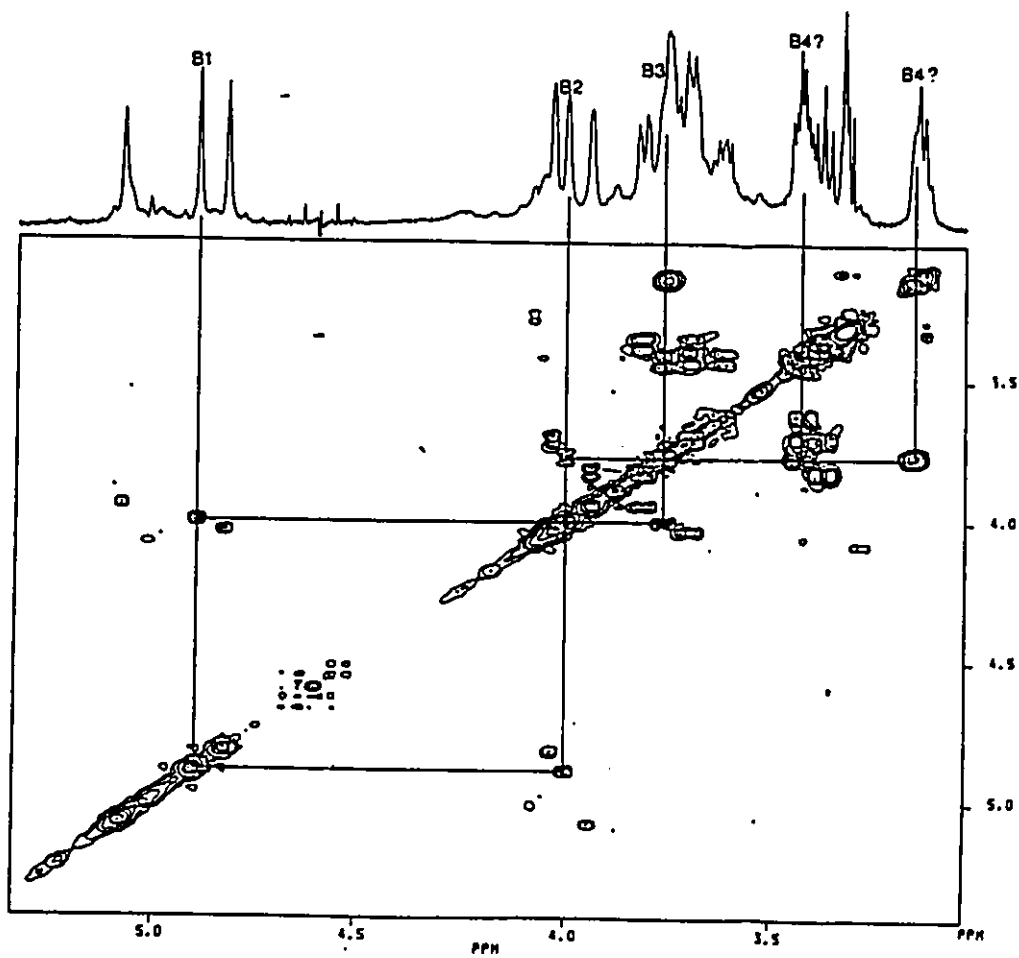


Figure 7: Portion of the ^1H - ^1H -COSY spectrum of AK1401 A-PS showing assignments of H1 to H3 of the B residue. Note that H4 cannot be assigned because there are two possible B3-B4 crosspeaks.

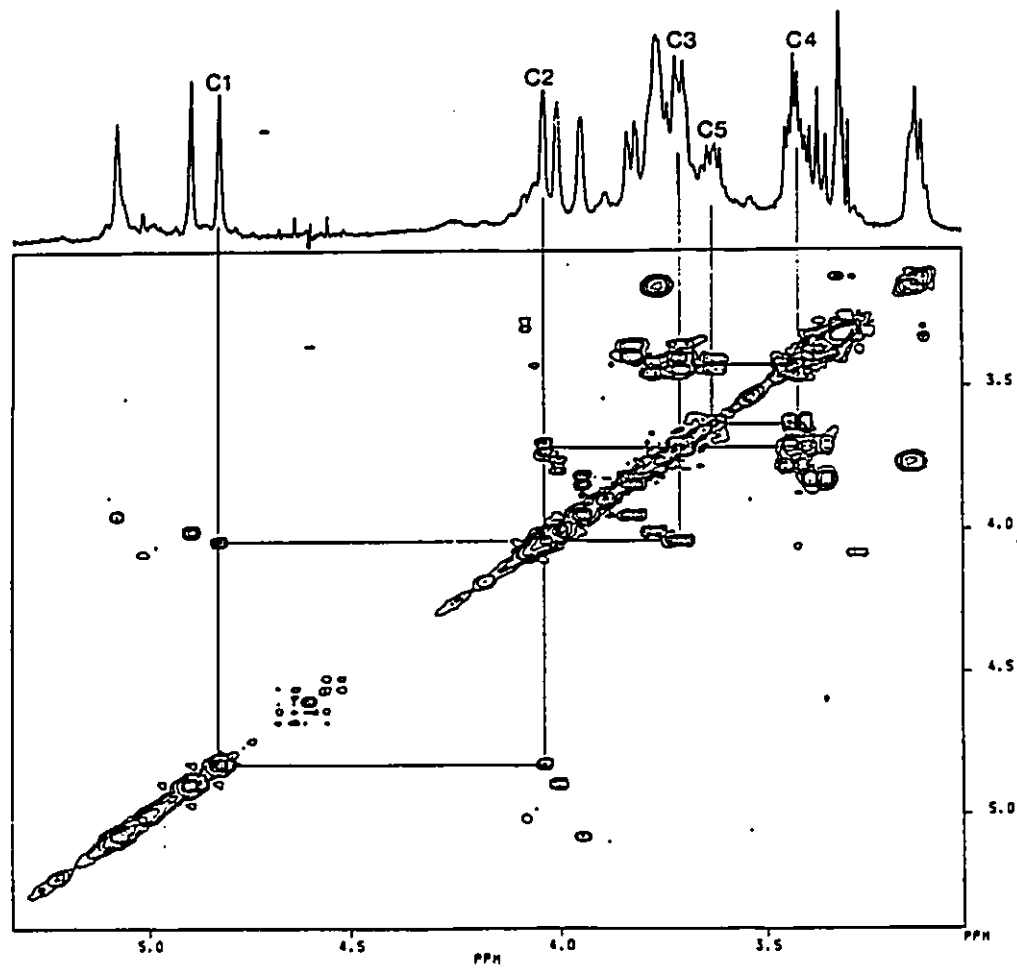


Figure 8: Portion of the ^1H - ^1H -COSY Spectrum of AK1401 A-PS showing assignments of H1 to H5 of the C residue

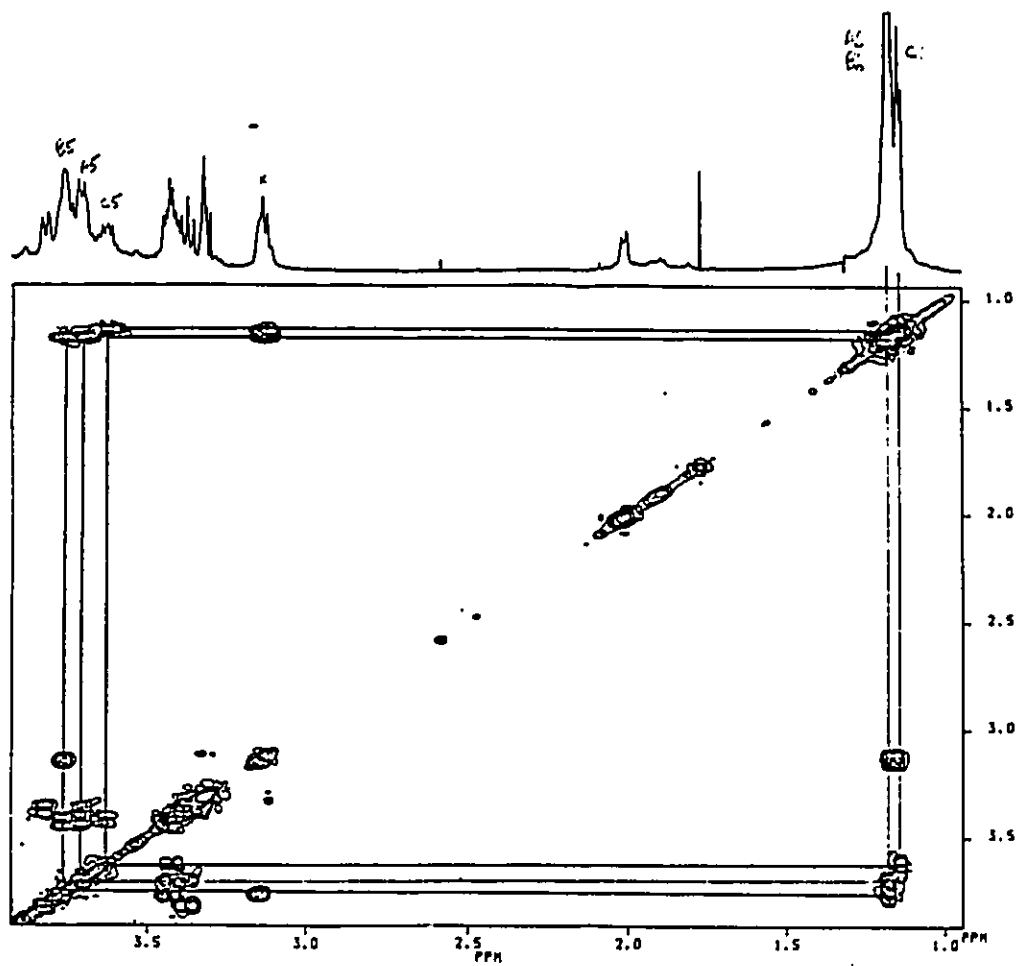


Figure 9: Portion of the ^1H - ^1H -COSY spectrum of AK1401 A-PS showing assignments of H5 and H6's (H6, H6', H6'') for each residue

be found in a similar fashion. In this way, all of the resonances of a given monosaccharide may be found by analysis of the nearest-neighbour connectivities shown in the COSY spectrum. The connectivity networks for H-1 to H-5 of each monosaccharide are outlined in Figure 6, 7, and 8, and the H-5 to H-6 correlations are shown on Figure 9. The complete assignment of the proton spectrum of residue B could not be made from the COSY spectrum alone, since there are two potential B3-B4 crosspeaks, one of which correlates B3 to the multiplet at 3.442 ppm, and the other correlates B3 with the resonance at 3.13 ppm (see Figure 7). This ambiguity may be the result of overlapping resonances at the position of the signal assigned to proton B3, or alternatively B3 has two neighbours in addition to B2.

3.3.3 Relayed Coherence Transfer Spectroscopy (RELAY)

The COSY experiment enabled the complete assignment of the protons of residues A and C, but residue B could not be completely assigned as outlined above. The use of the RELAY experiment in resolving the ambiguity caused by overlapping resonances is illustrated in Figure 10. Since this experiment shows next-nearest neighbour connectivities in addition to nearest-neighbour connectivities (the information contained in a COSY spectrum), the assignment of the signal for proton B4 is clarified by the presence of an additional crosspeak which correlates B2 to B4. Thus, the RELAY experiment shows a correlation between the known B2 resonance at 4.002 ppm and the B3 resonance at \approx 3.77 ppm (as in COSY), and also a correlation between the B2 resonance and the resonance at 3.442 ppm. Therefore, the signal at

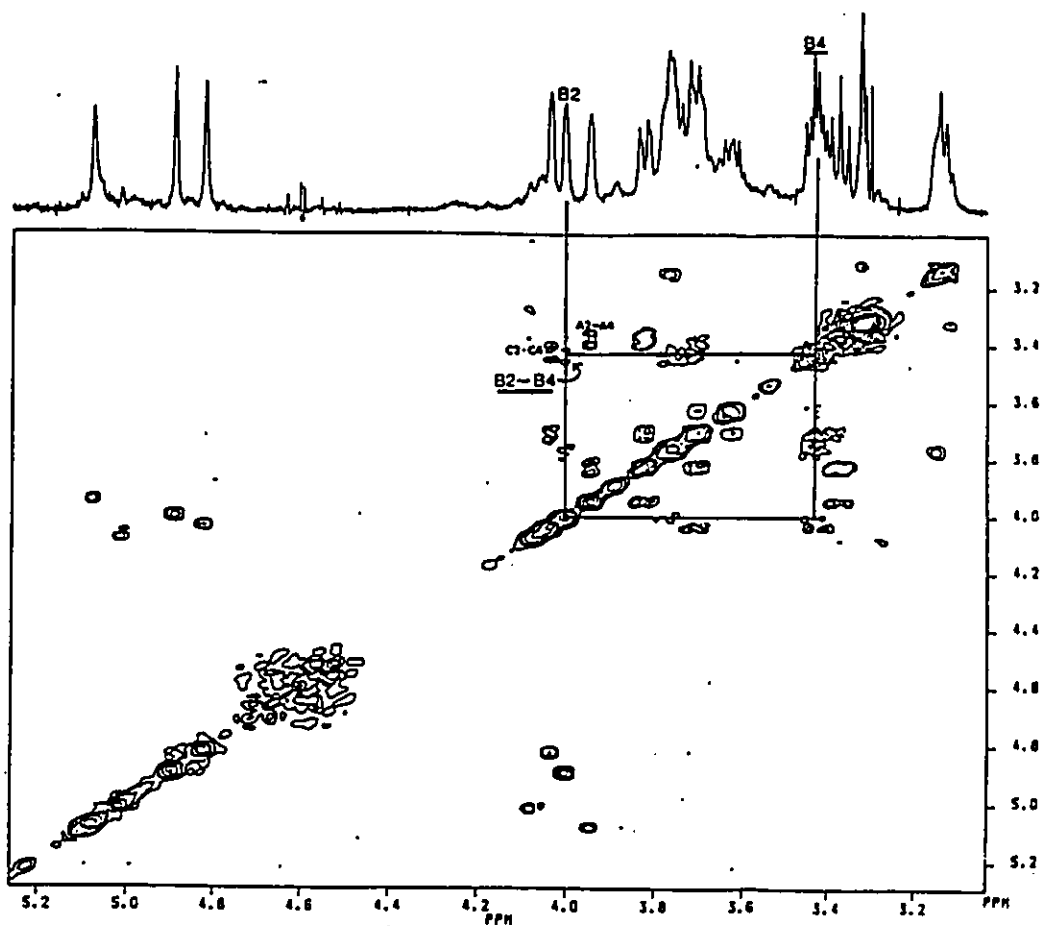


Figure 10: Portion of the RELAY spectrum of AK1401 A-PS showing B2-B4 correlation

3.442 ppm is assigned to proton B4, and the additional crosspeak seen in the COSY spectrum which correlated the B3 resonance to the resonance at 3.13 ppm must be the result of another resonance overlapped with that of B3. The nature of this additional resonance was not clarified by the RELAY spectrum, so that it and the resonance at 3.13 ppm remain unassigned.

The relay experiment also corroborated the assignments which were made based on the COSY spectrum. Additional crosspeaks were observed which correlated A2-A4, C2-C4, A3-A5, C3-C5, and H4-H6's for all three residues. No additional crosspeak was seen for B3-B5, but this is because the signals for B3 and B5 are nearly coincident. In addition, no H1-H3 crosspeaks were observed, but this is likely due to the small J_{H1-H2} 's relative to the other coupling constants, and the selection of τ in the pulse sequence.⁵⁵

A summary of the signal assignments derived from the COSY and RELAY experiments is given in Table 3. Some of the coupling constants were obtained by observation of the ¹H NMR spectrum at 80°C, however, the chemical shifts reported are those from the spectrum acquired at 30°C.

3.3.4 Unassigned resonances

One can infer that the resonances which remain unassigned after analysis of the COSY and RELAY spectra are not part of another monosaccharide, because there is no additional anomeric proton in the spectrum (there are also no additional anomeric carbon resonances). Furthermore, there is no anomeric proton signal hidden by the residual

Table 3: ^1H -NMR data for A-PS from AK1401 in D_2O

Proton	Chemical shift	Multiplicity	Coupling constant(s)
<i>Residue A</i>			
H-1	5.079	br s	$J_{1,2} = 1.7 \text{ Hz}^{(1)}$
H-2	3.946	br s	$J_{2,3} = 3.3 \text{ Hz}^{(1)}$
H-3	3.825	dd	$J_{3,4} = 10 \text{ Hz}$
H-4	3.374	apparent t	$J_{4,5} = 10 \text{ Hz}$
H-5	3.71	m ⁽²⁾	---
H-6,6',6''	1.175	d	$J_{5,6} = 5.5 \text{ Hz}$
<i>Residue B</i>			
H-1	4.894	br s	$J_{1,2} < 2 \text{ Hz}$
H-2	4.002	br s	$J_{2,3} = 3 \text{ Hz}$
H-3	3.77	br m ⁽³⁾	$J_{3,4} = 10 \text{ Hz}$
H-4	3.442	sextet ⁽⁴⁾	$J_{4,5} = 10 \text{ Hz}$
H-5	3.76	br m ⁽³⁾	---
H-6,6',6''	1.175	d	$J_{5,6} = 5.5 \text{ Hz}$
<i>Residue C</i>			
H-1	4.823	br s	$J_{1,2} < 2 \text{ Hz}$
H-2	4.037	br s	$J_{2,3} = 3 \text{ Hz}$
H-3	3.71	m ⁽²⁾	$J_{3,4} = 10 \text{ Hz}$
H-4	3.432	sextet ⁽⁴⁾	$J_{4,5} = 10 \text{ Hz}$
H-5	3.62	dq	---
H-6,6',6''	1.140	d	$J_{5,6} = 6 \text{ Hz}$

- (1) $J_{1,2}$ and $J_{2,3}$ for residue A were determined from the spectrum at 80°C .
- (2) The signals of H-5 of residue A and H-3 of residue C were overlapped.
- (3) H-3 and H-5 of residue B are part of the same multiplet, together with an unknown resonance.
- (4) The H-4 signals of residues B and C were overlapped.

HOD resonance at 4.60 ppm, since the spectrum at 80°C (see Appendix 2), in which the HOD resonance is shifted upfield by about 0.5 ppm, also shows only the three principal anomeric proton signals. The unknown spin system seems to be confined to a resonance at about 3.77 ppm (overlapped with B3), which is adjacent to the proton(s) at 3.13 ppm, which in turn is adjacent to a methyl group at about 1.15 ppm. It is interesting to note that the signal at 3.13 ppm is absent when the A-band LPS from AK1401 was obtained by extraction using a different procedure (phenol/chloroform/ petroleum ether; the ¹H-NMR spectrum of the material so obtained is in Appendix 2).

3.3.5 Determination of linkage stereochemistry

The anomeric carbon-anomeric proton coupling constants (J_{C1-H1}) were measured by inspection of the proton-coupled ¹³C-NMR spectrum shown in Figure 11. Since two of the lines were overlapped, the assignment of lines was verified by calculation of the midpoint of each doublet and comparison to the chemical shifts in the proton-decoupled ¹³C-NMR spectrum. These data are summarized in Table 4. Based on the magnitude of the C1-H1 coupling constants, all three anomeric carbons in the repeating unit have the α -configuration since $J_{C1-H1} = 169$ to 171 Hz for α -rhamnopyranosides, and 159 to 162 Hz for β -rhamnopyranosides.^{18,49} It should be noted that the assignment of the anomeric configuration by determination of the J_{H1-H2} could not be made in this case, because the signals for the anomeric protons had linewidths which were greater than the coupling constants ($J_{H1-H2} = 1.8$ Hz for α -rhamnopyranose, 1.1 Hz for β -rhamnopyranose, and 1.7 Hz for methyl α -rhamnopyranoside⁶⁵).



Figure 11: Anomeric carbon region of the ^1H - ^{13}C -coupled ^{13}C -NMR spectrum of the AK1401 A-PS

Table 4: Determination of linkage stereochemistry

=====

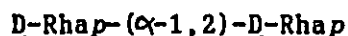
<u>Residue</u>	<u>Lines</u>	<u>J_{C1-H1} (Hz)</u>	<u>Midpoint (ppm)⁽¹⁾</u>	<u>ppm⁽²⁾</u>
X	13090-12917	173	103.40	103.43
Y	13062-12889	173	103.18	103.19
Z	12917-12741	176	102.01	102.01

(1) Calculated by finding the midpoint in Hz and dividing by the spectrometer frequency of 125.759 MHz

(2) Chemical shifts from the proton-decoupled spectrum

3.3.6 Nuclear Overhauser enhancement experiments and structure of the repeating unit

Since the repeating unit portion of the AK1401 A-PS is known to consist of a trisaccharide of two 1,3-linked and one 1,2-linked α -D-rhamnosides from the foregoing experiments, the sequence of and linkage positions between residues A, B, and C (defined in Figure 5) could be determined by observation of inter-residue nOe's. The result of a representative nOe experiment is shown in Figure 12, and the data are in Table 5; the complete set of nOe difference spectra are included in Appendix 2. If one considers the linkage:



it is apparent from a Dreiding model that the anomeric proton cannot approach within a distance of 3 Å to the H-3 of the next residue. Thus, an α -1,2-linkage would not show a significant nOe of the signal of H-3 upon irradiation of the anomeric proton of the neighbouring unit (see also reference 18 for a similar argument). Since irradiation of protons A1 and B1 resulted in nOe's of the signals of protons B3 and C3, respectively, neither of the linkages, A→B and B→C, can be α -1,2. Since irradiation of C1 gave a strong nOe of the signal of A2, but not of any H-3 signal, only C→A can be an α -1,2-linkage, whereas A→B and B→C are α -1,3-linkages. Furthermore, the results of the nOe difference experiments provide confirmatory evidence for the α -configuration of the linkages, as indicated, for example, by the absence of an nOe of H-3 or H-5 (of the same residue) upon irradiation of H-1. If the anomeric proton had been part of a β -D-pyranoside, an intense nOe of H-3 and H-5

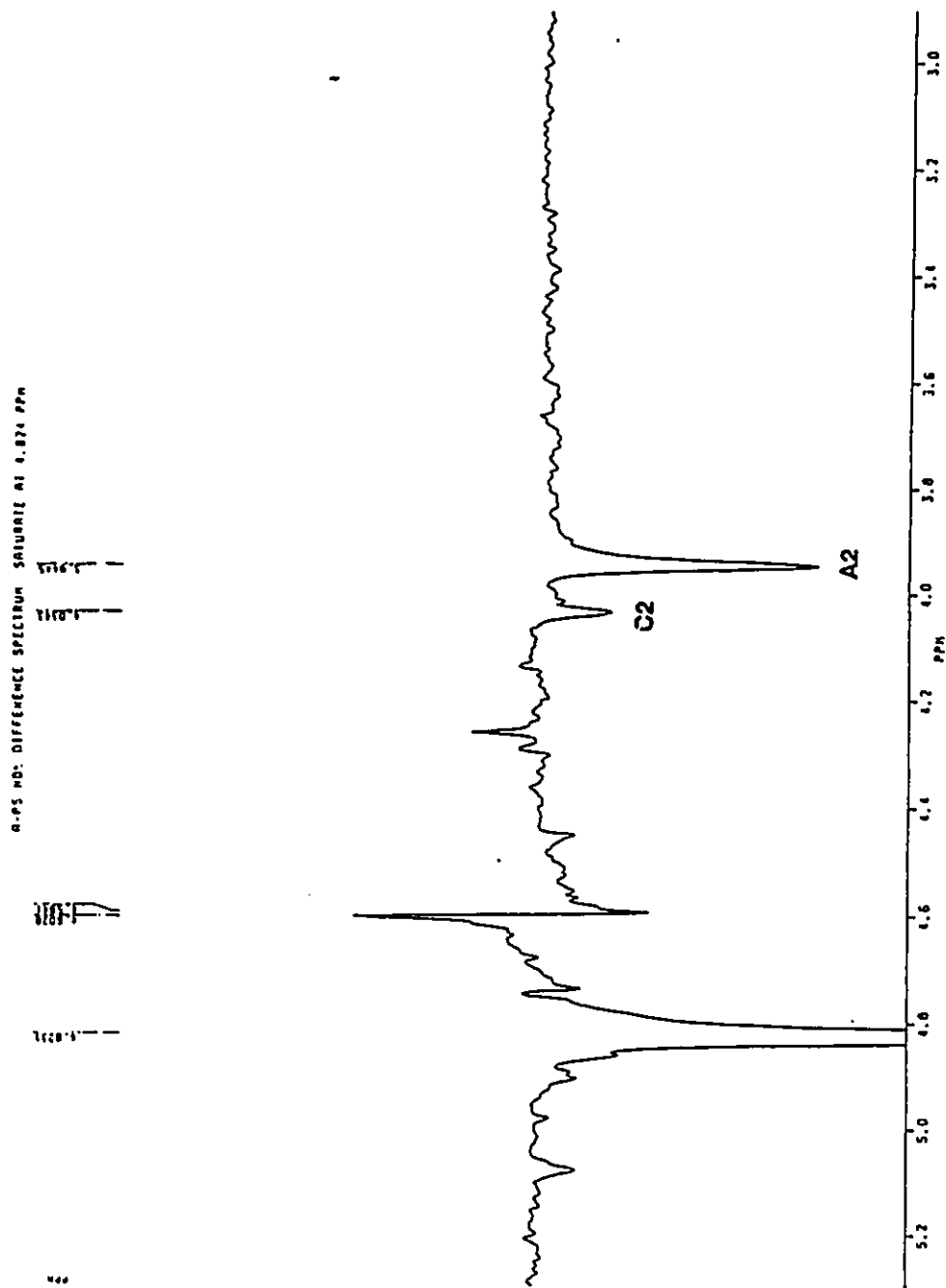


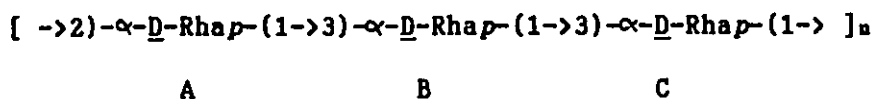
Figure 12: A representative n0e difference experiment. Proton C1 (4.823 ppm) was saturated, and negative enhancements of protons A2 and C2 were observed.

Table 5: Observed nuclear Overhauser enhancements

Irradiated proton	Enhanced signals ⁽¹⁾
A1	B3 (strong), C5, A2, H-6's
B1	B2, C3-A5 multiplet
C1	A2 (strong), C2
A2	C1 (strong), A3, A1
B2	B1, C3-A5 multiplet
C2	C1, B5, C3-A5 multiplet
A3	A2 (weak)
B3-B5	A1, C2, H-6's, B2
C3-A5	B1, H-6's, C2, B2, B4-C4 multiplet, A4
C5	H-6's, A1, B4-C4 multiplet
C6	C4-B4 (weak), C5
A6-B6	C3-A5, B5, A4, B4-C4 multiplet

(1) Enhanced signals are listed in order of decreasing intensity.

would have resulted. Thus, the repeating-unit structure of the A-PS from AK1401 is as follows:



where A, B, and C are the arbitrary designators of the monosaccharides defined in Figure 5. The complete assignment of the $^1\text{H-NMR}$ spectrum of this repeating unit was presented in Table 3. An idealized drawing of this repeating unit is shown in Figure 13.

It should be noted that inter-residue nOe's do not always show the greatest enhancement for the proton at the linkage site when the anomeric proton of the neighbouring residue is irradiated. Dabrowski⁴¹ has stated that the assignment of linkage positions is unambiguous except when the site of substitution has a vicinal equatorial proton, wherein the vicinal proton nOe is of a similar magnitude to that of the proton at the site of substitution. Note that in the case of the 3-substituted rhamnose of the A-PS, which has the C-2 *manno*-configuration, H-2 is equatorial, which could potentially give rise to an ambiguous assignment. However, the identification of the 2-substituted rhamnose by the argument presented above seems quite clear, and the assignment of the other two residues as 3-substituted rhamnosides may be made by deduction in light of the methylation analysis results. Furthermore, glycosylation induced shifts at the site of substitution and the vicinal protons^{41, 66} suggest that the linkage assignments presented above are correct, since proton A1 (vicinal to substitution site A2) is at lower

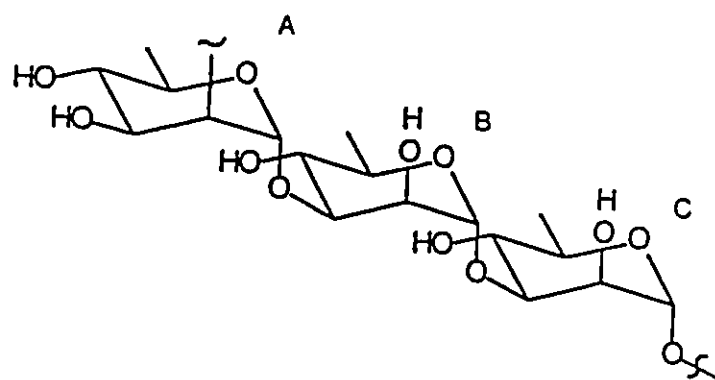


Figure 13: Structure of the repeating unit portion of AK1401 A-PS

field than B1 and C1, while protons B4 and C4 (vicinal to substitution sites: B3 and C3) are at lower field than A4.

3.3.7 Significance of the repeating unit structure

The repeating unit structure of AK1401 A-PS has been found previously in the LPS preparations from the plant pathogen *Pseudomonas syringae*^{16,17}, and from *P. aeruginosa* strain ATCC 27584 and *P. aeruginosa* serotype O7.^{14,18} Yokota *et al.*¹⁴ have proposed (on the basis of monoclonal antibody studies) that this structure represents a "common antigen" which is widely distributed among serotypes of *P. aeruginosa*.

The similarity between the A-band LPS described by McGroarty and co-workers^{12,13} and the "common antigen" described by Yokota *et al.*¹⁴ had been established by the use of monoclonal antibody MAb E87 (see ref. 20). The present data confirm this observation, since they show that the repeating unit of the polysaccharide portion of A-band LPS from AK1401 is the same as the repeating unit of the common antigen. Thus, there is a definable measure of chemical identity between the "common antigen" of *P. aeruginosa* and the A-band LPS described by McGroarty *et al.*. This work therefore validates the clinical studies of Lam *et al.*²⁰, who used AK1401 as a probe for the presence of a common antigen on *P. aeruginosa* cells from infected CF lungs.

The determination of the repeating unit structure of AK1401 A-PS also has implications in an ongoing controversy about antibody specificity. Kocharova *et al.*²¹ have suggested that MAb E87 is not specific for the rhamnan structure found by Yokota *et al.*, but rather

for another polysaccharide structure which has a repeating unit of L-rhamnose, D-ribose and D-glucose in the ratio 2:1:1. However, the results of the present work do not support their assertion. We have found no evidence of their polysaccharide in the PS preparation derived from AK1401 A-band LPS, which reacted with MAb E87 (although our PS preparation contains small amounts of ribose and glucose, the absence of L-rhamnose seems quite clear from the result of the chiral glycoside experiment discussed in Section 3.2.2). Instead, we have found that the principal structural feature of the AK1401 A-PS preparation is a D-rhamnan having the same repeating unit as found by Yokota *et al.*, suggesting that this may be the epitope recognized by MAb E87. Recent work by Yokota *et al.*⁶⁷ suggests this as well.

Although the repeating unit of AK1401 A-PS has the same structure as that found by other workers¹⁴⁻¹⁷, the present work represents the first complete assignment of the ¹H-NMR spectrum of the polysaccharide, thereby complementing the assignment of the ¹³C-NMR spectrum of this repeating unit reported by Tsvetkov *et al.*¹⁹

3.4 Studies on the minor monosaccharide components of AK1401 A-PS

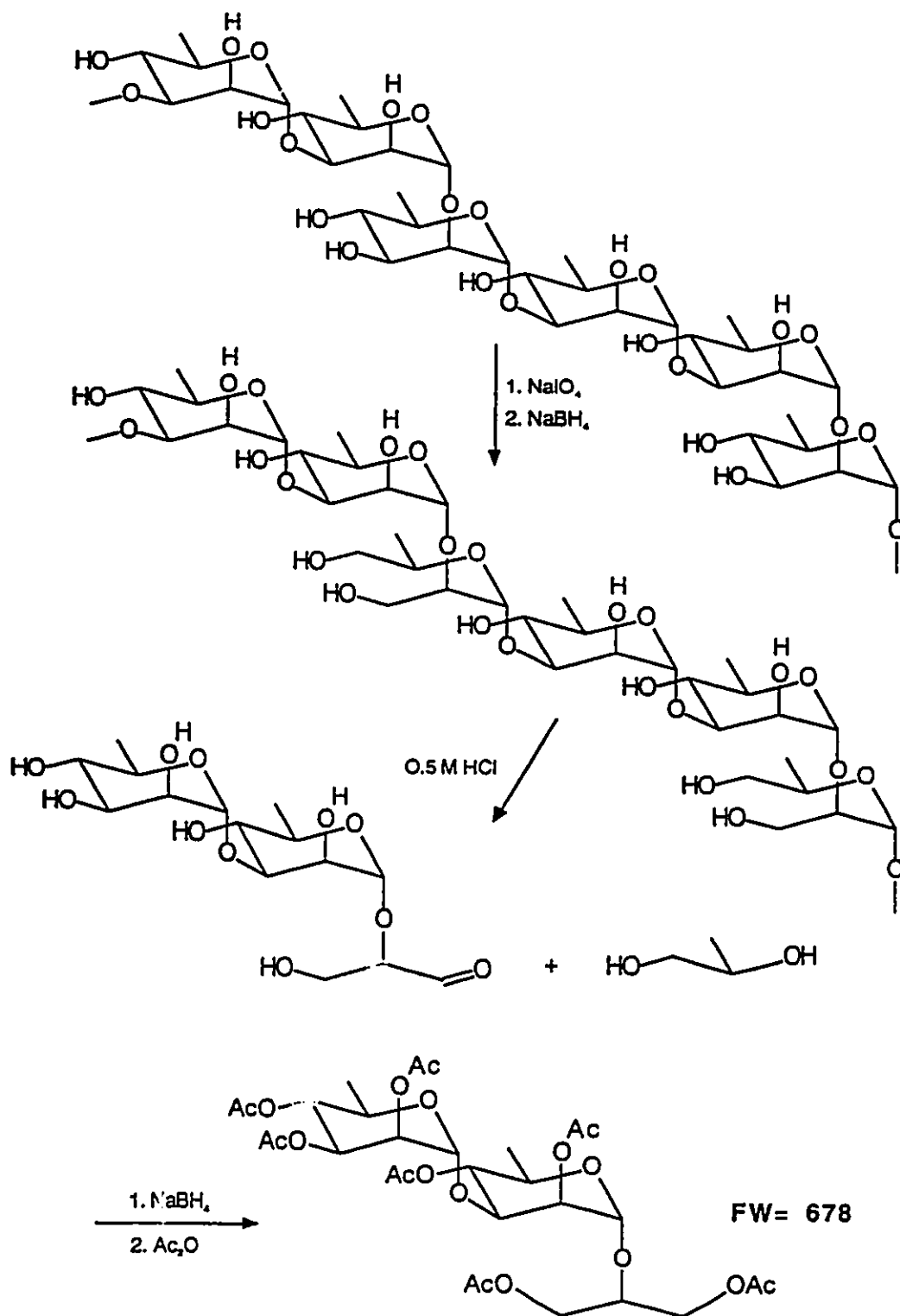
3.4.1 Rationale for the Smith degradation

Since the sequence and linkage structure of the repeating unit portion of the A-PS is now known, it remains to determine the role of the minor sugar constituents which were detected in the composition analysis. One may hypothesize that the minor sugars are grouped together, perhaps in a core arrangement, since the ¹H-NMR studies strongly suggest an unsubstituted, uninterrupted repeating unit

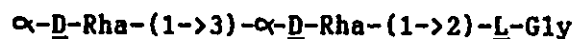
structure. Conceptually, one may isolate a core structure in one of two ways: one may investigate the LPS of rough mutants which do not produce side chain polysaccharide, but there are no mutants yet known to produce "rough A-band LPS". Alternatively, one may use chemical means (in certain cases) to selectively degrade the side chain polysaccharide in order to study the core oligosaccharide which remains after such treatment. An ideal situation for A-band LPS would be to degrade the repeating unit portion with an enzyme (in analogy to the studies of Dutton *et al.*,⁶⁸). There is a literature report¹⁶ of a bacteriophage that bears an enzyme capable of depolymerizing the LPS of a strain of *Pseudomonas syringae* that has the same repeating unit as the AK1401 A-PS. However, this bacteriophage was unavailable to us, so a selective chemical method was used instead (Smith degradation, outlined in Chapter 1).

One can take advantage of the structure of the repeating unit of AK1401 A-PS to degrade it in a controlled fashion. Since every third monosaccharide in the polysaccharide is a 1,2-linked rhamnose residue and since these residues possess a vicinal diol on carbons 3 and 4, they may be selectively oxidized by sodium periodate without oxidation of the 1,3-linked rhamnose residues. Reduction of the resulting dialdehydes and mild acid hydrolysis (to selectively hydrolyse the acyclic acetals in the presence of cyclic ones) results in depolymerization of the main chain into oligosaccharides of predictable structure, which are derivatized prior to analysis. This series of reactions (Smith degradation) is illustrated for the known portion of the A-PS structure in Scheme 1. It is apparent that the expected major product of the mild

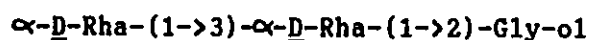
SCHEME 1



hydrolysis will be:



where L-Gly is L-glyceraldehyde derived from carbons 1, 2, and 3 of the former 1,2-linked rhamnose residue. For practical reasons the aldehyde is reduced prior to further derivatization, so the final product is actually:



where Gly-ol is glycerol.

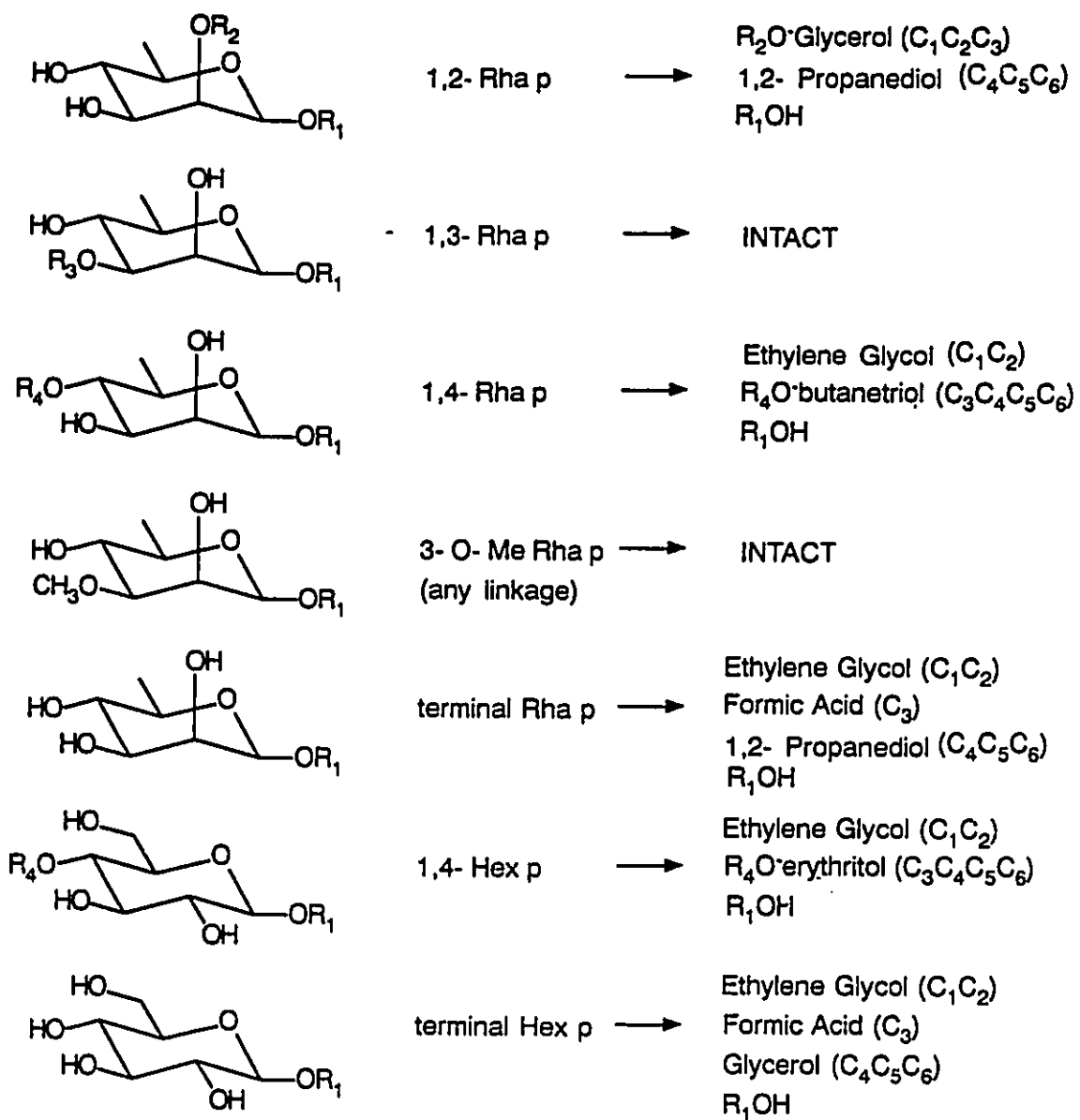
If one can isolate and identify other Smith degradation products which contain the minor monosaccharides, one may be able to use their structures to infer the locations of the minor monosaccharides in the polysaccharide. However, the determination of the structure of each of these putative fragments is not trivial; compounds of very similar structure (for example, a compound similar to the major product above, but with replacement of one rhamnose by a different monosaccharide) may not be separable by liquid chromatography. A better analytical scheme would use capillary gas chromatography, which has at least an order of magnitude better resolving power than HPLC. Nevertheless, the use of GC as a separation method has some drawbacks: the method is inapplicable to higher mass oligosaccharides because of their low vapour pressures, and preparative separations may not be practical because these must be carried out on lower-resolution packed columns. This last criterion may exclude further degradative analysis (such as compositional or methylation analysis) of the fractions observed in the capillary GC. Therefore, one may have to rely entirely on GC- mass spectrometry (GC-MS) to determine these structures.

Ammonia chemical ionization mass spectrometry (NH_3 -CIMS) of the peracetylated or permethylated derivatives of oligosaccharides can be used to provide molecular weight (these derivatives invariably show $[\text{M}+\text{NH}_4]^+$ pseudomolecular ions) and fragmentation information. Unfortunately, the sensitivity of GC-CIMS with ammonia reagent gas is significantly lower than GC-MS with electron impact ionization (unpublished observation). The pseudomolecular ion $[\text{M}+18]^+$ dominates the spectrum of the lower oligosaccharides, so there is little evidence of fragment ions in the spectra of GC-scale sample amounts. Thus, the GC-CIMS experiment yields only molecular weight information, and the fragmentation must be deduced entirely from the GC-EIMS spectra.

One should note that the number of potential structures of the Smith degradation products is limited: by definition, there should be no monosaccharides having a vicinal-diol structure if the periodate oxidation was carried to completion. Thus, rhamnopyranose may only be present as a component of one of the products if it is 1,3-linked; 1,2- and 1,4-linked sugars would have suffered periodate oxidation. A similar analysis on all of the known component monosaccharides of the AK1401 A-PS is shown in Scheme 2, which gives a list of possible components of the oligosaccharides resulting from Smith degradation.

Finally, one may analyse the polymer resulting from periodate oxidation/ borohydride reduction by alditol acetate and methylation analysis to gain further insight into the overall structure.

SCHEME 2



3.4.2 Liquid chromatography of the oligosaccharide acetates
resulting from Smith degradation of the A-PS

The A-PS was degraded as outlined in Scheme 1, and the products were acetylated. TLC of the product mixture on silica (developed in CH_2Cl_2 - CH_3OH (19:1 v/v) showed a major product (oblong spot, $R_f=0.5$), and at least two minor products (sharp spots, $R_f=0.31$, 0.26) contained within a streak from the origin to the top spot. The product mixture was separated into two fractions by column chromatography, one containing the major component, and the other containing both of the minor components.

HPLC analysis of the entire product mixture showed an unresolved doublet ($t_r=5.2$, 5.4 min., approximate ratio 2:1) which, when collected as a single fraction gave only the spot with $R_f=0.5$ on TLC. No evidence of the other components observed by TLC was seen in the HPLC chromatogram, probably because of the insensitivity of the refractive index detection method and the relatively small amount of the minor components.

It should be noted that the above HPLC conditions easily allowed the separation of lactose octaacetate ($t_r=5.6$ min.) from raffinose undecaacetate ($t_r=7.6$ min.). The much shorter difference in retention time between the two peaks observed for the acetates from the Smith-degraded A-PS suggests that they are not oligomers, and the similarity of the retention times to that of lactose octaacetate suggests that they are disaccharides.

3.4.3 Gas chromatography and GC-MS of the oligosaccharide acetates resulting from Smith degradation of the A-PS

GC of the major fraction isolated by column chromatography and of the whole mixture gave the same chromatogram (Figure 14), suggesting that the higher polarity spots were involatile. Note also that this chromatogram clearly shows that the mixture is much more complex than TLC or HPLC had indicated. GC-MS of the whole mixture gave the chromatogram shown in Figure 15a; that obtained using GC-MS- NH_3CI is shown in Figure 15b (note that the chromatographic resolution is not as good as it was in the GC-MS-EI experiment because the column had to be overloaded in order to overcome the relative insensitivity of the GC-CIMS experiment).

Interpretation of the mass spectra of these components is not straight-forward because literature spectra do not exist (based on a search of probable compositions in the Chemical Abstracts Formula index and the EPA/NIH mass spectral data base). However, the principal component seen in the GC (peak B on Figure 15a) shows an intense m/z 696 in the NH_3 -CIMS experiment, suggesting that it has a formula weight of 678; this can be interpreted as the expected major component derived in Scheme 1, thus providing a standard spectrum. Interpretation of the spectrum of this component is facilitated by the presence of a related compound of lower molecular weight (peak X on Figure 15a). The NH_3 -CI spectrum of peak X shows an ion at m/z 466, suggesting that the formula weight is 448. The EI spectrum of peak X is shown in Figure 16, and is interpreted in Scheme 3. All of these assignments are based on analogous fragmentations in monosaccharide peracetates.⁶⁹ Peak X is

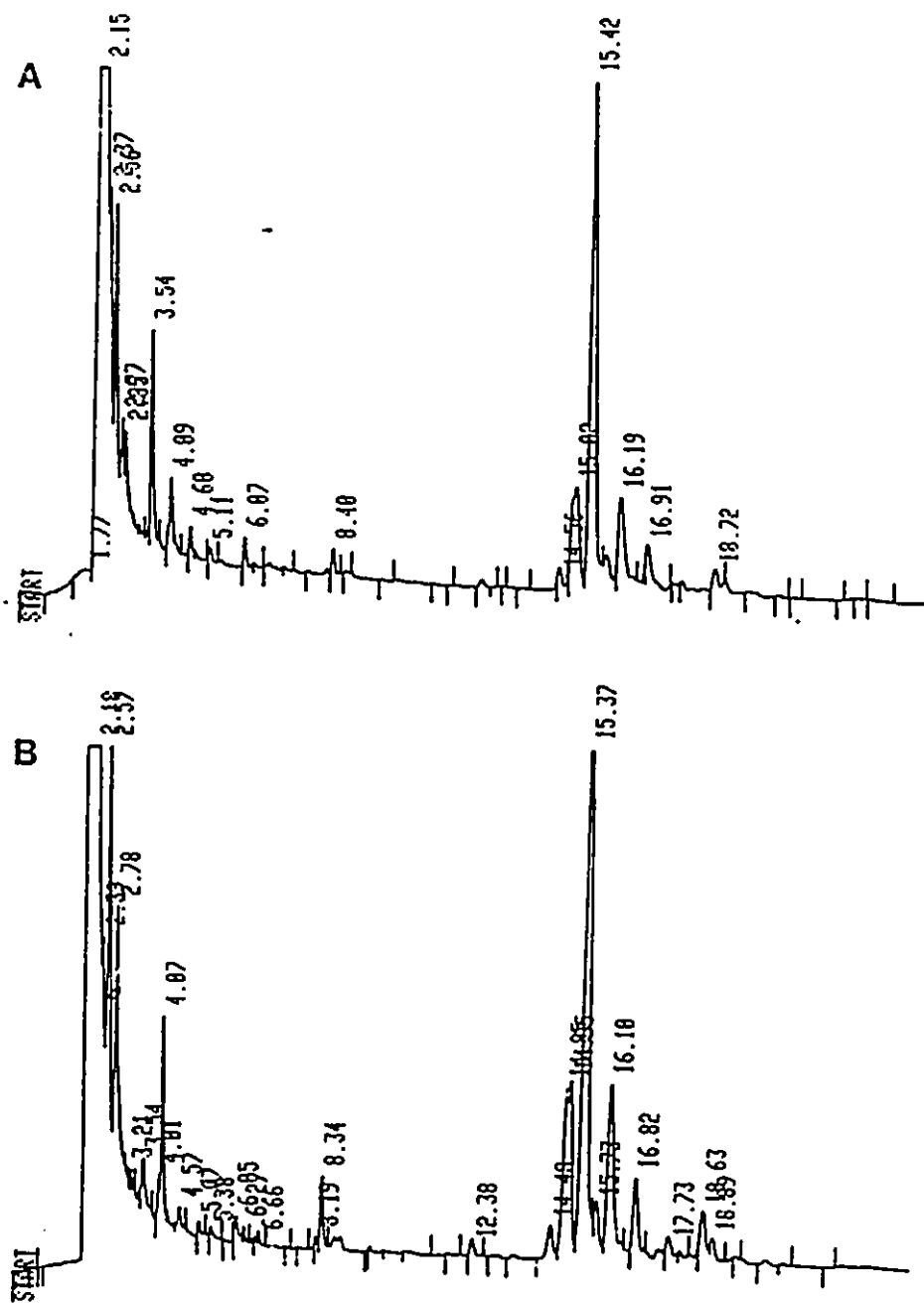


Figure 14: Gas chromatography of oligosaccharide acetates resulting from Smith degradation of the AK1401 A-PS. A) total mixture, and B) fraction isolated by column chromatography ($R_f = 0.5$ on TLC)

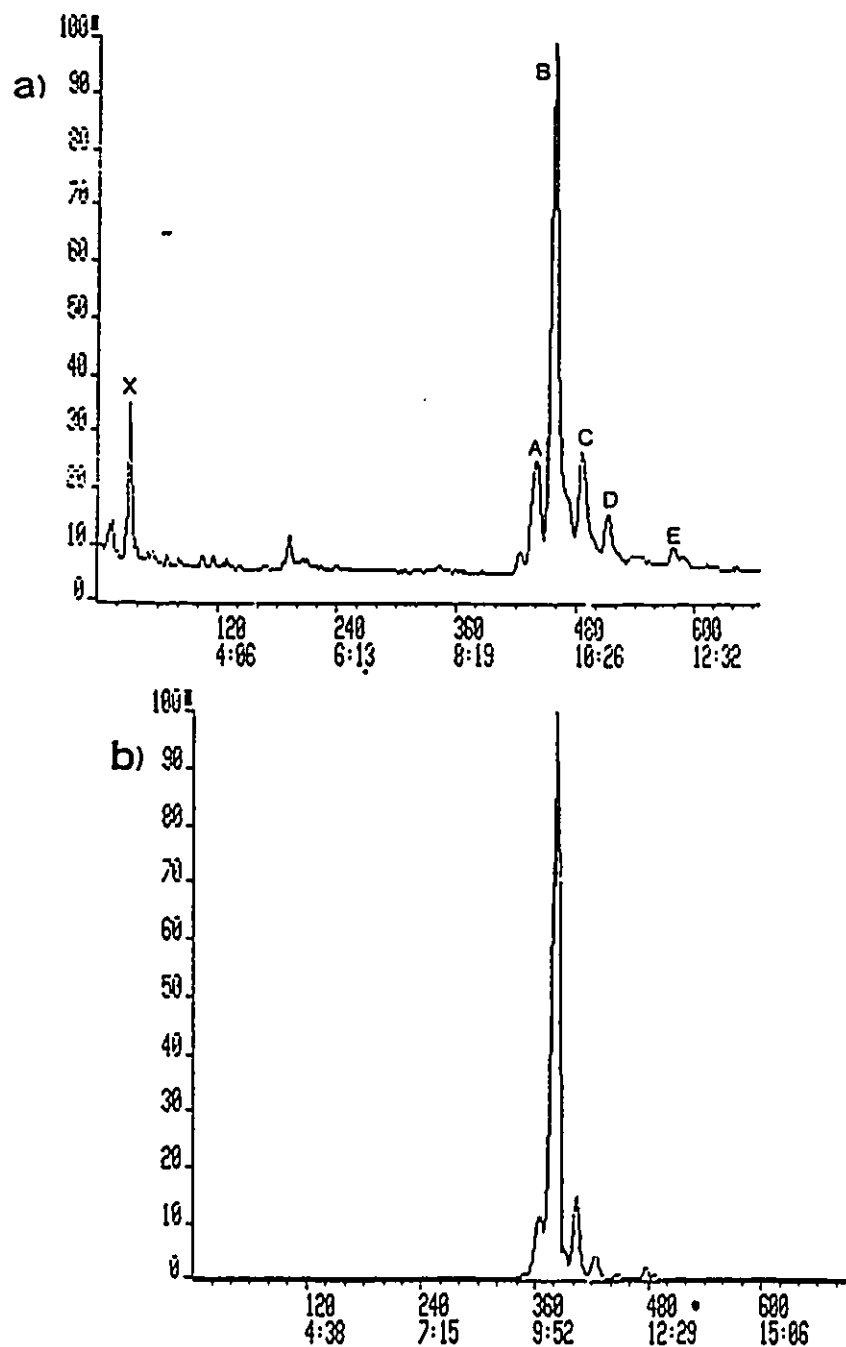


Figure 15: Total ion current chromatograms of oligosaccharide acetates from Smith-degraded AK1401 A-PS. a) electron impact ionization, and b) ammonia chemical ionization experiments

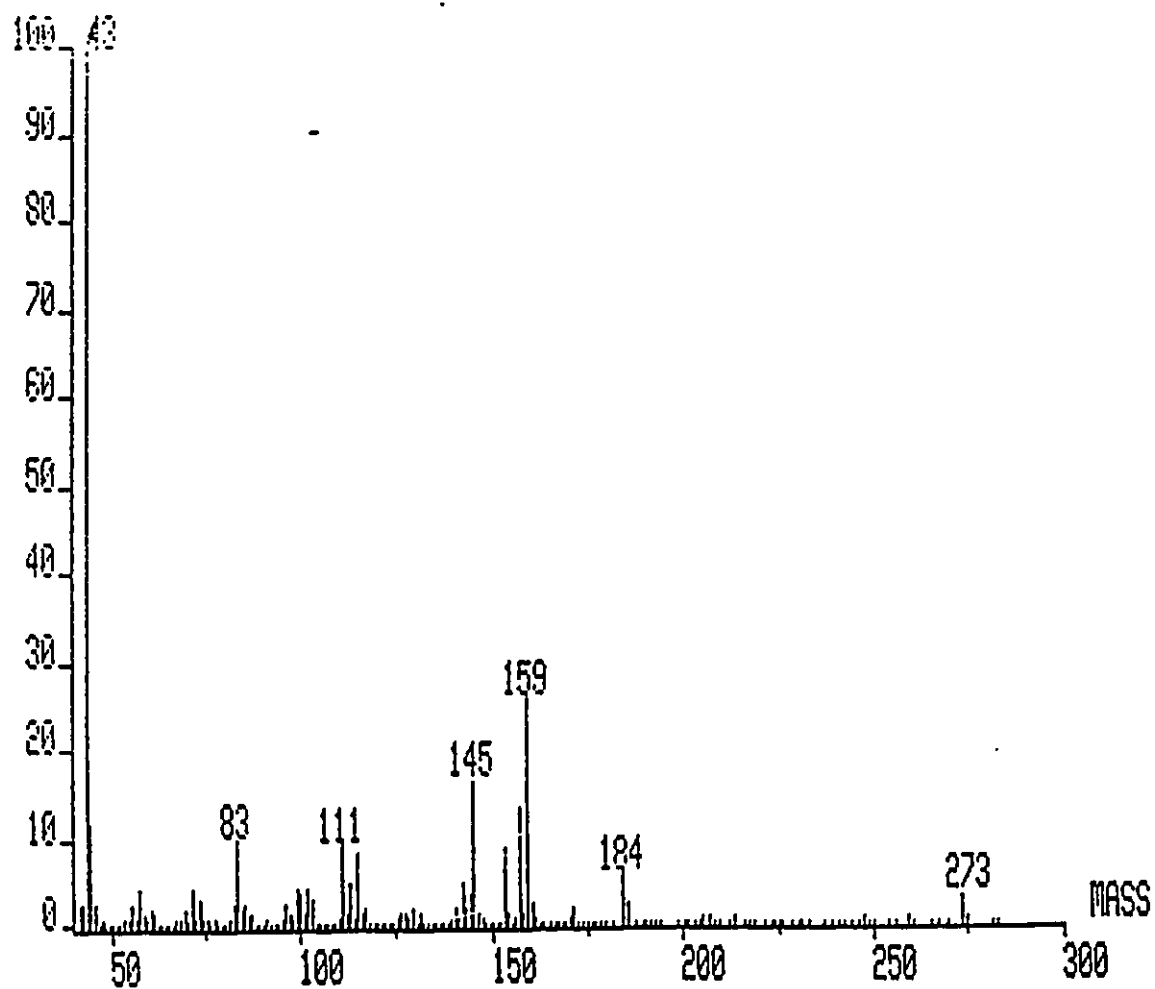
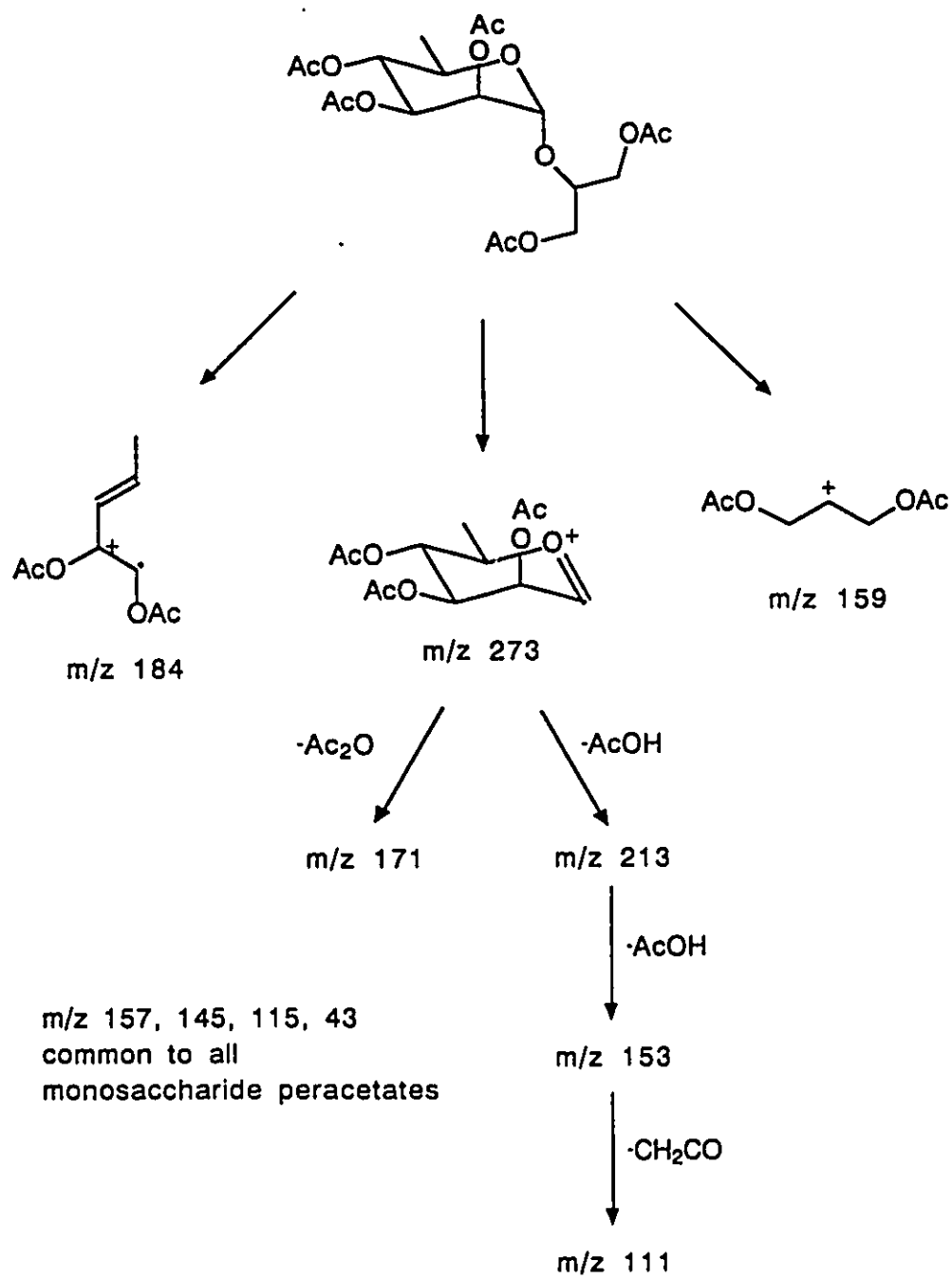
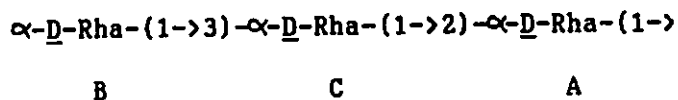


Figure 16: EI mass spectrum of Peak X (molecular weight= 448)
[Rha-(1->2)-Gly-ol (OAc)₅]

SCHEME 3



therefore assigned as Rha-(α 1,2)-Gly-ol (OAc)_s, which can result either from over-hydrolysis of the Smith-degraded PS, or from the non-reducing terminus of the PS if the end sequence is:

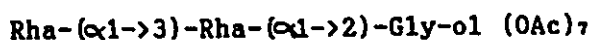


where B is oxidized and lost, C survives intact, and A results in the glycerol portion (A, B, and C are the same designators used in the assignment of the NMR spectrum).

This last possibility is intriguing, especially because there is no evidence of any rhamnose-rhamnitol disaccharide heptaacetate which should also be present if the Smith-degraded PS was over-hydrolysed. If the origin of this component is due only to the non-reducing end, then the ratio of the major component (peak B) to peak X should give an estimate of the degree of polymerization (D.P.) of the A-PS repeating unit. This ratio is approximately 11 \pm 1: 1 from integration of replicate GC-FID chromatograms, indicating an average D.P. of 12 trisaccharide repeats. Note, however, that there is a large uncertainty in this estimate because of the large difference in molecular weights of the two components (448 versus 678), which could give rise to substantially different flame ionization detector response factors: the ratio of peak areas was uncorrected, since the standard materials are unavailable for determination of response factors.

The major component (peak B) shows an ion at m/z 696 in the NH₃-CI spectrum which corresponds to the composition expected for the major

degradation product derived from the repeating unit portion of the PS:



The electron impact spectrum of this component is shown in Figure 17, and is interpreted in Scheme 4. The ion at m/z 273 is prominent in this component, as are its daughter ions, thus indicating that rhamnose is the terminal monosaccharide; the ion at m/z 159 is again indicative of the presence of the glycerol portion. The presence of m/z 503 shows that this compound contains a rhamnose-rhamnose disaccharide moiety, which, when coupled with the glycerol component gives the expected composition. The ion at m/z 259 is assigned in analogy to the fragment ion described by Peltier *et al.*⁷⁰ The ion at m/z 477 is analogous to an ion in the spectrum of N-arylglycosylamine disaccharide peracetates⁷¹, disaccharide peracetates^{72,73}, and permethylated disaccharides.^{74,75} The ion at m/z 415 could not be assigned with certainty. Note that m/z 259 and 477 result from decomposition of the ring at the "non-reducing" terminus (hereafter called the A ring, as opposed to the ring at the "reducing" terminus (hereafter called the B ring)). Therefore, if the two sugars in a disaccharide have different masses, these ions can be used to determine the sequence of residues.

Given the assignments of the EI spectra of Rha-Gly-ol (OAc)₅ and of Rha-Rha-Gly-ol (OAc)₇, an attempt has been made to assign the spectra of the other components observed in Figure 15a. The most straightforward of these is peak D (see spectrum, Figure 18), which has m/z 159 (glycerol), and an intense m/z 259, but no m/z 273; this suggests that the terminal residue is not rhamnose, and that the ion at 259 amu arises

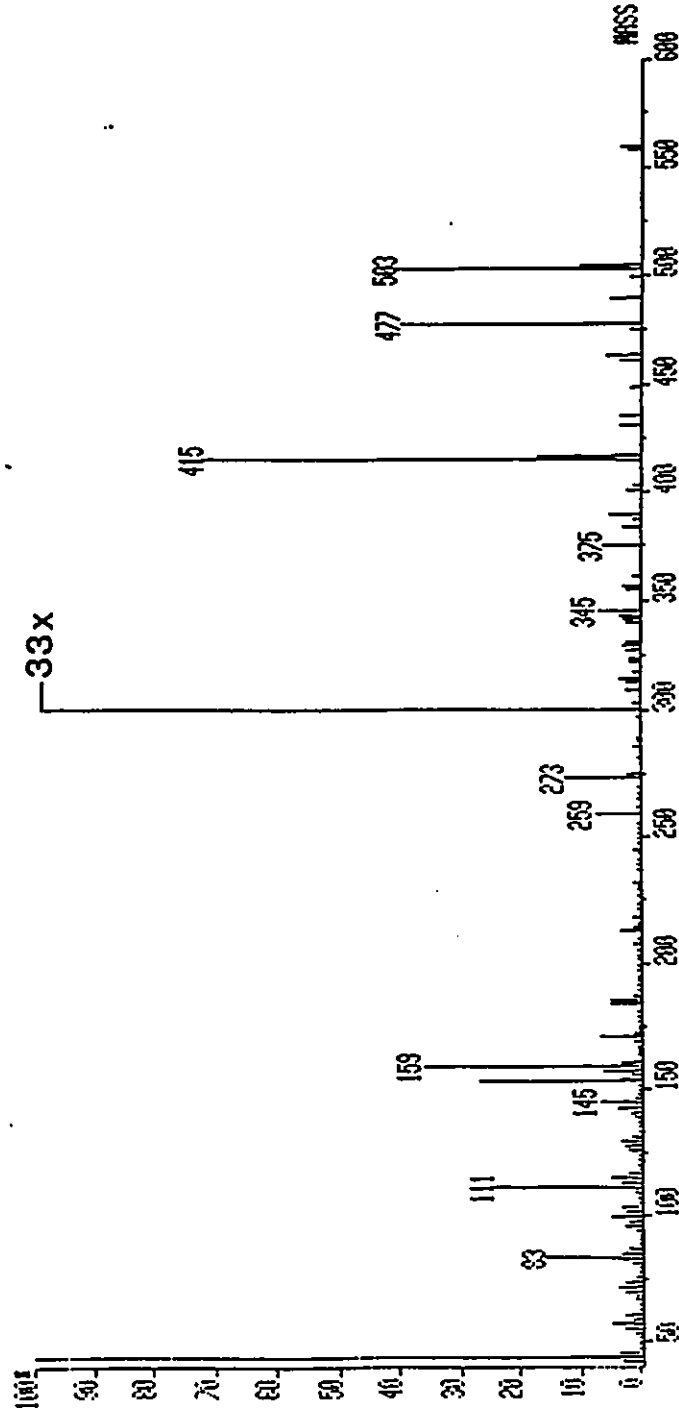
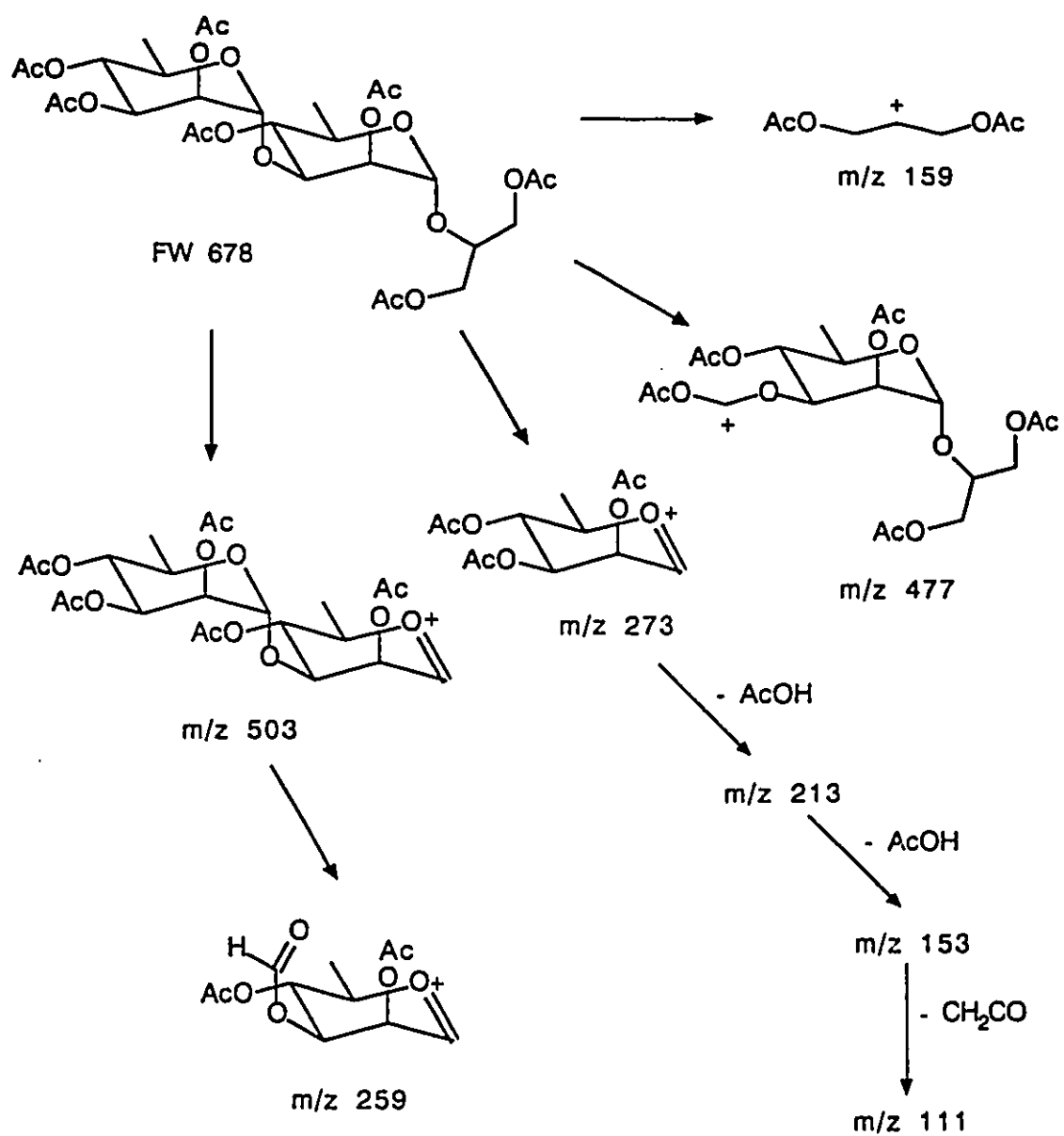


Figure 17: EI mass spectrum of Peak B (molecular weight= 678)
[Rha-(1->3)-Rha-(1->2)-Gly-ol (OAc)₇]

SCHEME 4



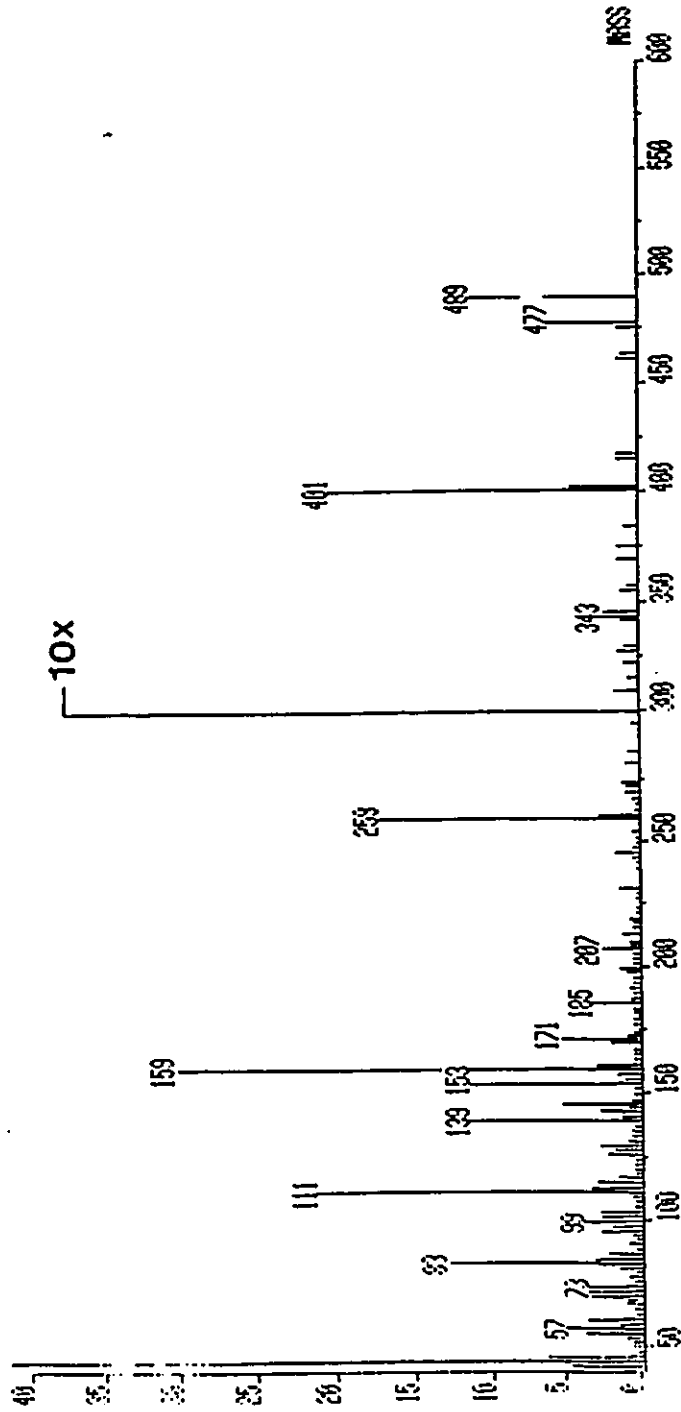
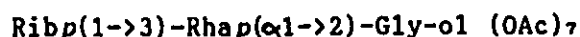


Figure 18: EI mass spectrum of Peak D (molecular weight= 664)
 [Rib-(1->3)-Rha-(1->2)-Gly-ol (OAc)]₇

from a different (additional) route from that accounted for in the major component. The analogous ion to m/z 273 for a pentoside is m/z 259, so the terminal residue might be ribose; this is confirmed by the shifting of the disaccharide oxonium ion from m/z 503 to m/z 489. Note that the unknown ion at m/z 415 in peak B is absent, but is replaced by an ion at m/z 401, which also corresponds to replacement of a rhamnose by ribose. The mass of the disaccharide oxonium ion (m/z 489) suggests that the other monosaccharide is rhamnose, and this is confirmed by the presence of the A ring fragmentation ion at m/z 477 (same mass as in the major component); the other A ring fragmentation ion is still m/z 259, but this can now arise by an additional route, and therefore is more intense than in the spectrum of the major component. The EI data suggest the composition of component D is Rib-Rha-Gly-ol (OAc)₇ (FW= 664), and this is confirmed by the observation of m/z 682 ($M+18^+$) in the NH_3 -CI spectrum.

A more specific structure can be assigned to component D if one considers the possibility of different ring sizes. If the ribose was present as the furanoside, one would expect fragmentation of the molecular ion at C4-C5 of the pentofuranoside to give m/z 591 ($M-CH_2OAc$) and m/z 73 (CH_2OAc^+). Since neither of these fragments is present, component D probably contains a ribopyranoside. From an analysis of possible linkages, a ribopyranoside would only survive Smith degradation if it was 1,3-linked or branched in the PS; similarly, the rhamnose residue in this component must be 1,3-linked. Thus, the structure of component D can be defined as:



where only the absolute configuration of ribose, and the stereochemistry of the ribose-rhamnose linkage are uncertain. This proposed structure is consistent with the EI and CI mass spectra of this component, but the structure could only be proved by examination of the GC retention time and mass spectrum of the proper synthetic standard.

The EI spectra of the other components are not so easily assigned, unfortunately. Components A and C both have an ion of m/z 682 in their NH_3 -CI spectra, suggesting that they have the same formula weight as component D. The EI mass spectrum of component A, however, lacks an ion at m/z 159, implying that glycerol was not present. It was originally thought that a 1,1-linked glycerol might be present instead, but the intensity of m/z 159 is approximately the same in the EI spectra of β -D-Gal-(1,4)- β -D-Glc-(1,2)-Gly-ol (OAc)₉ and of β -D-Gal-(1,4)- β -D-Glc-(1,1)-Gly-ol (OAc)₉ (samples kindly provided by W.A. Szarek, Queen's University, Kingston); presumably this occurs because the 1° glycerol cation can quickly rearrange to the highly stabilized 2° cation.

The EI mass spectrum of component A (Figure 19) has a very intense m/z 145 ion ; this ion is present in the spectra of all carbohydrate acetates at low abundance, but an additional fragmentation to give a highly stabilized ion must occur in this case. Ions in the spectrum which can easily be assigned are: m/z 273, 213, 153 and 111 (oxonium ion of terminal rhamnose unit and its daughter ions); m/z 503 (oxonium ion of rhamnose-rhamnose disaccharide); m/z 415 (unknown structure, but the same mass as in the rhamnose-rhamnose disaccharide); and m/z 259 (ring A fragmentation ion). Note that the other ring A fragmentation ion is shifted by 14 amu less to m/z 463; since this is

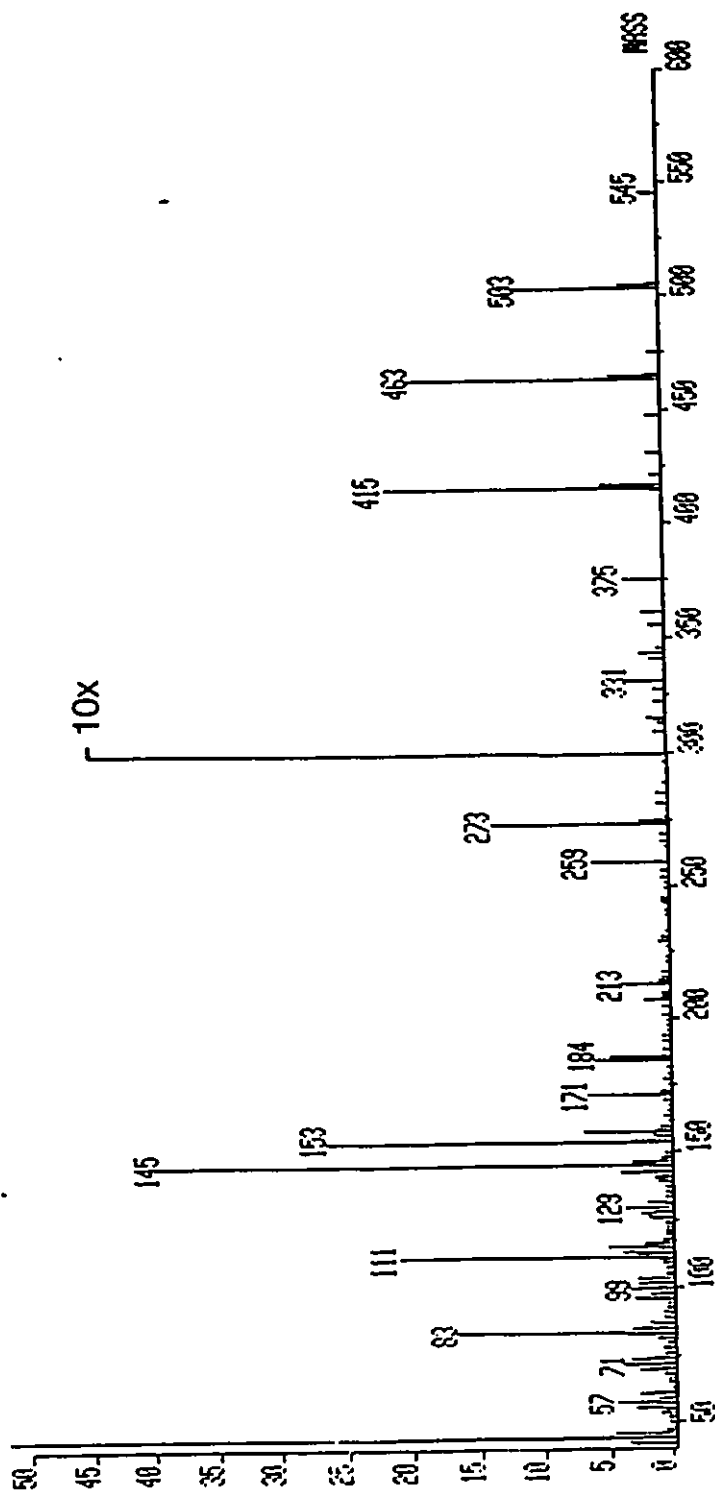
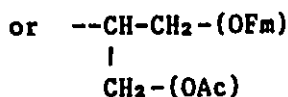
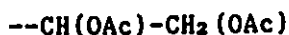


Figure 19: EI mass spectrum of Peak A (molecular weight = 664)

the only ion in Scheme 4 which contains the aglycone (glycerol in component B and D), and since the above data indicate a rhamnose-rhamnose disaccharide, and furthermore since the formula weight is 14 amu less than that of component B, the probable composition of component A is Rha-Rha-OR, where R has a mass of 14 amu less than glycerol diacetate.

R may thus be:



Although a partial structure can be assigned for component A, the origin of such a degradation product is not obvious.

The EIMS of component C (Figure 20), on the other hand, does have an ion of m/z 159, so glycerol is a constituent. NH_3 -CIMS shows a pseudomolecular ion at m/z 682, and EIMS shows a disaccharide oxonium ion at m/z 489, so Rib-Rha-Gly-ol is a possible composition (same as component D). However, the EI spectrum does not give a clear indication of the structure: both m/z 259 and 273 are present, so the identity of the terminal monosaccharide is in doubt. Similarly, both m/z 477 and 463 are present, so the identity of the monosaccharide joined to glycerol is in doubt as well. Furthermore, m/z 415, which would result from a rhamnose-rhamnose disaccharide, is present along with the ion expected for the composition Rib-Rha-Gly-ol (m/z 401). Thus, no conclusions can be drawn regarding the structure of this component; it is possible that peak C represents a coelution of more than one

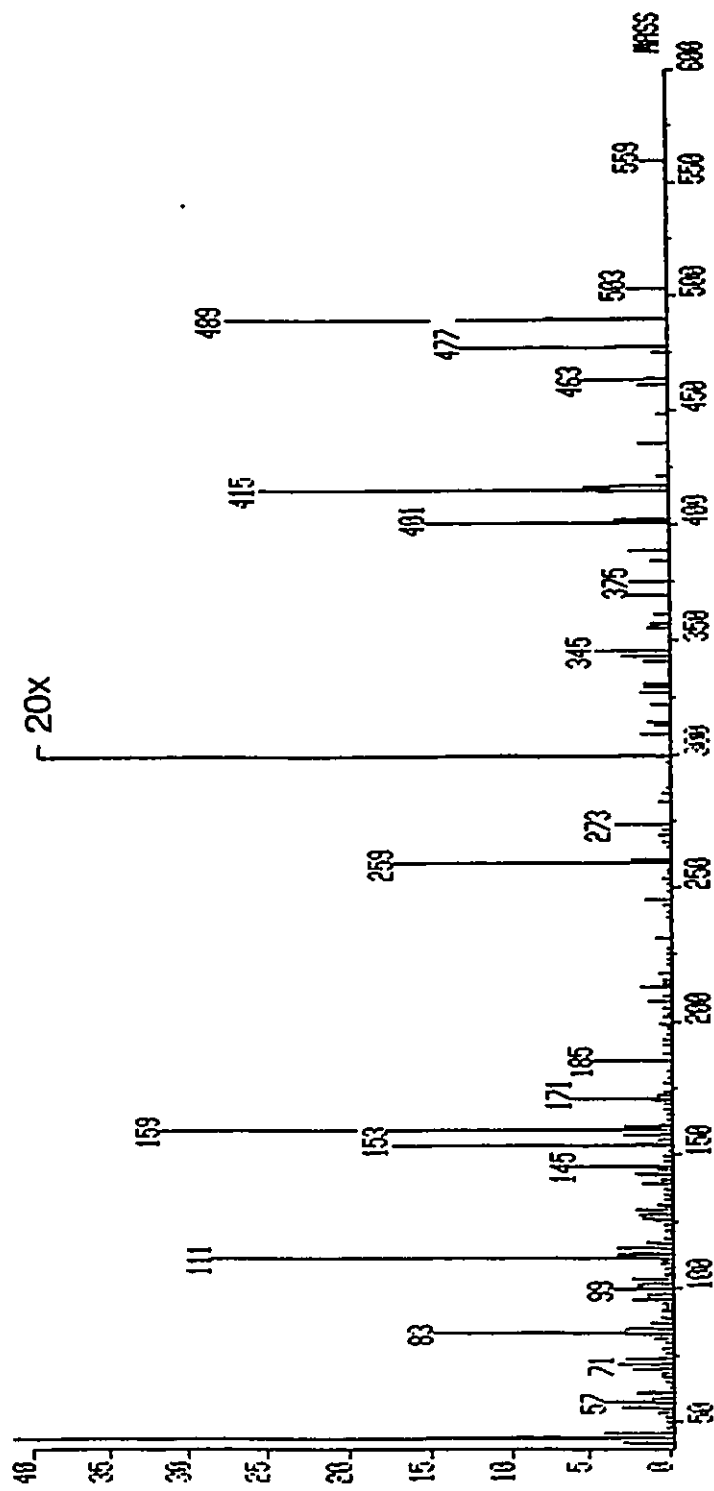


Figure 20: EI mass spectrum of Peak C (molecular weight= 664)

compound.

Peak E, although a very minor component of the mixture, is quite interesting; by $\text{NH}_3\text{-CI}$ its formula weight is 692 (14 amu more than component B). The EI spectrum (Figure 21) shows no m/z 159 (no glycerol), and contains ions indicative of a rhamnose-rhamnose disaccharide moiety (m/z 503, 415, 273, 259, 153, 111). The aglycone must therefore have the extra 14 amu, however, this cannot be verified by the EI spectrum because the aglycone-containing ion (m/z 477 in component B) is absent (no m/z 477 nor 491). What can be noticed readily, though, is the appearance of new ions at m/z 101 and 87; these ions cannot be assigned, but m/z 87 could be $[\text{CH}(\text{OAc})\text{-CH}_3]^+$, which would suggest the presence of either a rhamnofuranoside or 1,2,3-trihydroxybutane as the aglycone. This latter possibility would imply a very small amount of 1,4-linked rhamnose in the PS. However, this aglycone cannot be confirmed from the spectrum, since the A ring fragmentation ion should be observed at m/z 491, and one would expect an intense ion at m/z 173 with a similar stabilization to that seen for m/z 159 from glycerol. Thus the identity of component E is also not clear.

The deduced structures of the various oligosaccharide acetates from the Smith-degraded A-PS are summarized in Table 6.

3.4.4 Alditol acetate analysis of the product of periodate oxidation and borohydride reduction of the A-PS

In this experiment, the dialdehydes resulting from the periodate oxidation of the AK1401 A-PS were reduced with sodium borohydride, and the polymer was subjected to complete hydrolysis. The mixture of

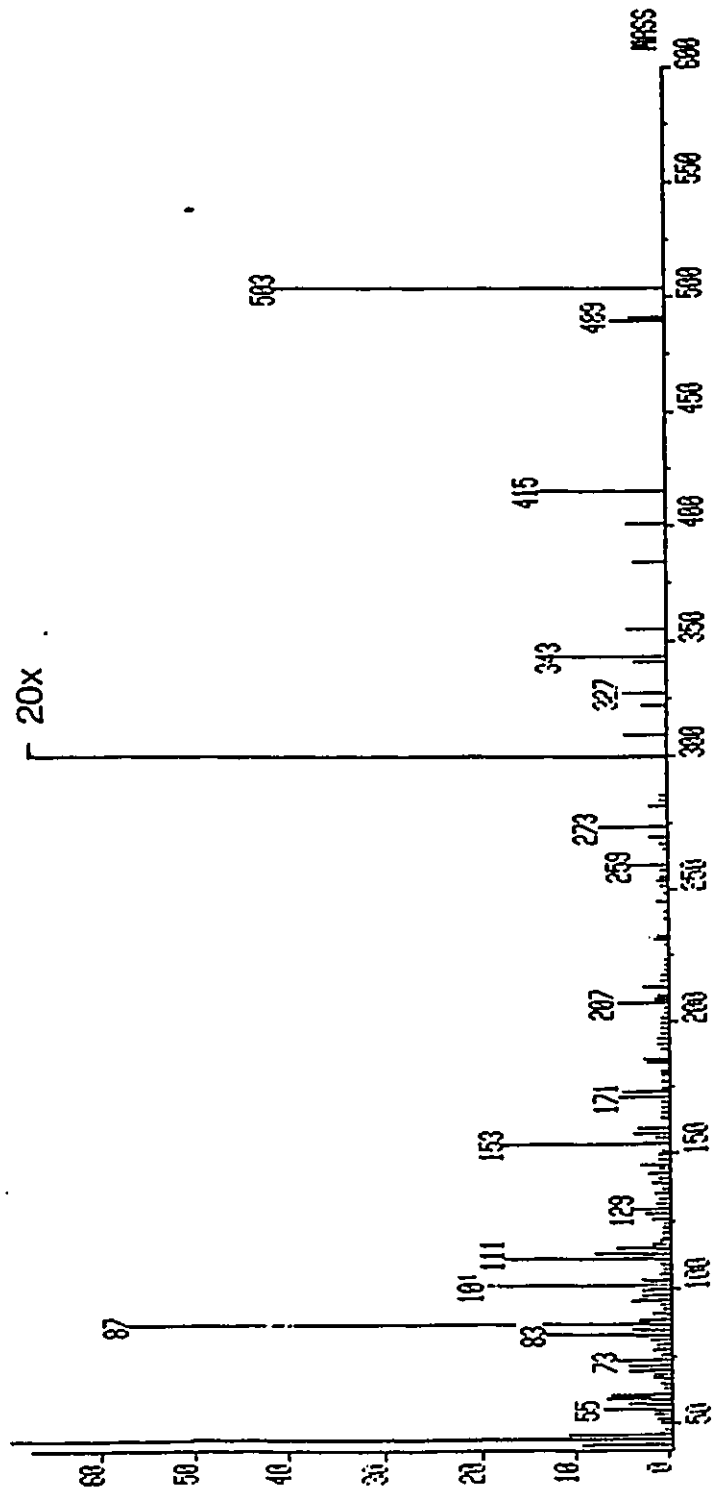
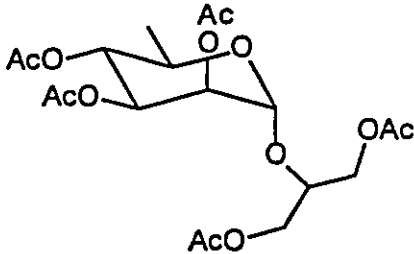
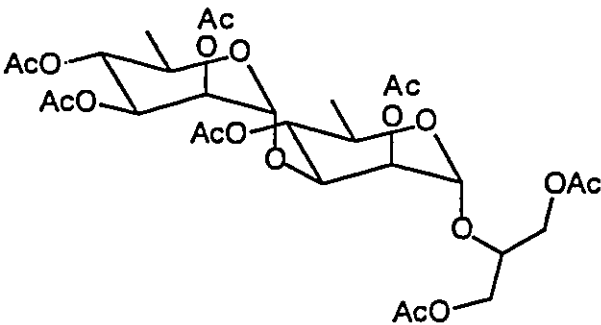
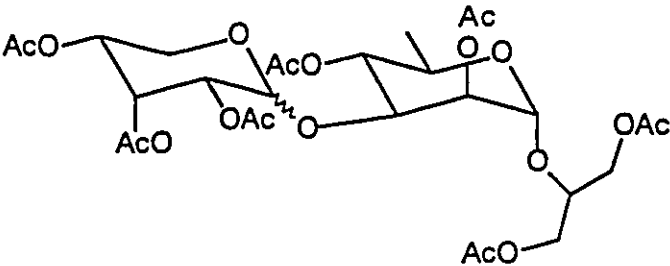


Figure 21: EI mass spectrum of Peak E (molecular weight = 692)

Table 6: Structures of oligosaccharide acetates resulting from Smith degradation of the AK1401 A-PS

COMPONENT	FW	STRUCTURE
X	448	
A	664	RHA-RHA-OR, R= 145 amu
B	678	
C	664	MORE THAN ONE COMPOUND ?
D	664	
E	692	RHA-RHA-OR, R= 173 amu

monosaccharides was then reduced with sodium borodeuteride so that each component containing deuterium represented a portion of the periodate oxidized polymer which had an anomeric carbon. The results (Table 7 and spectra in Appendix 1) show that rhamnose, 3-O-methyl rhamnose, ribose, and trace amounts of 2- and 3-O-methyl hexoses are the only aldoses which survive periodate oxidation. Hexitol-d₁ hexaacetates were absent in this analysis, indicating that the glucose and mannose were completely oxidized to erythritol, as was expected from the 1,4-hexopyranose linkages found by methylation analysis. The absence of these components verifies that the periodate oxidation reaction went to completion.

It should be noted that no trace of 1,2-propanediol diacetate (anticipated product from carbons 4, 5, and 6 of 1,2-linked rhamnopyranose) nor of ethylene glycol diacetate (from 1,4-linked hexopyranoses, see Scheme 2) was found in this analysis. This is most likely due to loss by evaporation, as there is also less glycerol triacetate than would have been expected, that is, 1 mole for every 2 moles of rhamnose. The relative intensities presented in Table 7 should therefore be interpreted with caution.

An interesting note here is that glycerol is present both with and without deuterium. The glycerol-d₁ represents glyceraldehyde in the periodate oxidized polymer which is derived from carbons 1, 2, and 3 of 1,2-linked rhamnopyranoses, but the glycerol which does not contain deuterium is not easily explained. Although a terminal hexopyranose (Scheme 2) would give undeuterated glycerol from carbons 4, 5, and 6, the amount of terminal hexopyranose is insufficient to account for all

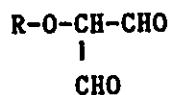
Table 7: Alditol acetates from the polymer remaining after periodate Oxidation and borohydride reduction of the AK1401 A-PS

Retention time (min) ⁽¹⁾	Identity	Relative intensity ⁽²⁾
6.81	glycerol <i>and</i> glycerol-d ₁ triacetate	5
7.90	erythritol tetraacetate	16
8.65	3-O-methyl rhamnitol-d ₁ tetraacetate	13
8.79	rhamnitol-d ₁ pentaacetate	100
8.86	ribitol-d ₁ pentaacetate	35
9.68	2-O-methyl hexitol-d ₁ pentaacetate	<5
9.89	3-O-methyl hexitol-d ₁ pentaacetate	<5

(1) GC-MS conditions: 30 metre DB-1701, 1 min. at 40°C, 40° per minute to 280°C, hold.

(2) From the integrated total ion current chromatogram of a single chromatographic run; the values therefore have a large uncertainty.

of this product. It is possible that some hydrolysis of the oxidized residues occurs in the oxidation reaction mixture, resulting in oligosaccharides having the following reducing end group:



If this occurs, the borohydride reduction step prior to the mild acid hydrolysis step could then produce undeuterated glycerol end groups.

3.4.5 Methylation analysis of the polymer remaining after periodate oxidation and borohydride reduction of the A-PS

The result of the previous experiment is useful because it defines what types of monosaccharides may be components of the oligosaccharides which result from Smith degradation. In an attempt to further define the monosaccharide types that are present in these oligosaccharides, the periodate oxidized/ borohydride reduced polymer was subjected to methylation analysis. The results of this experiment are listed in Table 8. The mass spectra of the components are in Appendix 1.

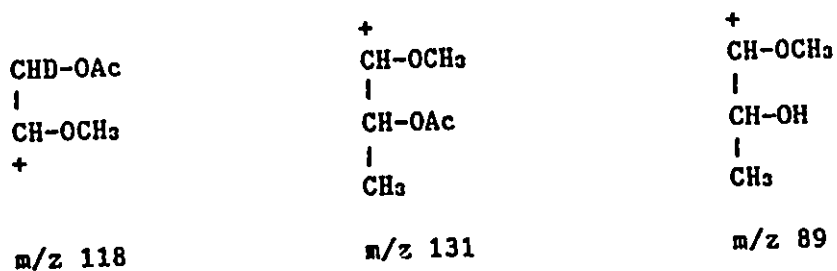
There are many unidentified components in the mixture. The putative PMAA derivatives of glycerol and erythritol (which are known components of the periodate oxidized/ borohydride reduced polymer, see Table 7) could not be positively identified because standard mass spectra of these derivatives are unavailable. As well, the components with retention times of 14.72 and 16.62 minutes could not be identified by computer search of the Wiley library, nor by inspection of the spectra. The spectra show some features which could be ascribed to

Table 8: Partially methylated alditol acetates from the polymer remaining after periodate oxidation and borohydride reduction of the A-PS

Retention time (min) ⁽¹⁾	Identity	Origin
12.00	a PMAA derivative of glycerol ? (di- O-methyl ?)	----
13.37	a PMAA derivative of glycerol ? (1- or 2-O-methyl ?)	----
14.45	glycerol triacetate	----
14.65	a PMAA derivative of erythritol ?	----
14.72	Unknown	----
16.62	Unknown	----
18.17	1,5-di-O-acetyl-2,3,4-tri-O-methyl rhamnitol-d ₁	term. Rhap
19.69	Unknown PMAA derivative ?	----
20.68	1,4,5-tri-O-acetyl-2,3-di-O-methyl rhamnitol-d ₁	1,4- 3-O-MeRhap ²
20.88	1,3,5-tri-O-acetyl-2,4-di-O-methyl rhamnitol-d ₁	1,3- Rhap
22.85	1,3,4,5-tetra-O-acetyl-2-O-methyl rhamnitol-d ₁	1,3,4- Rhap ⁽³⁾
23.38	1,2,3,5-tetra-O-acetyl-4-O-methyl rhamnitol-d ₁	1,2,3- Rhap ⁽³⁾
24.95	rhamnitol-d ₁ pentaacetate	----
25.30	1,4,5-tri-O-acetyl-2,3,6-tri-O-methyl hexitol-d ₁	1,4- 3-O-MeHexp
26.04	1,4,5-tri-O-acetyl-2,3,6-tri-O-methyl hexitol-d ₁	1,4- 3-O-MeHexp

- (1) GC-MS conditions: DB-1701 30 metre narrow bore, 1 min. at 50°C, 10°C to 200°C, hold.
- (2) Must be derived from 2- or 3-O-methyl rhamnose in order to survive periodate oxidation (see text).
- (3) These PMAA's could represent the indicated branch points, but they may also be the result of undermethylation of 1,3-linked rhamnopyranose (the major monosaccharide type in this sample). This latter possibility seems very likely, as there is also a small amount of rhamnitol-d₁ pentaacetate, which would result from a complete lack of methylation.

partially-methylated partially-acetylated pentosides, but definitive structures could not be assigned. A GC-MS NH_3 -CI experiment might be able to provide the molecular weights of these components, which could assist in the interpretation of the EI spectra, but this experiment was not attempted. Finally, the component at 19.69 minutes appears to be a PMAA derivative because of the presence of ions at m/z 118, 131, and 89, which may be formulated as:



These ions suggest that the component is a PMAA derivative of a deoxy-sugar (which must be rhamnose, given the composition analysis). Since the retention time of this component is between a di-*O*-acetyl-tri-*O*-methyl rhamnitol (18.17 min.) and the tri-*O*-acetyl-di-*O*-methyl rhamnitol (20.68 and 20.88 min.), it is reasonable to assume that the component is related to these compounds. If one considers the fragments above to be derived from C1 and C2 (m/z 118), and from C4, C5 and C6 (m/z 131 and 89), one can generate two possible structures by considering C3 to be either CH-OCH₃ or CH-OAc: however, the observed spectrum is a poor match for both possibilities, and both possible rhamnitol derivatives are already present elsewhere in the chromatogram. Thus, the identity of the the component with a retention time of 19.69 min. remains unknown.

Derivatives of ribose were absent in this analysis, as they were in the methylation analysis of the intact AK1401 A-PS (section 3.2.3).

Possible reasons for the absence of ribose derivatives have been presented already in section 3.2.3.

Comparison of the PMAA's that were identified in this analysis to those found by methylation analysis of the intact A-PS (Table 2) shows several interesting features. Firstly, the absence of the PMAA derived from 1,2-linked rhamnopyranose in the periodate oxidized polymer indicates that the periodate oxidation reaction went to completion. Secondly, the PMAA derived from 1,4-linked rhamnopyranose is still present in essentially the same relative amount (see Figure 22), even though 1,4-linked rhamnopyranose should not survive periodate oxidation since it has a 2,3-glycol. However, if either the 2 or 3 position (or both) has a naturally occurring *O*-methyl group, the monosaccharide would be periodate-resistant, and would still give the same PMAA (*i.e.*, 1,4,5-tri-*O*-acetyl-2,3-di-*O*-methylrhamnitol- d_1). Since 3-*O*-methyl rhamnose is a known constituent of the AK1401 A-PS, one can infer that this PMAA is derived from 1,4-linked 3-*O*-methyl rhamnopyranose. The ratio of this component to that derived from 1,3-linked rhamnopyranose is 22.1 to 100 before periodate oxidation and 19.4 to 100 after periodate oxidation. These values are based on the integration of the total ion current chromatograms of a single run, and thus have low precision, so one cannot tell whether or not there is a significant difference in the amount of 1,4,5-tri-*O*-acetyl-2,3-di-*O*-methylrhamnitol- d_1 after periodate oxidation. Thus, the possibility that a very small amount of 1,4-linked rhamnopyranose is present cannot be ruled out, but the result presented in Figure 22 suggests that the 1,4,5-tri-*O*-acetyl-2,3-di-*O*-methyl rhamnitol- d_1 found in the methylation analysis of the intact A-PS is

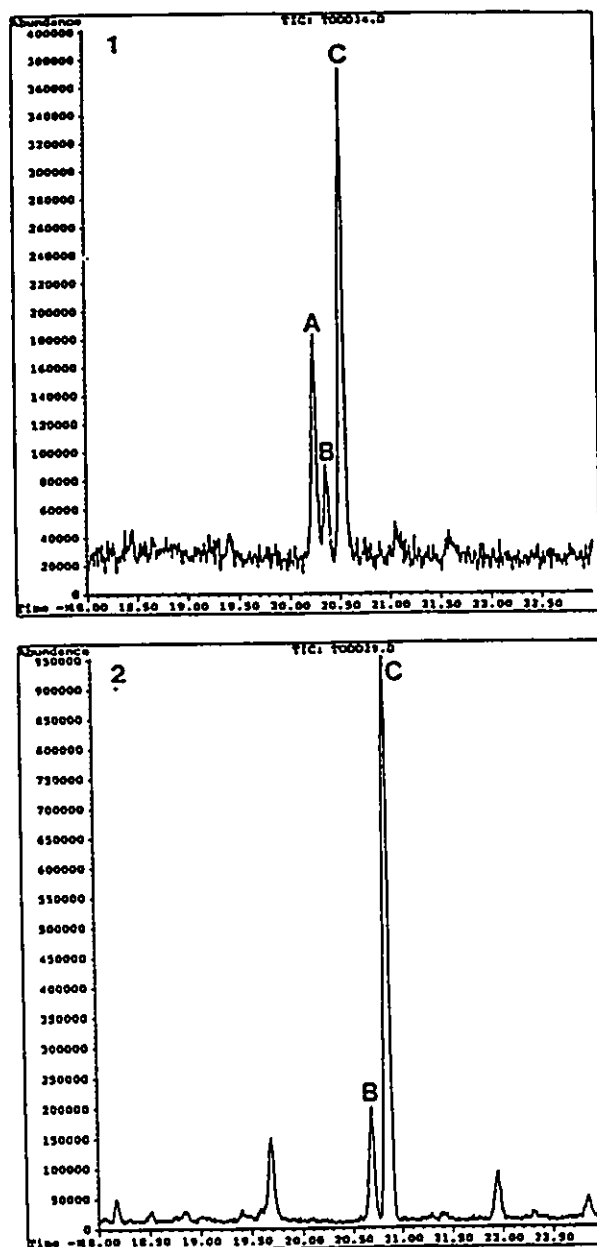


Figure 22: Portion of total ion current chromatograms showing PMAA derivatives from 1) AK1401 A-PS, and 2) periodate oxidized/borohydride reduced A-PS. The ratio of A:B:C is 52.1 :22.1 :100 in (1), and 0 :19.4 :100 in (2)

- A 1,2,5 tri-*O*-acetyl-3,4-di-*O*-methylrhamnitol-d, (from 1,2-Rha)
- B 1,4,5 tri-*O*-acetyl-2,3-di-*O*-methylrhamnitol-d, (from 1,4-Rha)
- C 1,3,5 tri-*O*-acetyl-2,4-di-*O*-methylrhamnitol-d, (from 1,3-Rha)

mostly (if not entirely) derived from 1,4-linked 3-*O*-methyl-rhamnopyranose.

One should note that similar reasoning suggests that the two 1,4,5-tri-*O*-acetyl-2,3,6-tri-*O*-methylhexitol-d₁'s found in the periodate oxidized polymer must be derived from 1,4-linked 2- or 3-*O*-methylhexoses, since 1,4-linked hexopyranoses should not survive periodate oxidation.

Finally, potential branch point PMAA's (components at 22.85 and 23.38 min) were detected in very small amounts, but these cannot be distinguished from undermethylation of 1,3-linked rhamnopyranose residues.

3.4.6 Summary of the experiments on Smith degradation

The polymer remaining after periodate oxidation and borohydride reduction of the A-PS was found to contain glyceraldehyde, glycerol, erythritol, 3-*O*-methylrhamnose, rhamnose, ribose, 2-*O*-methylhexose, and 3-*O*-methylhexose. Methylation analysis of this polymer revealed a 1,4-linked 3-*O*-methylrhamnose, 1,3-linked rhamnose, a small amount of terminal rhamnopyranose, and two 1,4-linked 3-*O*-methylhexoses. PMAA derivatives of glycerol, erythritol and ribose could not be positively identified.

When the periodate oxidized/ borohydride reduced A-PS was hydrolyzed under mild acid conditions, a mixture of oligosaccharides resulted which was derivatized and analyzed by TLC, HPLC, GC, and GC-MS. GC-MS revealed several components in addition to the major one that was predicted based on the repeating unit structure derived earlier. The

deduced structures of the oligosaccharide acetates resulting from Smith degradation of the A-PS are shown in Table 6. The identified components confirm the repeating unit structure, suggest a possible non-reducing end sequence, and give some indication of the way in which ribose is incorporated into the A-PS.

3.4.7 Attempts to analyse the involatile oligosaccharide acetates resulting from Smith degradation of AK14C1 A-PS

The total mixture of oligosaccharide acetates derived from the Smith-degraded A-PS contained a major and two minor fractions when analysed by TLC (section 3.4.2). The components observed in the GC analysis (section 3.4.3) were all contained within the major TLC fraction. In an attempt to study the minor components, they were isolated (as a single fraction) by liquid chromatography and analysed by mass spectrometry using Direct Chemical Ionization with ammonia reagent gas (NH_3 -DCI-MS). The DCI method involves coating the sample on a platinum wire probe which is inserted directly into the ion volume of the mass spectrometer ion source and rapidly heated to desorb the sample.⁷⁶ Since the sample does not have to travel far off the probe in order to be ionized, molecules may be desorbed into the ion source with a minimum of thermal energy input. Furthermore, since the probe can be so rapidly heated that the sample does not stay resident long enough to decompose, one may study molecules that are too involatile to be introduced by a conventional solids probe.

The involatile oligosaccharide acetates derived from the Smith-degraded A-PS showed a weak ion current at about 1600 amu in the NH_3 -DCI

mass spectrum. In order to improve the signal to noise ratio, a multi-channel analyser was used over a narrow mass range (m/z 1700 to m/z 1200). The mass spectrometer was tuned to about 1800 resolution and calibrated using Fomblin-Y in the absence of ammonia reagent gas. However, upon introduction of the reagent gas, the resolution was found to decrease well below nominal mass resolution (Figure 23a), so that isotope peaks were unresolved. This presumably results because the tuning characteristics of the ion source are considerably different in the presence and absence of reagent gas. In order to circumvent this problem, the mass spectrometer was retuned to greater than nominal mass resolution in the presence of reagent gas by using a standard mixture of malto-oligosaccharide acetates (the calibrant, Fomblin-Y, could not be used for this purpose because it is not ionized by the NH_3 plasma). This retuning introduces a calibration error which can be corrected by acquiring the NH_3 -DCI spectrum of the malto-oligosaccharide acetates and determining the difference between the observed masses and the calculated masses of the pseudomolecular ions listed in Table 9. The malto-oligosaccharide acetates were not used directly as a calibrant mixture because the NH_3 -DCI spectrum has too few ions to be useful for this purpose. Figure 23b shows the improvement in the NH_3 -DCI spectrum after retuning in the presence of reagent gas.

The high mass region of the NH_3 -DCI spectrum of the involatile oligosaccharide acetates derived from the Smith-degraded A-PS is shown in Figure 24. This spectrum may be interpreted as the $[\text{M} + \text{NH}_4]^+$ pseudomolecular ions of two species of molecular weights 1560 and 1546, and ions corresponding to losses of ketene ($\text{C}_2\text{H}_2\text{O}$, 42 amu) from each.

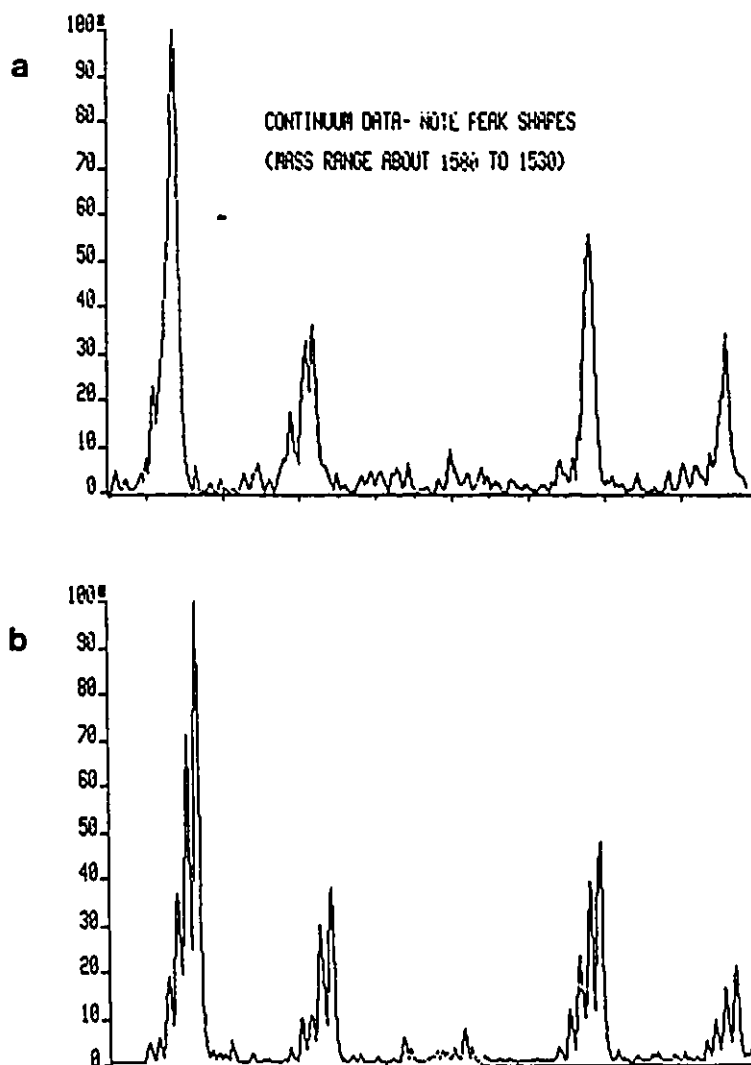


Figure 23: 1600 amu mass region of the NH_3 -DCI mass spectrum (time data only, non-centroided, non-mass converted) of the involatile oligosaccharide acetates from the Smith-degraded A-PS. a) spectrum without retuning in the presence of reagent gas; b) with retuning.

Table 9: Calculated masses of (M + NH₄)⁺ pseudomolecular ions of malto-oligosaccharide acetates

Oligomer ⁽¹⁾	Formula	Mass	M+1 rel. abund. (%)
M2	C ₂₈ H ₄₂ O ₁₉ N ₁	696.235	31
M3	C ₄₀ H ₅₈ O ₂₇ N ₁	984.320	44
M4	C ₅₂ H ₇₄ O ₃₅ N ₁	1272.404	57
M5	C ₆₄ H ₉₀ O ₄₃ N ₁	1560.489	70
M6	C ₇₆ H ₁₀₆ O ₅₁ N ₁	1848.573	84

(1) M2 refers to Maltose peracetate, M3 to Maltotriose peracetate, etc.

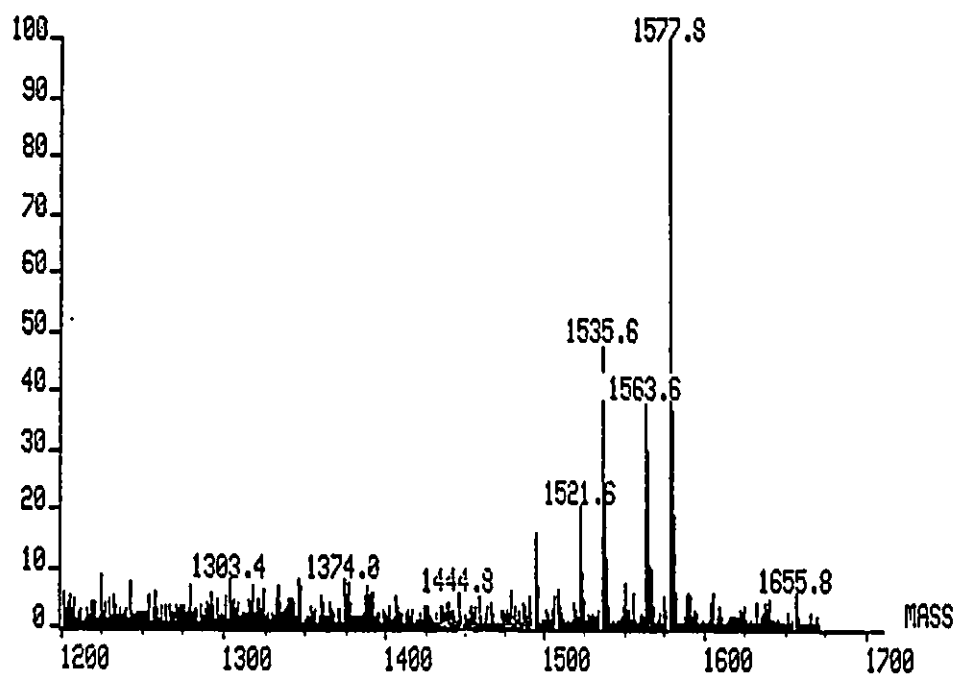


Figure 24: 1200 to 1700 amu region of the NH_3 -DCI mass spectrum of the involatile oligosaccharide acetates from the Smith-degraded AK1401 A-PS. Note that the indicated masses are 1.0 amu low as indicated by a calibration check with malto-oligosaccharide peracetates (see text).

It was thought that these components might be the products of incomplete oxidation or incomplete hydrolysis of the A-PS repeating unit, but the expected compositions do not have the above formula weights.

The complete NH_3 -DCI spectrum appears very complex (Figure 25, note that some ions appear to be 1 amu higher in mass due to calibration errors). However, an interesting feature is the occurrence of several pairs of ions which differ by 2 amu (m/z 682, 684; 710, 712; 884, 886; and 912, 914). This phenomenon has been noted previously⁷⁷ in the NH_3 -DCI spectra of permethylated oligosaccharides. The pairs of ions were interpreted as being indicative of the sequence of monosaccharides where the ions were formed by cleavage of successive glycosidic bonds. Each ion was found to include the non-reducing terminus, so the series allowed the determination of the monosaccharide sequence starting from the non-reducing end of the oligosaccharide. In each pair of ions, the higher mass ion was interpreted as being the product of glycosidic cleavage with retention of the glycosidic oxygen, hydrogen transfer⁷⁸ from the portion that was lost, and ammonium ion attachment. The ion 2 amu less than the hydrogen transfer ion cannot be unambiguously formulated⁷⁷, but it is clear that it is also a non-reducing terminal series ion.

In light of this fragmentation mechanism, it appears that the ions which differ by 2 amu in Figure 25 are all part of a terminal series. Note that $914-712 = 202$ (alternatively $912-710$), and that $886-684 = 202$ (or $884-682$) as well. The increment 202 amu corresponds to the incorporation of an acetylated *O*-methylrhamnose, so two ion series are apparent (possibly corresponding to the two components observed in

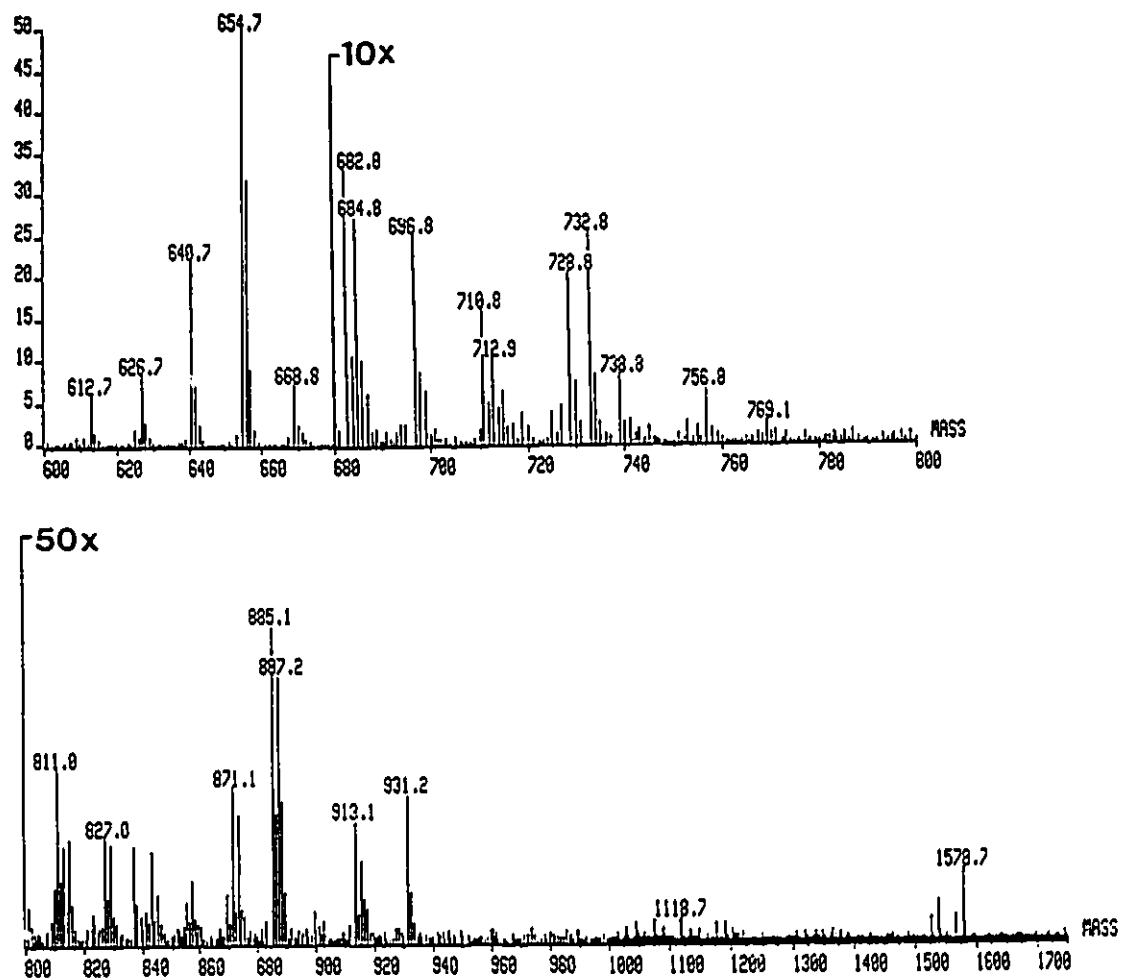
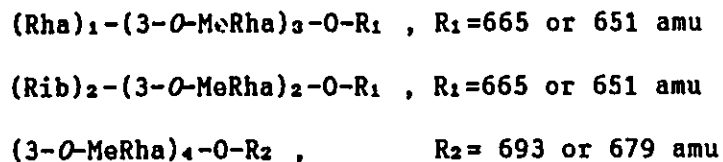


Figure 25: NH_3 -DCI mass spectrum of the involatile oligosaccharide acetates from the Smith-degraded AK1401 A-PS. Note that the indicated masses are 0.6 to 0.8 amu high.

the TLC of this sample) which each have a 3-*O*-methylrhamnose constituent. These two components can be formulated as in Figure 26. When one considers possible compositions for the residual masses (bearing in mind that 3-*O*-methylrhamnose, rhamnose, ribose, and *O*-methylhexoses are the only possible monosaccharide constituents, based on the composition analysis of the polymer remaining after periodate oxidation), the partial compositions:



may be formulated. A BASIC computer program (see Appendix 3, Program 1) was written and used to confirm that no other combinations of the constituent aldoses could produce the same observed m/z .

Similarly, a BASIC program (Appendix 3, Program 2) was used to determine possible compositions of the residual masses at the reducing end (R_1 and R_2 in Figure 26). This program includes the aldoses and alditols found in the composition analysis of the polymer remaining after periodate oxidation and borohydride reduction (Table 7) and the aglycones which might have been present in the oligosaccharide acetates analyzed by GC-MS (Table 6). The program identified the following compositions:



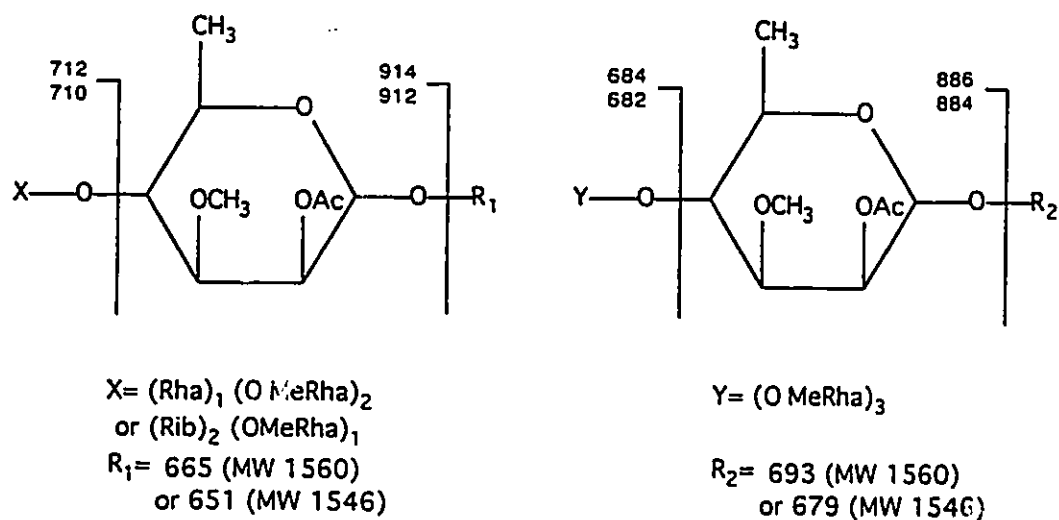
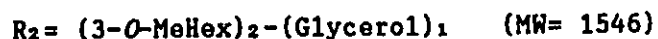
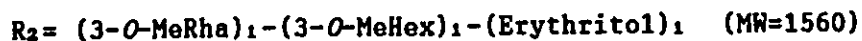
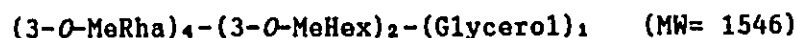
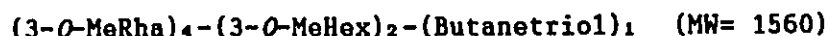


Figure 26: Schematic representation of possible components of the involatile oligosaccharide acetates from the Smith-degraded AK1401 A-PS. Note that the higher mass ion in each pair represents the product of glycosidic cleavage with hydrogen transfer, $[M+H+NH_4]^+$, while the lower mass ions are of the form $[M-H+NH_4]^+$.

where "Unknown" is the aglycone of 14 amu less than glycerol diacetate (Table 6), and



Note that this program returned two other possible compositions, but these were discounted since each contained three aglycone constituents. Combining the information provided by Programs 1 and 2, one can deduce that the compositions:



are the only possible combinations of the known and inferred constituents of the Smith degraded A-PS which can account for the observed ammonia DCI-MS spectrum.

There are four possible compositions for the component with a molecular weight of 1560, and these could not be distinguished by examination of the observed spectrum. However, there is only one possible composition for the component with a molecular weight of 1546. Furthermore, note that the sequence of monosaccharides in this component

is fortuitously defined (assuming that the oligosaccharide is not branched) simply by knowing the compositions of the residual masses on either side of the internal 3-O-methylrhamnose that was inferred from examination of the fragment ions in the spectrum.

The overall spectrum is not easily assigned, in spite of the limited number of possible compositions, because it is the spectrum of a mixture. Nevertheless, the data seem to indicate that 3-O-methylrhamnose (and possibly ribose) play a role in the structures of the involatile oligosaccharides derived from Smith degradation of the A-PS, and since they are grouped together, they may represent a core oligosaccharide or a branch from the main chain of the A-PS. These findings suggest that a re-examination of the involatile oligosaccharide acetates from the Smith degradation, using a more efficient separation method in order to obtain pure fractions, might provide a more detailed structure of the portion of the A-PS containing the minor monosaccharides.

The computer programs used here are not elegant, but they are very effective in ensuring that possible compositions are not overlooked. Nevertheless, this method has several limitations. It does not guarantee an assignment of the spectrum, for example, when several compositions are possible (as in the case of the component of MW= 1560). It also depends heavily on the composition analysis of the polysaccharide to provide a basis for calculation of residual masses. This limitation may provide misleading results if components that are in very small amounts are missed in the composition analysis, since they may be very significant in degradation products of low abundance like

the involatile oligosaccharide acetates studied in these experiments. In spite of this, the computer calculations provide a useful way to attempt an assignment of an observed mass spectrum when other information about the analytes is lacking.

3.5 Assessing the possibility of RNA contamination of the A-PS preparation

Experiments were conducted to determine whether RNA was present in the A-PS preparation, since aqueous solutions of the AK1401 A-PS were found to absorb ultraviolet light with an absorption maximum near the nominal absorption maximum of RNA (260 nm). If RNA were present in the preparation, it could account for the detection of ribose in the composition analysis of the A-PS.

Ultraviolet spectroscopy of AK1401 A-PS (0.25 mg mL^{-1} in water) gave an absorption maximum at 252 nm (absorbance = 1.05), with an $A_{260} = 0.95$, which corresponds to a concentration of $36 \mu\text{g mL}^{-1}$ of RNA ($40 \mu\text{g mL}^{-1}$ of RNA gives $A_{260} = 1.61$), so the PS preparation could be interpreted to contain 14% RNA by weight. However, the mere observation of UV absorbance does not conclusively prove that RNA is present.

In an attempt to ascertain whether the UV absorbance was due to RNA or to some other unidentified component, the PS preparation was digested with Nuclease P1 and Alkaline Phosphatase (which would release ribonucleosides from any RNA that might be present), and analyzed by HPLC. The result of this experiment is shown in Figure 27, along with the chromatograms obtained with a standard nucleoside sample and a positive control (yeast transfer-RNA). The absence of nucleosides in

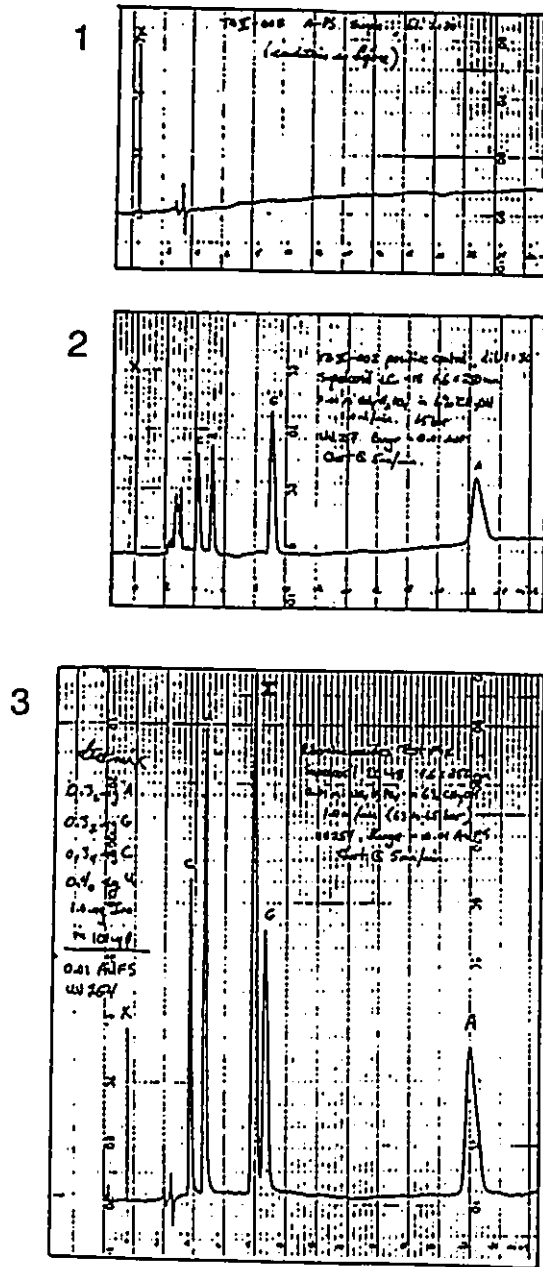


Figure 27: HPLC chromatograms of the products of Nuclease P1 and Alkaline phosphatase digestion of 1) AK1401 A-PS, 2) yeast transfer RNA (positive control), and 3) a standard test mix of ribonucleosides (C= cytidine, U=uridine, I= inosine, G= guanosine, and A= adenosine)

the PS sample suggests that RNA was not present, and that the UV absorbance must be due to some other (unidentified) compound.

Additional control experiments included:

1. a sample containing t-RNA and AK1401 A-PS, which resulted in a similar chromatogram to the positive control sample: this result indicates that AK1401 A-PS is not an inhibitor of either enzyme.
2. a sample of t-RNA to which no Nuclease P1 was added (to control for enzyme activity, since it is possible that a false positive would result if the nuclease was inactive and the standard t-RNA sample contained mononucleotides). This experiment produced no nucleosides, thus proving the integrity of both the t-RNA standard and the nuclease.

Thus, it appears clear that the AK1401 A-PS preparation does not contain RNA, even though the presence of ribose and the UV absorbance of the A-PS could be taken as evidence of RNA contamination.

The nature of the UV absorbance in the A-PS preparation is still unknown, and it is not known whether the chromophore is part of the molecule or a contaminant in the preparation. The NMR spectra of the A-PS contain a few unassigned resonances, and there are several unassigned components in some of the degradative analyses, but these could not be related to any potential UV absorbing constituent.

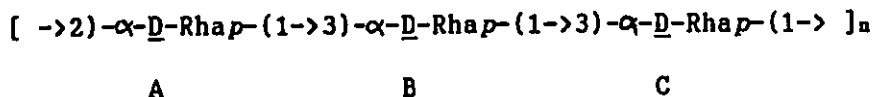
CHAPTER 4

Conclusions

The polysaccharide portion of A-band lipopolysaccharide (A-PS) from *Pseudomonas aeruginosa* rough mutant AK1401 was investigated by means of degradative and spectroscopic analyses. The PS was found to consist principally of D-rhamnose, with lesser amounts of 3-*O*-methylrhamnose, ribose, mannose, and glucose. These monosaccharides were found to exist as 1,3-linked rhamnopyranose, 1,2-linked rhamnopyranose (2:1 ratio), 1,4-linked 3-*O*-methylrhamnopyranose, and 1,4-linked manno- and gluco-pyranoses; the linkage position to ribose was not determined directly, although a product was isolated upon Smith degradation whose EI mass spectrum was consistent with a structure which incorporated a 1,3-linked ribopyranose. Very small amounts of non-reducing terminal rhamnopyranose and terminal hexopyranose were also detected, suggesting that the A-PS has at least one branch point, although a degradation product corresponding to the branching monosaccharide was not found.

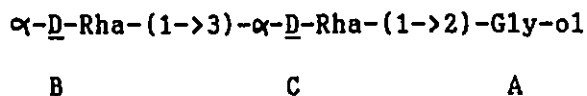
¹H- and ¹³C-NMR showed the presence of three principal monosaccharides, all of which were 6-deoxy-sugars having the C₂-manno-configuration (based on the small H₁-H₂ coupling constant). Proton-coupled ¹³C-NMR showed that all three principal monosaccharides were α-D-rhamnosides. These results, together with the degradative analyses, suggest a trisaccharide repeating unit structure composed of two α-

(1,3)-linked rhamnopyranosides and one α -(1,2)-linked rhamnopyranoside. The $^1\text{H-NMR}$ spectrum of the repeating unit portion of the A-PS was assigned by use of COSY and RELAY experiments. This assignment was used to interpret Nuclear Overhauser Enhancement experiments, which allowed the assignment of the sequence of monosaccharides⁷⁹. The deduced structure of the repeating unit of AK1401 A-PS is:

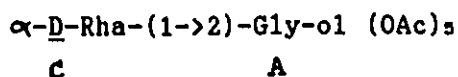


where A, B, and C designate those monosaccharides corresponding to the anomeric proton resonances labelled A1, B1, and C1 in Figure 5a. This work represents the first assignment of the $^1\text{H-NMR}$ spectrum of this repeating unit structure, which complements a previously published assignment of the $^{13}\text{C-NMR}$ spectrum.¹⁹

Because of its regular repeating unit structure, the bulk of the A-PS is converted into an oligosaccharide of predictable structure by Smith degradation, namely:

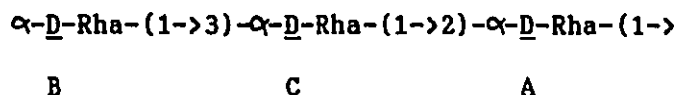


Indeed, the heptaacetate derivative of this compound was found to be the principal oligosaccharide acetate resulting from acetylation of the products of Smith degradation. The presence of a similar component:



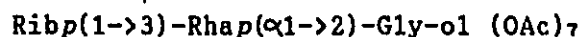
C A

suggests that the non-reducing end sequence of the A-PS is:



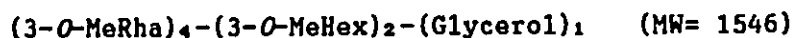
where residue B is oxidized and lost during the Smith degradation.

Another product found by GC-MS of the mixture of oligosaccharide acetates resulting from Smith degradation of the A-PS had an EI mass spectrum consistent with the structure:



The presence of this component is an important finding because it implies that ribose is actually part of the A-PS, and is not just the result of contamination of the A-PS preparation by ribonucleic acid (RNA).

The mixture of oligosaccharide acetates resulting from Smith degradation of the A-PS also contained components which were not observed by GC-MS, presumably due to low volatility. These components were separated from the volatile constituents by liquid chromatography, and analyzed by Direct Chemical Ionization (DCI) mass spectrometry with ammonia reagent gas. This analysis showed that the involatile components were higher oligosaccharides, and their structures could be partially defined. One possible component is:



Four other possible compositions were found that could correspond to another component having a molecular weight of 1560. These could not be uniquely identified, but it appears that 3-*O*-methylrhamnose (and possibly ribose and 3-*O*-methylhexose) play a role in these structures. Since these monosaccharides are grouped together, they may represent a core oligosaccharide or a branch from the main chain of the A-PS.

Finally, experiments were conducted to determine whether RNA was present in the AK1401 A-PS preparation, since aqueous solutions of the A-PS were found to absorb ultraviolet light at a wavelength near the nominal absorption maximum for RNA. Nuclease digestion, dephosphorylation by alkaline phosphatase, and analysis for ribonucleosides by HPLC suggested that the A-PS preparation used in this work did not contain RNA. However, the nature of the UV absorbance in the A-PS preparation is still unknown.

The present work is significant for several reasons. The rough mutant strain of *Pseudomonas aeruginosa* (AK1401) has been used to test for the presence of antibodies to A-band LPS in the sera of Cystic Fibrosis (CF) patients, and A-band LPS was found to be the principal cell surface antigen of *P. aeruginosa* isolates from CF lungs.²⁵ This was an important finding because it suggested the potential for A-band LPS derivatives to be used as vaccines for the production of antibodies which would be effective against established colonies in CF lungs. The

structure of A-band LPS was believed to be similar to the common antigen described by Yokota *et al.*¹⁴ because both LPS's were reactive with monoclonal antibody E87.¹⁹ However, Kocharova *et al.*²¹ suggested that E87 recognized a completely unrelated polysaccharide, so the relationship between A-band LPS and the common antigen became uncertain. The results of the present study show that A-band LPS from AK1401 has the identical repeating unit polysaccharide to the common antigen reported by Yokota *et al.*¹⁴, so the results of Lam's clinical study²⁵ are in fact representative of the distribution of the common antigen in CF patients. The structural identity between A-band LPS and the common antigen is quite clear as a result of this work.

The structure of the A-band LPS from AK1401 is not unique, since it was found to contain the same repeating unit structure found previously in the LPS of *P. syringae*^{16,17} and other strains of *P. aeruginosa*.^{14,15} However, the minor sugar components are different from those found in related LPS's, so there is some diversity in structure between strains.

The approach used in an attempt to determine the role of minor sugar constituents is unique. Although Yokota *et al.*¹⁴ carried out a Smith degradation of their polysaccharide, their studies were limited to composition analyses of two fractions isolated by size exclusion chromatography. The efforts in the present work to analyze all oligosaccharides resulting from the Smith degradation by GC-MS and DCI-MS have not been previously attempted. This work shows the potential of these methods for a detailed examination of oligosaccharides resulting from degradative analyses, but also shows that these methods are

currently limited by a lack of standard spectra and reference compounds. The DCI-MS studies on the higher mass oligosaccharide fraction, in particular, merit reinvestigation if the two (or possibly more) oligosaccharides present can be separated, since a complete assignment of the structures of these compounds would be very revealing about the role of minor monosaccharide constituents in the overall A-PS structure.

Through an assignment of the $^1\text{H-NMR}$ spectrum, a detailed examination of the polysaccharide structure by various degradative analyses, and several novel approaches to furthering the study of minor constituents in the overall polysaccharide structure, this work has contributed to the body of knowledge about A-band LPS, which is now becoming recognized as an important cell surface antigen of *Pseudomonas aeruginosa*.

A study based on the results of this work is currently being conducted by Dr. W.A. Szarek and coworkers at Queen's University, Kingston, Ontario. This group is synthesizing oligomers derived from the structural features of the A-band LPS found in this work, and also preparing protein conjugates of these compounds for biological testing. The results will hopefully shed some light on whether or not A-band-derived sequences can be used as vaccines against *P. aeruginosa*.

Research is also in progress to determine the manner in which the A-PS is joined to the core oligosaccharide. This information will allow the formulation of a more complete A-band LPS structure, which will establish a prototype for this new class of LPS.

APPENDIX 1

Mass Spectra

Alditol Acetates from AK1401 A-PS

- 1 3-*O*-Methylrhamnitol tetraacetate
(coelution with ethyl palmitate)
- 2 3-*O*-Methylrhamnitol tetraacetate
(standard sample)
- 3 Rhamnitol pentaacetate
- 4 Ribitol pentaacetate
- 5 3-*O*-Methylhexitol pentaacetate
- 6 Mannitol hexaacetate
- 7 Glucitol hexaacetate
- 8 Ethyl stearate (impurity)

(-)-2-octyl-D-rhamnoside triacetates from AK1401 A-PS

- 9 (*R*)-2-octyl-L-rhamnoside triacetates standard (NH₃-Cl)
- 10 (*R*)-2-octyl- α -D-rhamnopyranoside
- 11 (*R*)-2-octyl- β -D-rhamnopyranoside
- 12 (*R*)-2-octyl- α -D-rhamnofuranoside

Partially Methylated Alditol Acetates (PMAA's) from AK1401 A-PS

- 13 1,5-di-*O*-acetyl-2,3,4-tri-*O*-methyl-rhamnitol-d₁
- 14 1,2,5-tri-*O*-acetyl-3,4-di-*O*-methyl-rhamnitol-d₁
- 15 1,4,5-tri-*O*-acetyl-2,3-di-*O*-methyl-rhamnitol-d₁
- 16 1,3,5-tri-*O*-acetyl-2,4-di-*O*-methyl-rhamnitol-d₁

- 17 1,5-di-*O*-acetyl-2,3,4,6-tetra-*O*-methyl-hexitol-d₁
- 18 1,4,5-tri-*O*-acetyl-2,3,6-tri-*O*-methyl-hexitol-d₁
- 19 1,4,5-tri-*O*-acetyl-2,3,6-tri-*O*-methyl-hexitol-d₁

Alditol Acetates from Periodate Oxidized/ NaBH₄ Reduced AK1401 A-PS

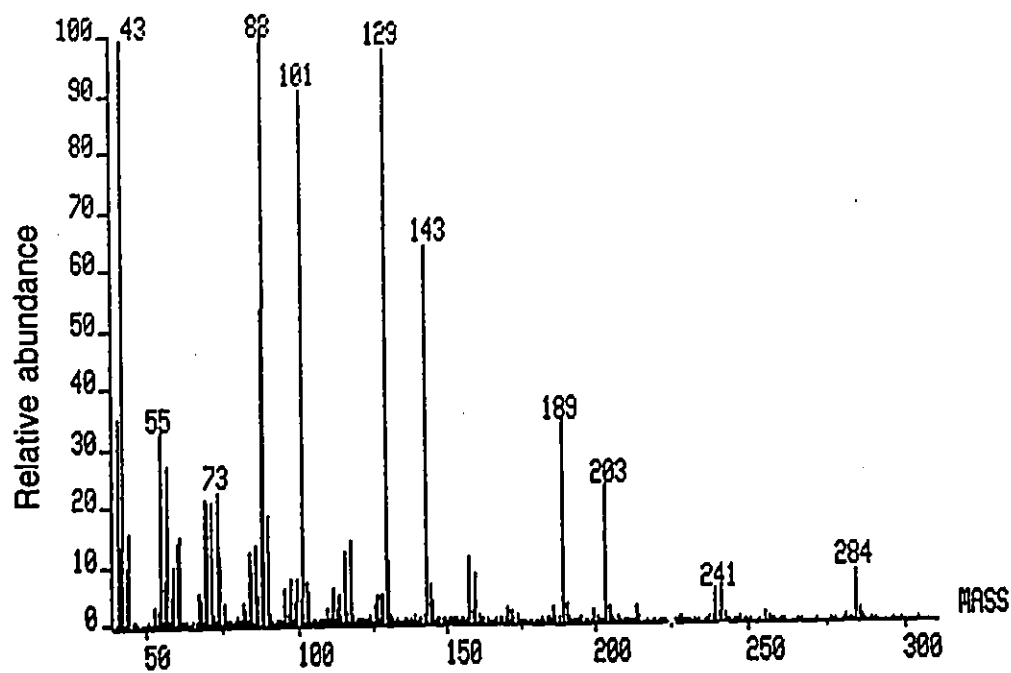
- 20 glycerol and glycerol-d₁ triacetate
- 21 erythritol tetraacetate
- 22 3-*O*-methyl rhamnitol-d₁ tetraacetate
- 23 rhamnitol-d₁ pentaacetate
- 24 ribitol-d₁ pentaacetate
- 25 2-*O*-methyl hexitol-d₁ pentaacetate
- 26 3-*O*-methyl hexitol-d₁ pentaacetate

PMAA's from Periodate Oxidized/ NaBH₄ Reduced AK1401 A-PS

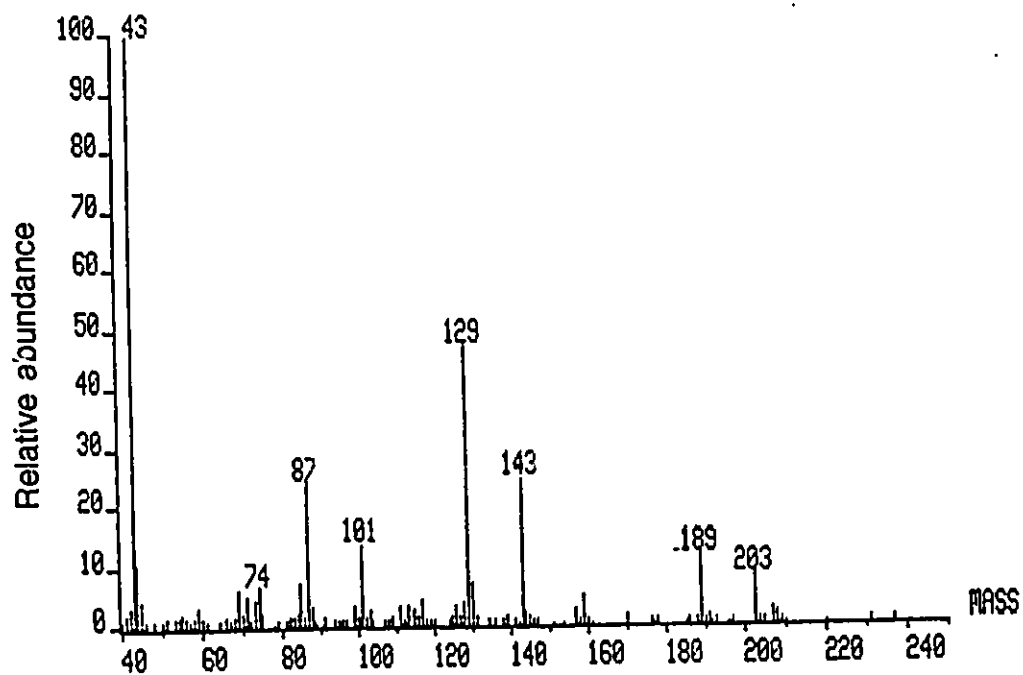
- 27 a PMAA derivative of glycerol ?
- 28 a PMAA derivative of glycerol ?
- 29 glycerol triacetate
- 30 a PMAA derivative of erythritol ?
- 31 Unknown (retention time 14.72 min)
- 32 Unknown (retention time 16.62 min)
- 33 1,5-di-*O*-acetyl-2,3,4-tri-*O*-methyl rhamnitol-d₁
- 34 Unknown PMAA derivative
- 35 1,4,5-tri-*O*-acetyl-2,3-di-*O*-methyl rhamnitol-d₁
- 36 1,3,5-tri-*O*-acetyl-2,4-di-*O*-methyl rhamnitol-d₁
- 37 1,3,4,5-tetra-*O*-acetyl-2-*O*-methyl rhamnitol-d₁

- 38 1,2,3,5-tetra-*O*-acetyl-4-*O*-methyl rhamnitol-d₁
39 rhamnitol-d₁ pentaacetate
40 1,4,5-tri-*O*-acetyl-2,3,6-tri-*O*-methyl hexitol-d₁
41 1,4,5-tri-*O*-acetyl-2,3,6-tri-*O*-methyl hexitol-d₁

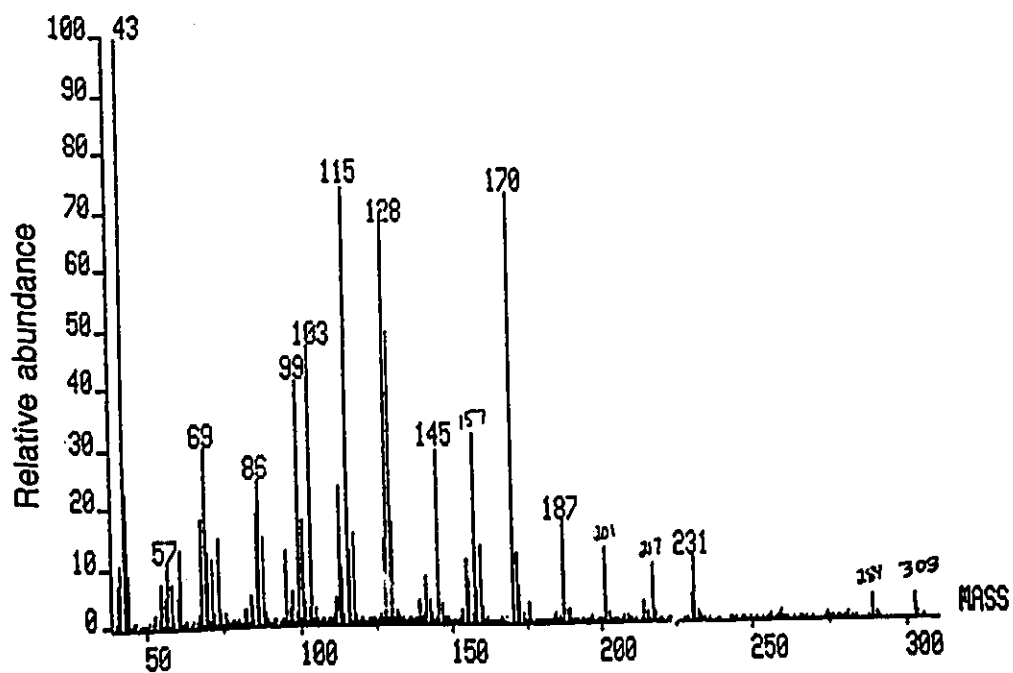
- 1 3-O-Methylrhamnitol tetraacetate
(coelution with ethyl palmitate)



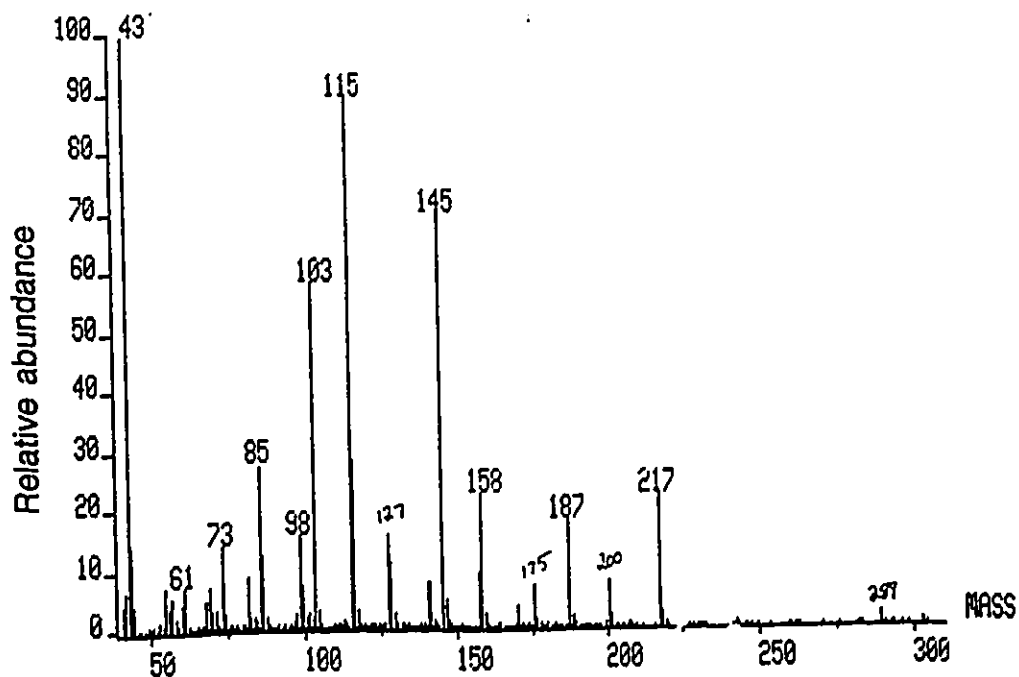
- 2 3-O-Methylrhamnitol tetraacetate
(standard sample)



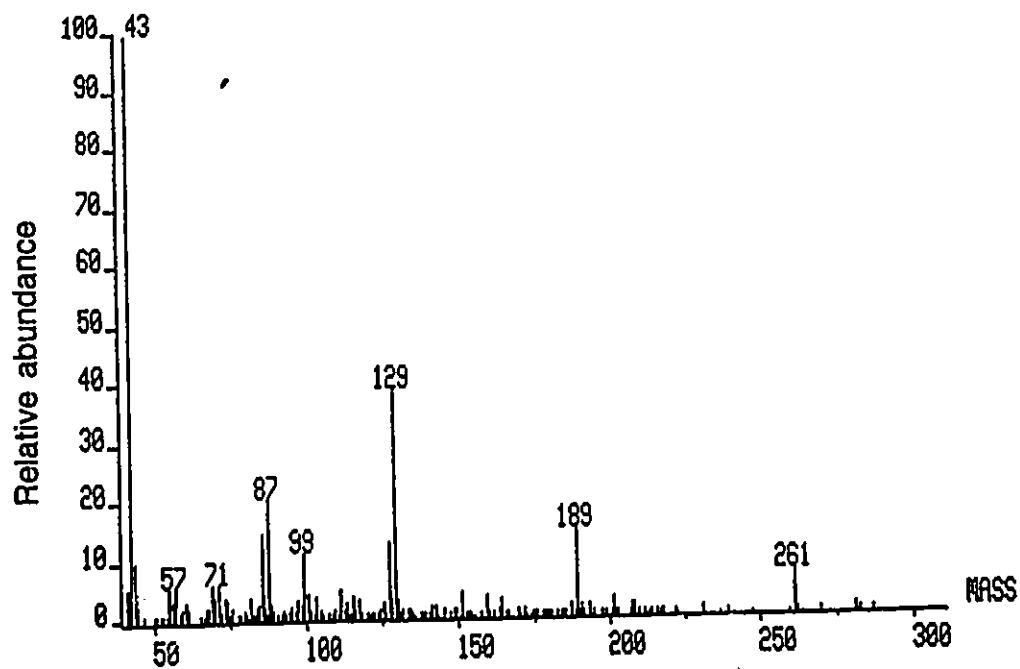
3 Rhamnitol pentaacetate



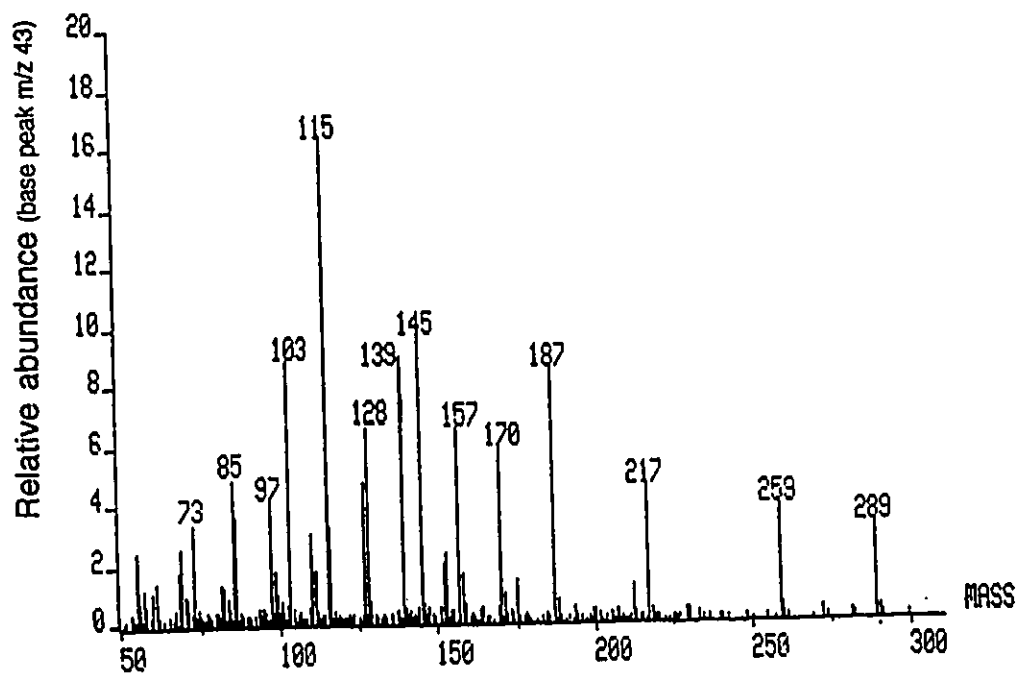
4 Ribitol pentaacetate



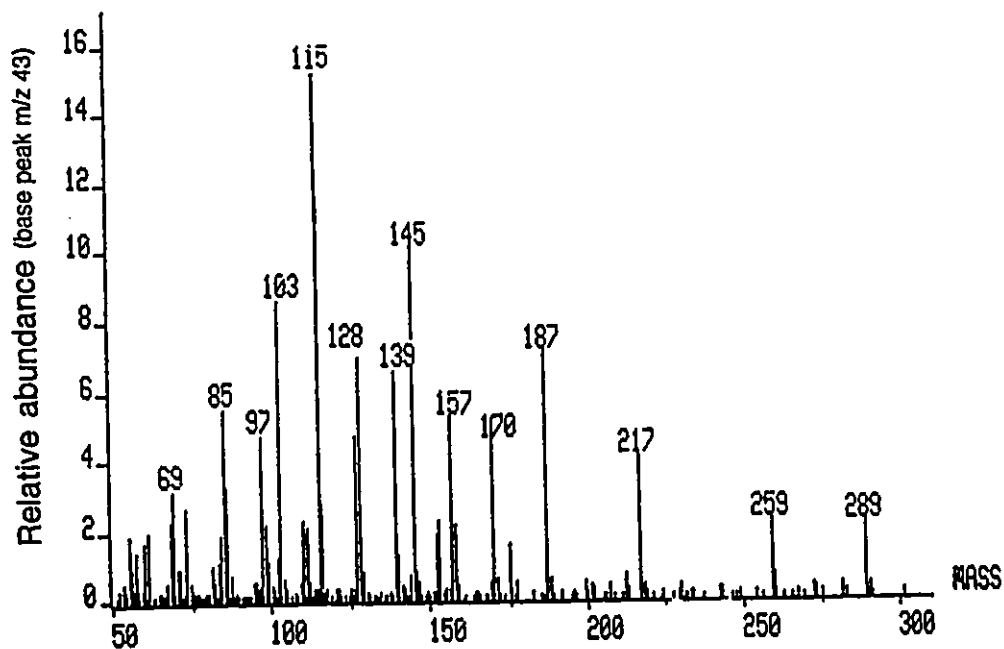
5 3-O-Methylhexitol pentaacetate



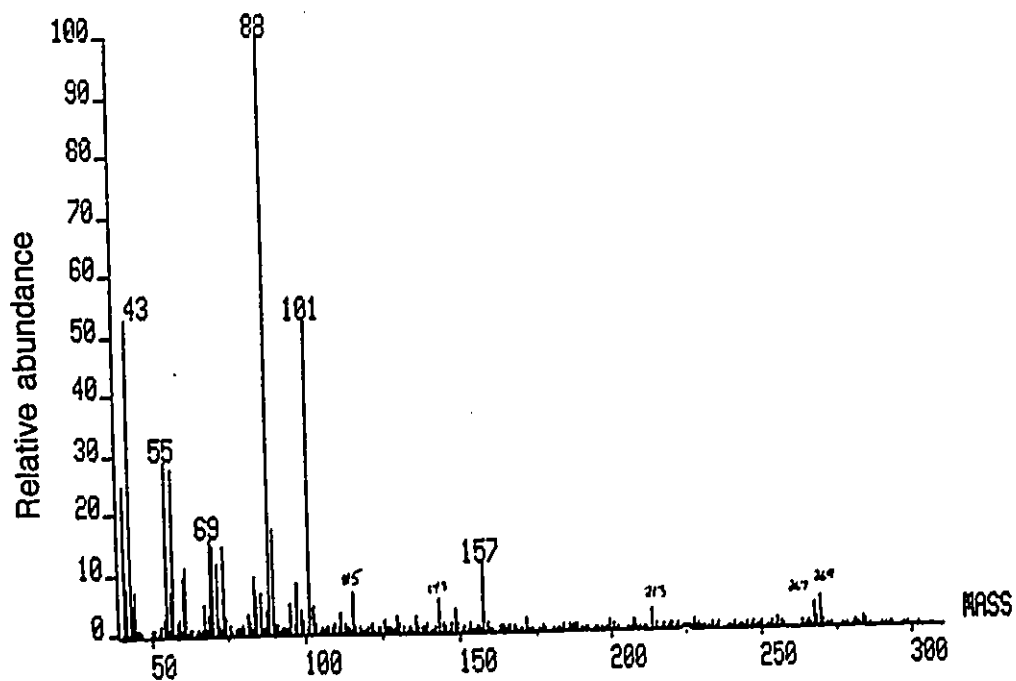
6 Mannitol hexaacetate

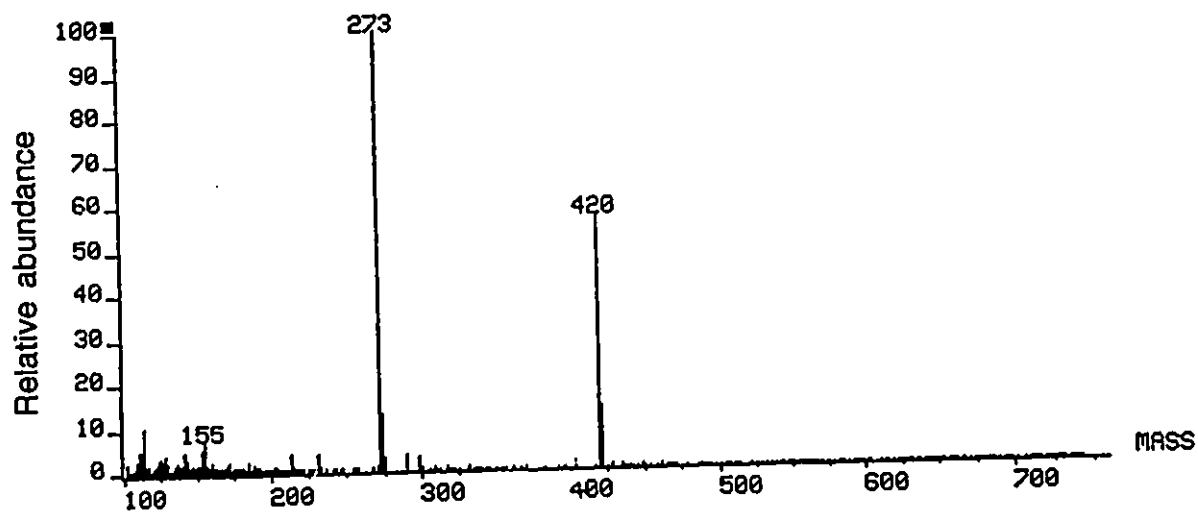
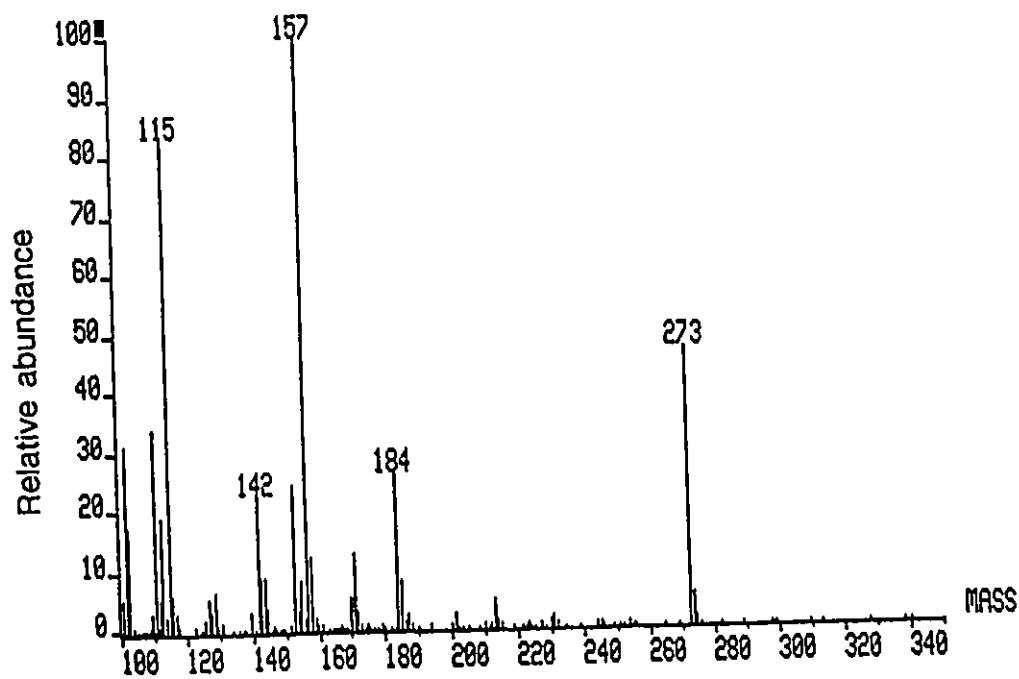


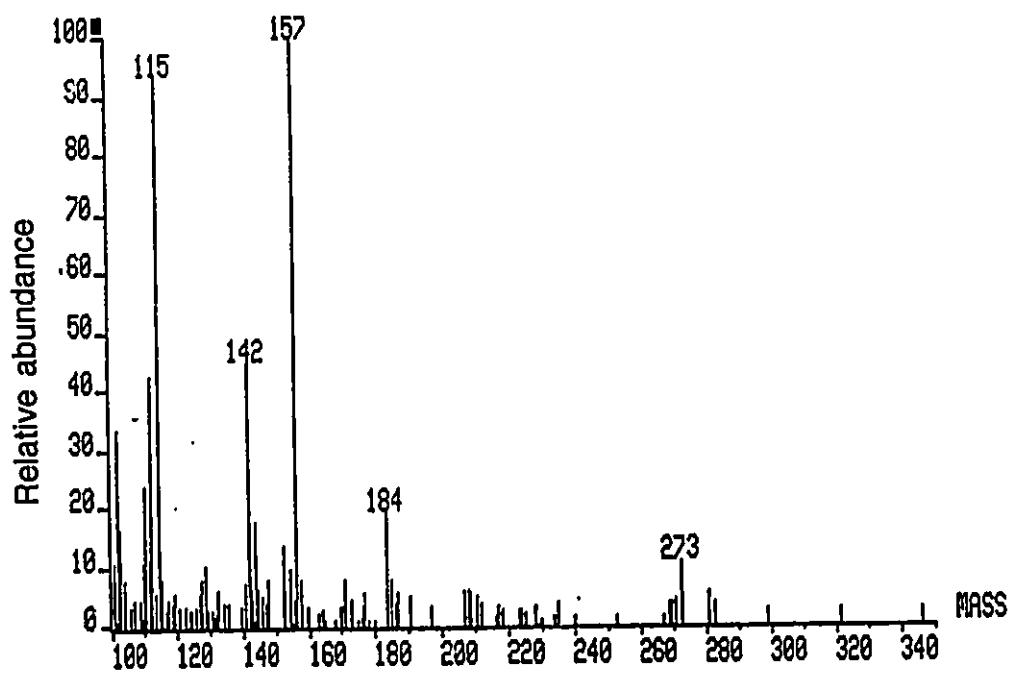
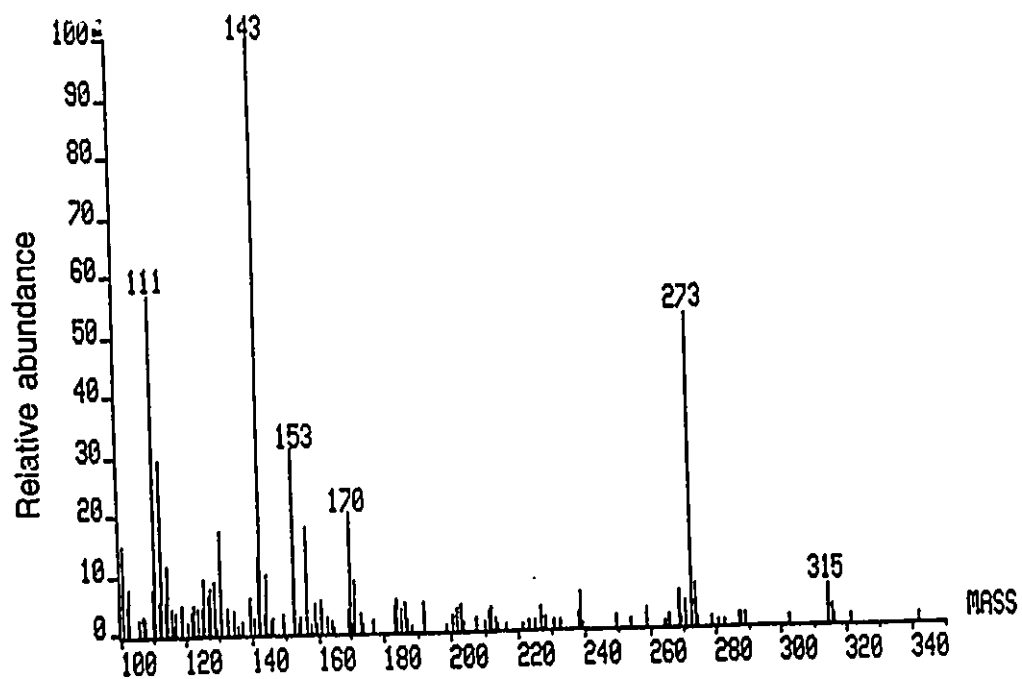
7 Glucitol hexaacetate

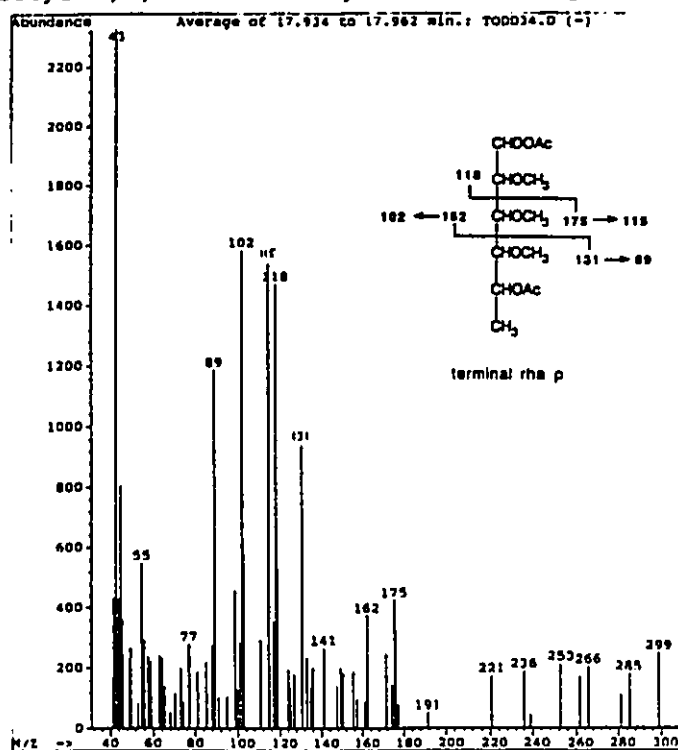
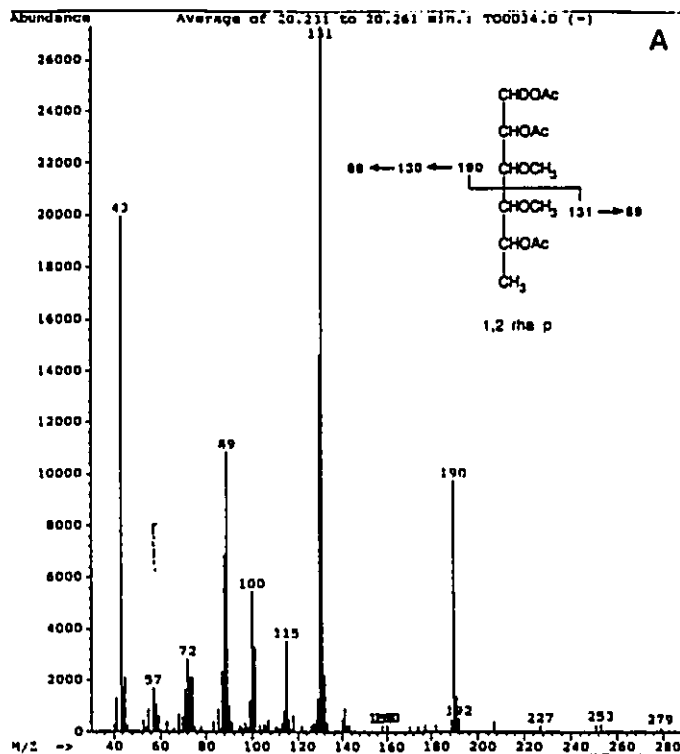


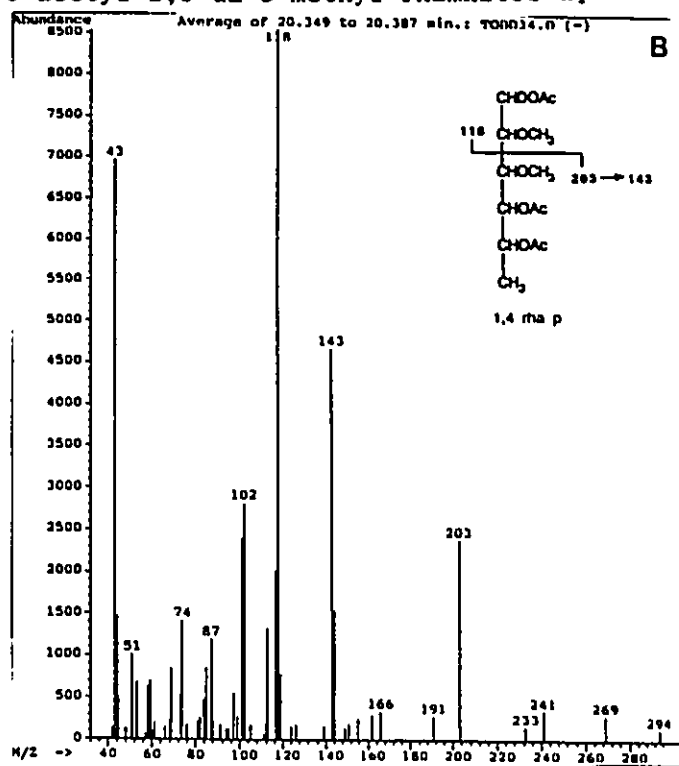
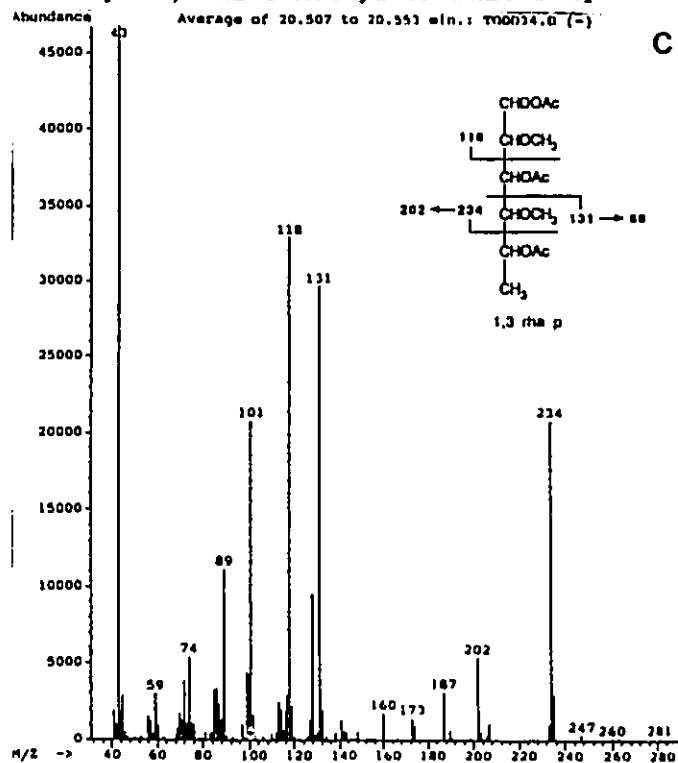
8 Ethyl stearate (impurity)

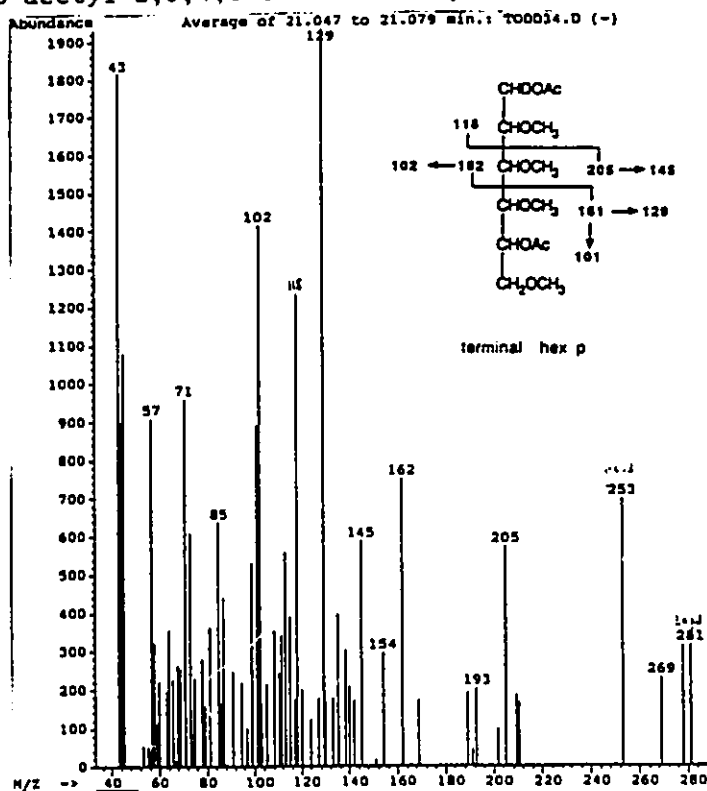
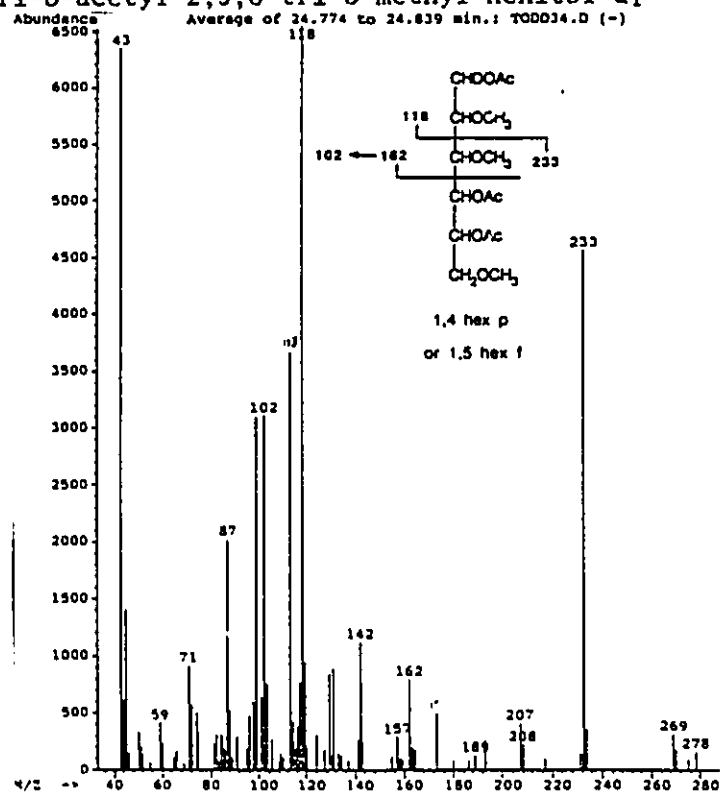


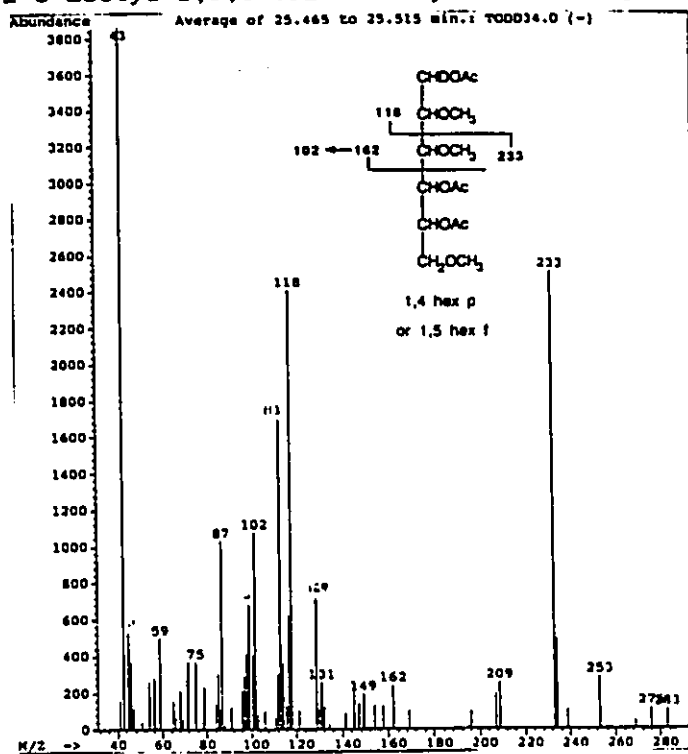
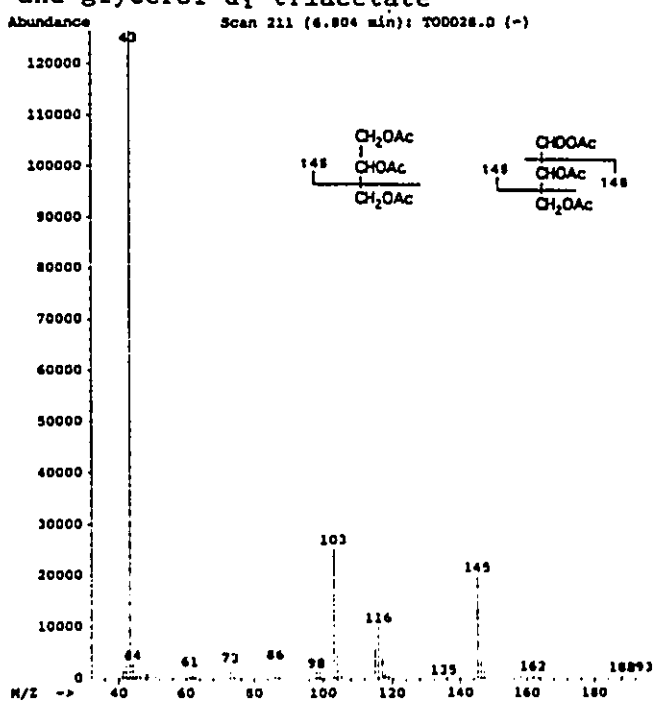
9 (R)-2-octyl-L-rhamnoside triacetates standard (NH₃-CI)10 (R)-2-octyl- α -D-rhamnopyranoside

11 (R)-2-octyl- β -D-rhamnopyranoside12 (R)-2-octyl- α -D-rhamnofuranoside

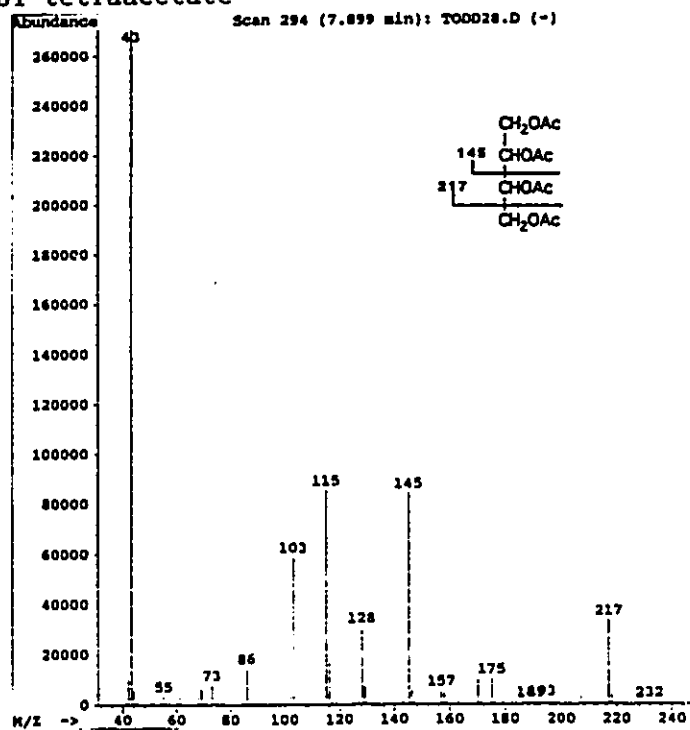
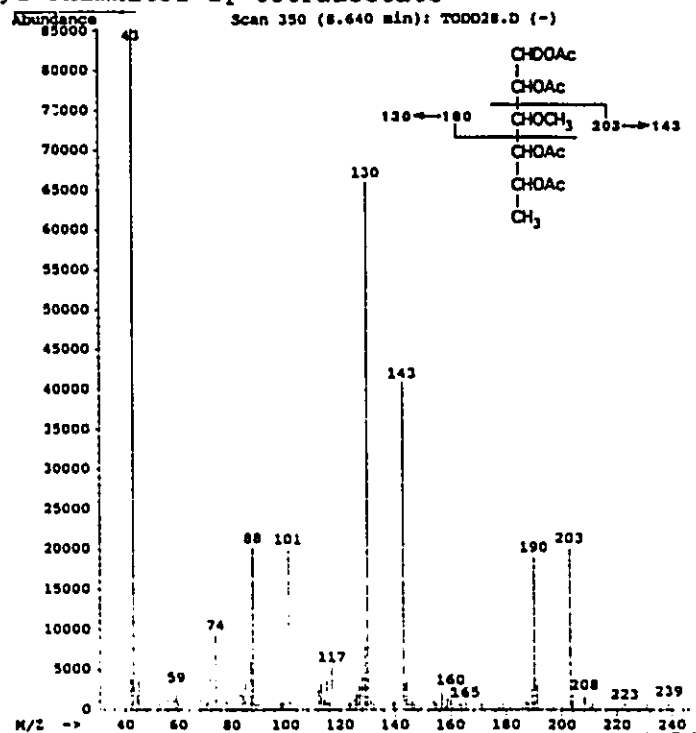
13 1,5-di-*O*-acetyl-2,3,4-tri-*O*-methyl-rhamnitol-d₁14 1,2,5-tri-*O*-acetyl-3,4-di-*O*-methyl-rhamnitol-d₁

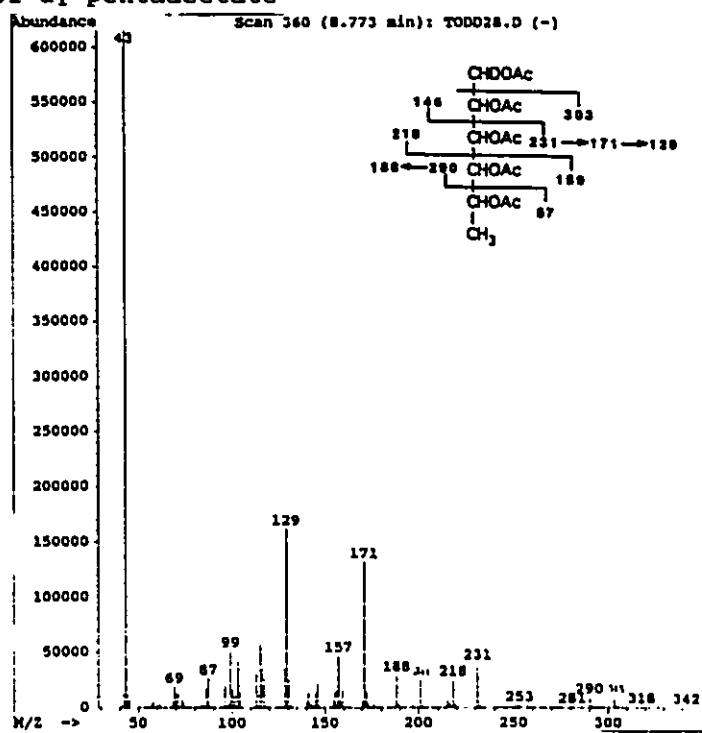
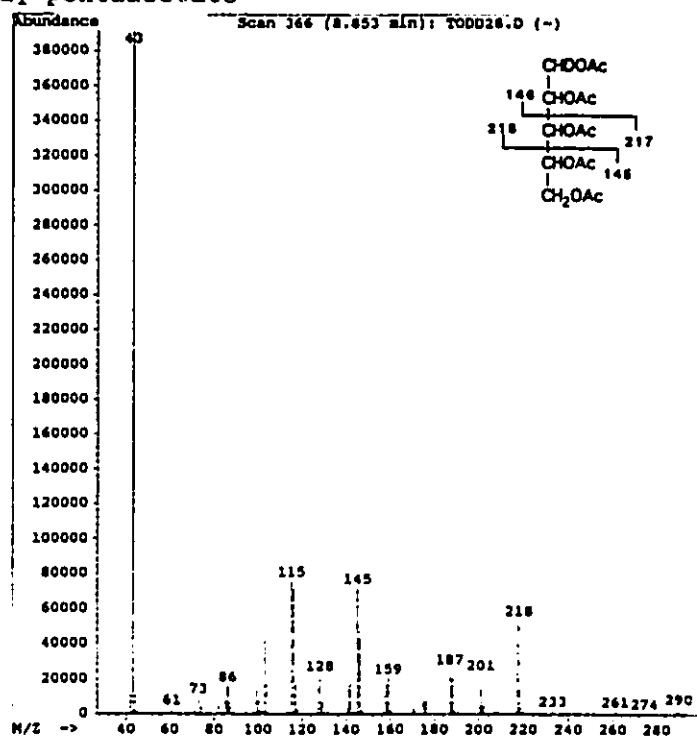
15 1,4,5-tri-*O*-acetyl-2,3-di-*O*-methyl-rhamnitol-d₁16 1,3,5-tri-*O*-acetyl-2,4-di-*O*-methyl-rhamnitol-d₁

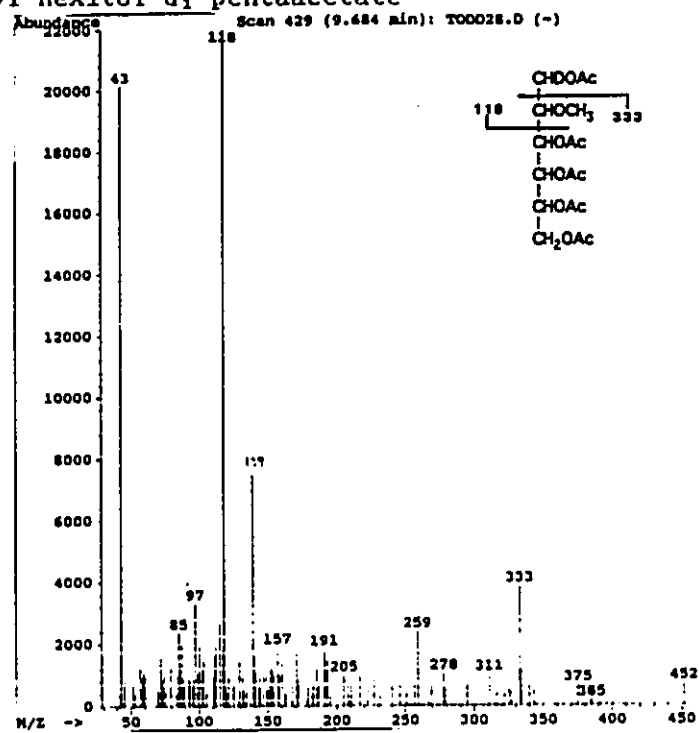
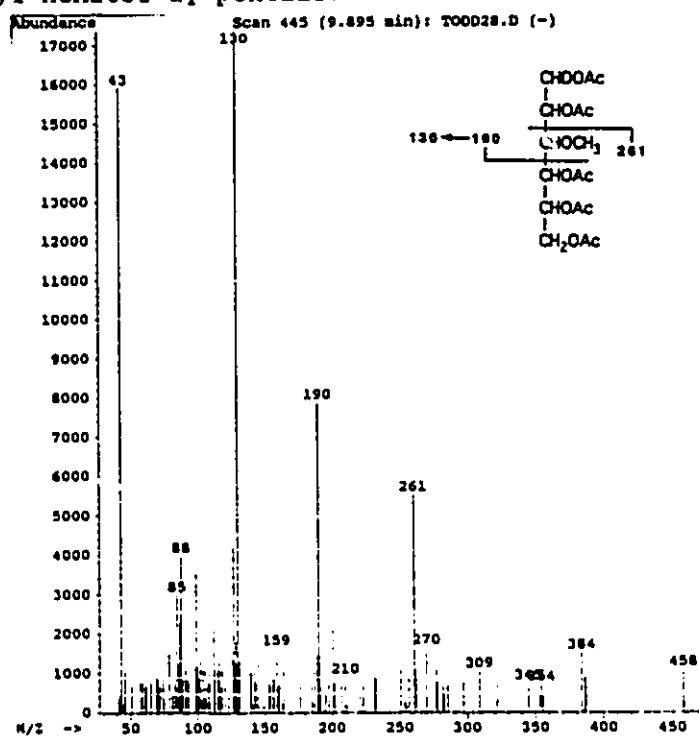
17 1,5-di-*O*-acetyl-2,3,4,6-tetra-*O*-methyl-hexitol-d₁18 1,4,5-tri-*O*-acetyl-2,3,6-tri-*O*-methyl-hexitol-d₁

19 1,4,5-tri-*O*-acetyl-2,3,6-tri-*O*-methyl-hexitol-*d*₁20 glycerol and glycerol-*d*₁ triacetate

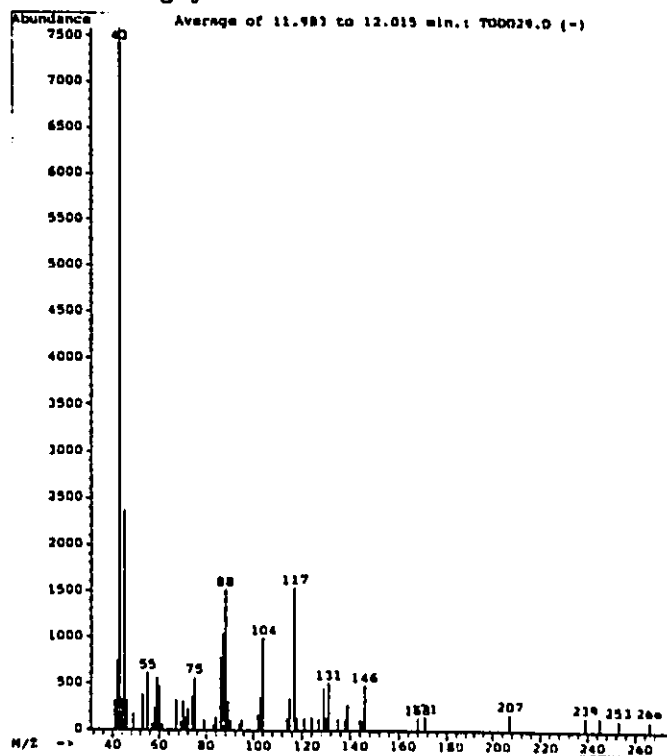
21 erythritol tetraacetate

22 3-O-methyl rhamnitol-d₁ tetraacetate

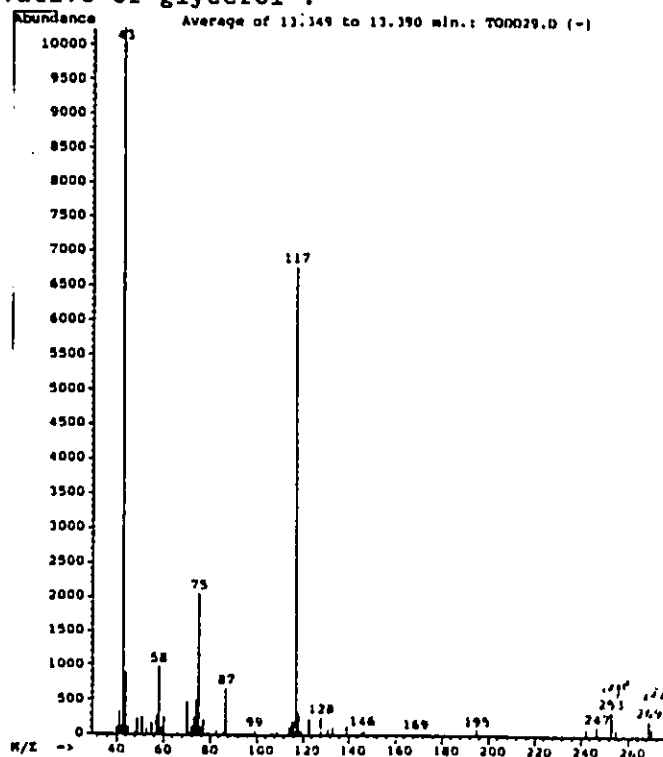
23 rhamnitol-d₁ pentaacetate24 ribitol-d₁ pentaacetate

25 2-O-methyl hexitol-d₁ pentaacetate26 3-O-methyl hexitol-d₁ pentaacetate

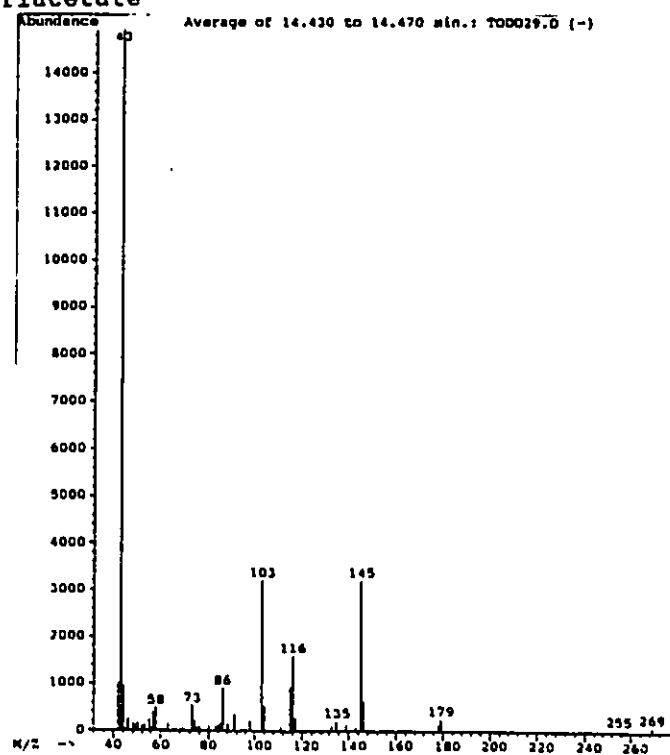
27 a PMAA derivative of glycerol ?



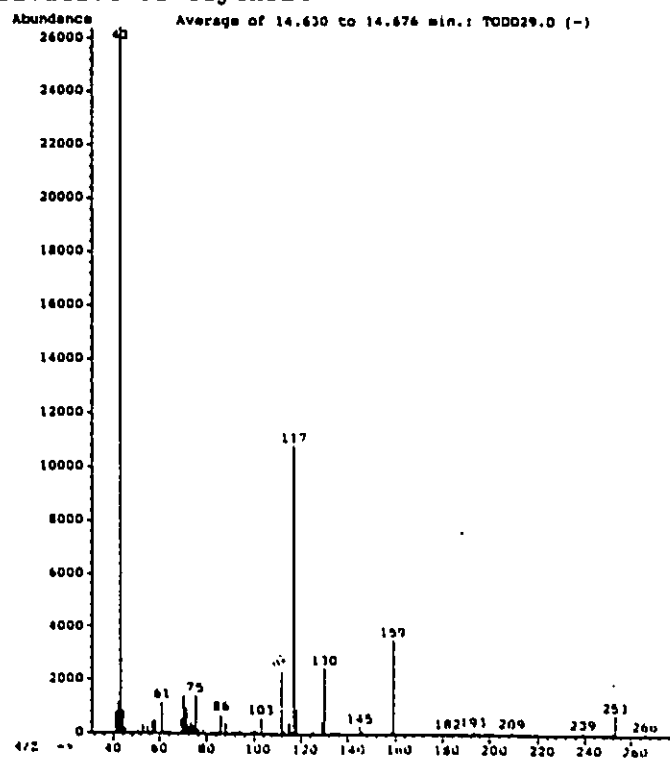
28 a PMAA derivative of glycerol ?



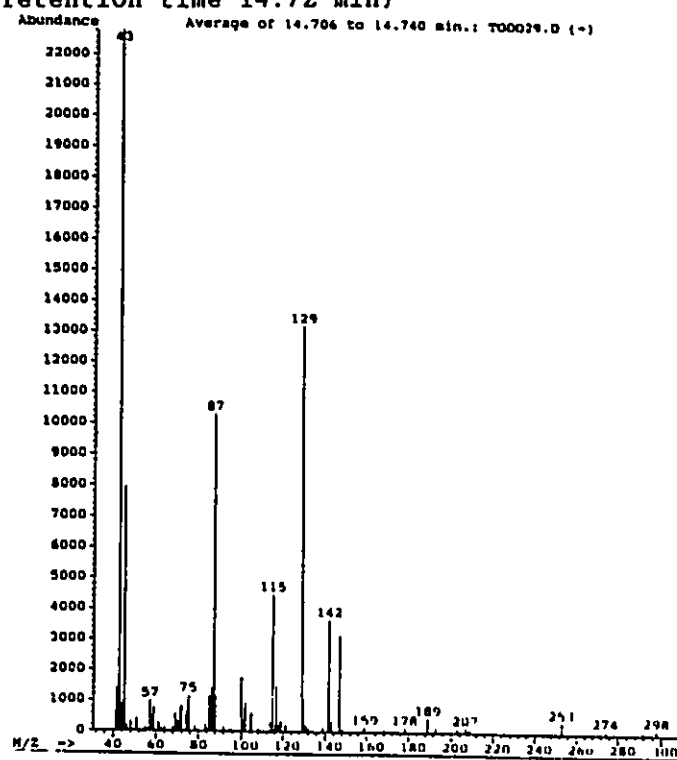
29 glycerol triacetate



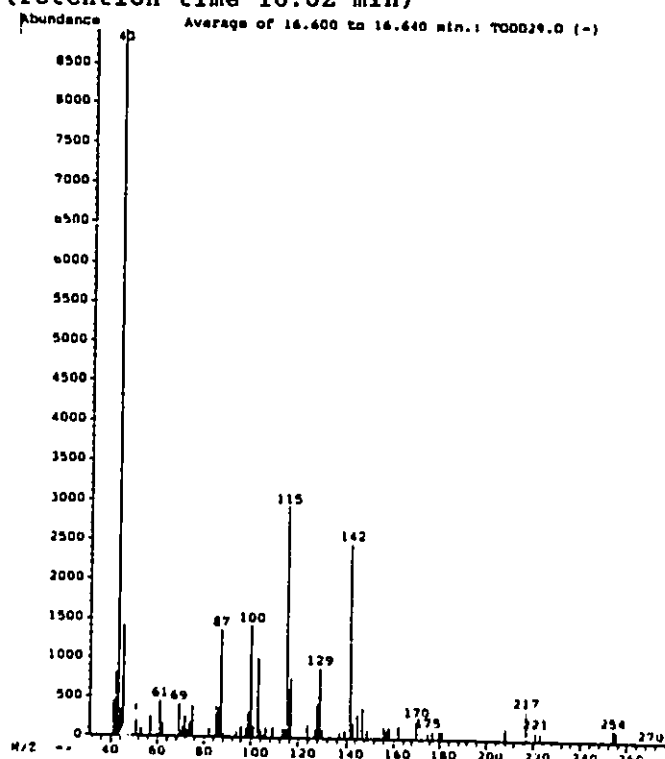
30 a PMAA derivative of erythritol ?

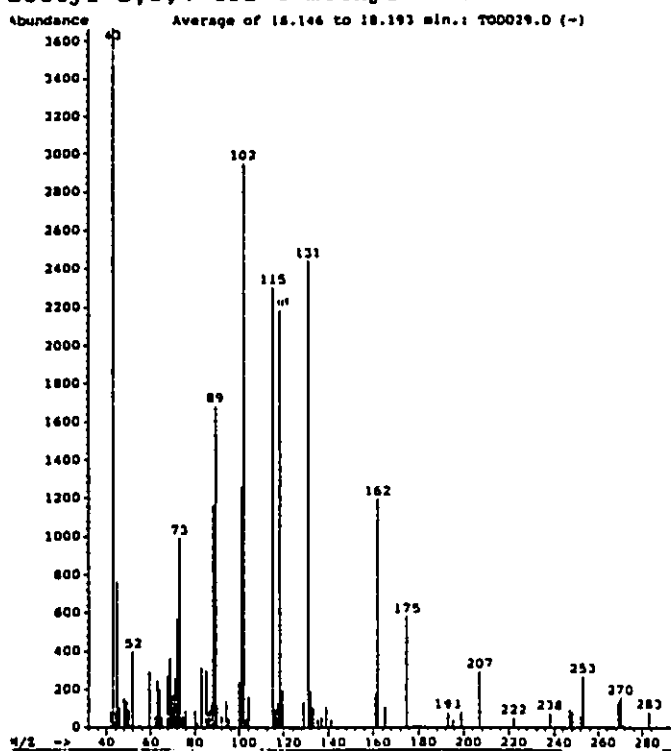


31 Unknown (retention time 14.72 min)

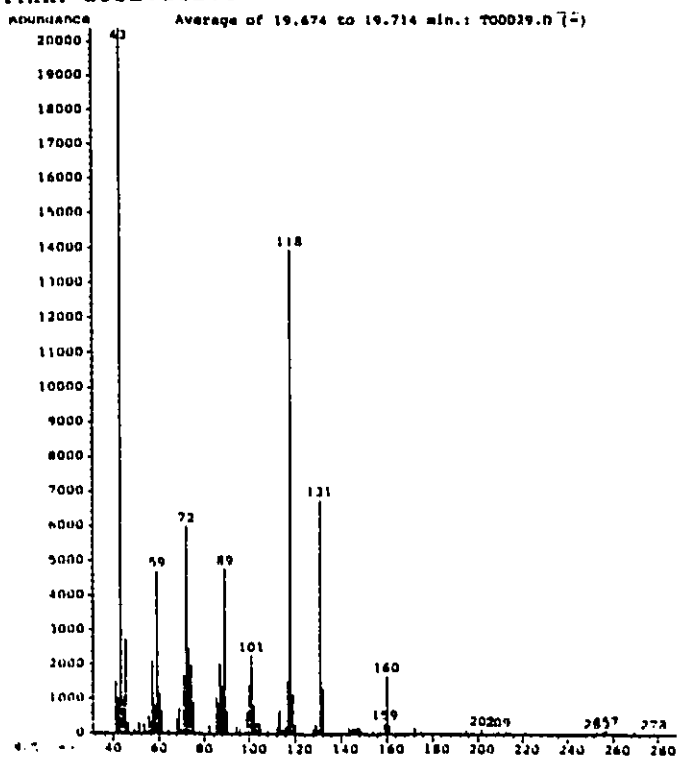


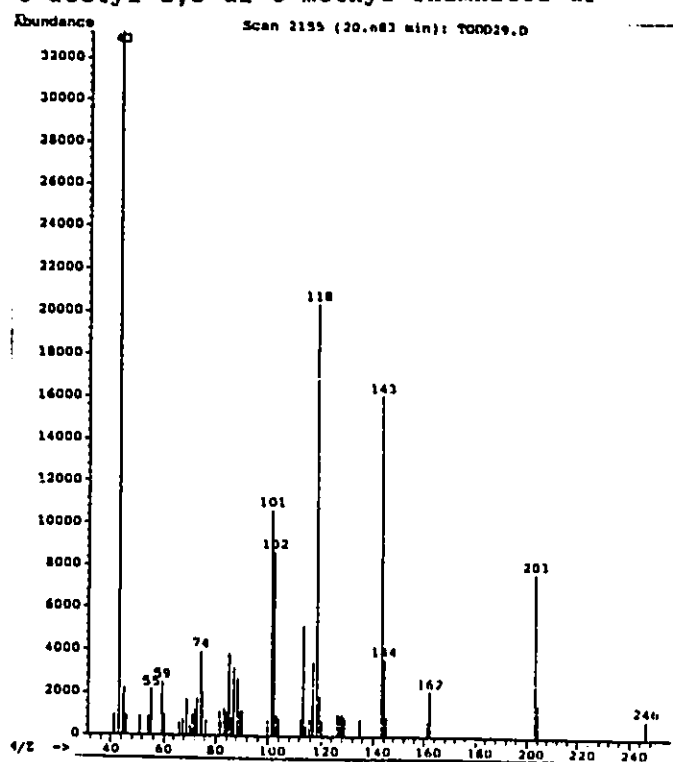
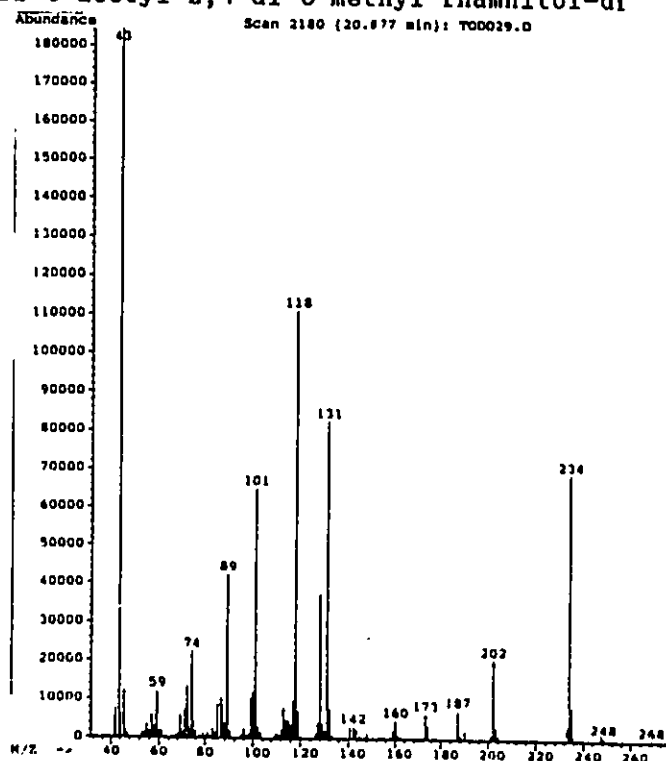
32 Unknown (retention time 16.62 min)

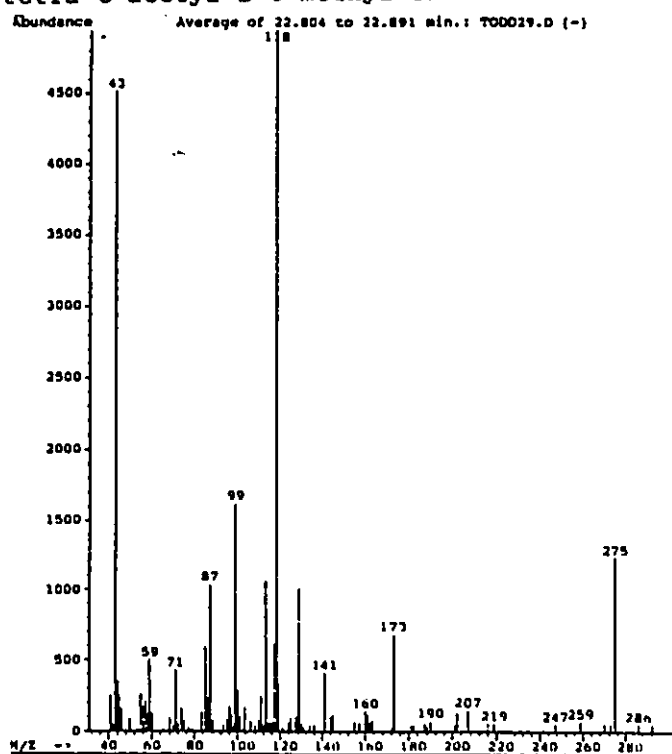
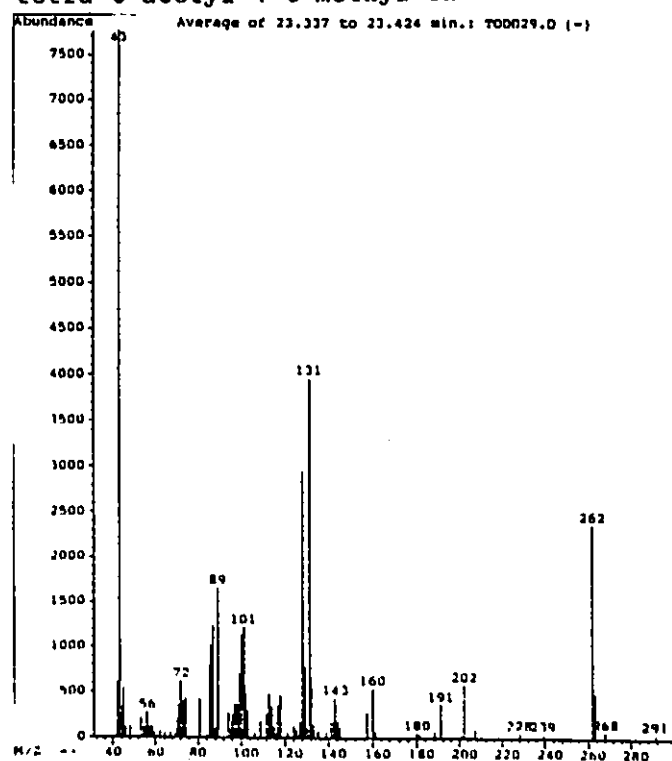


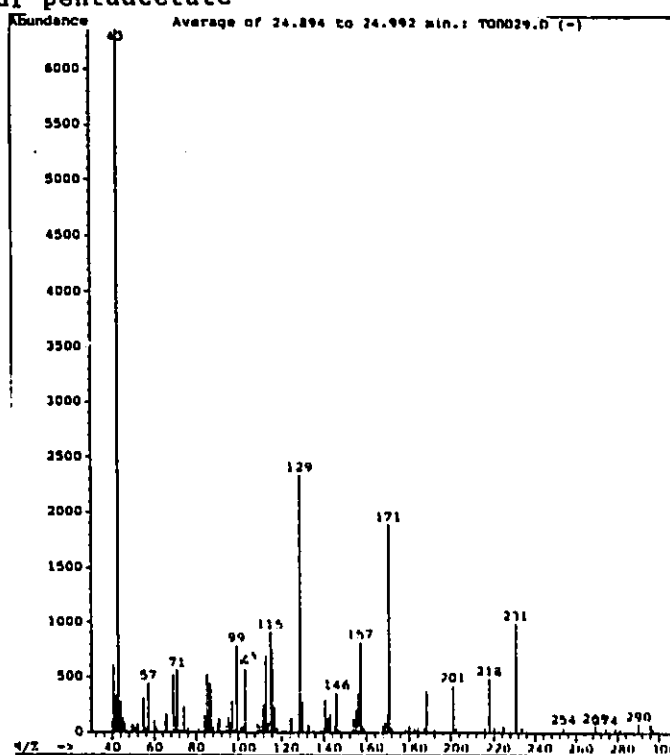
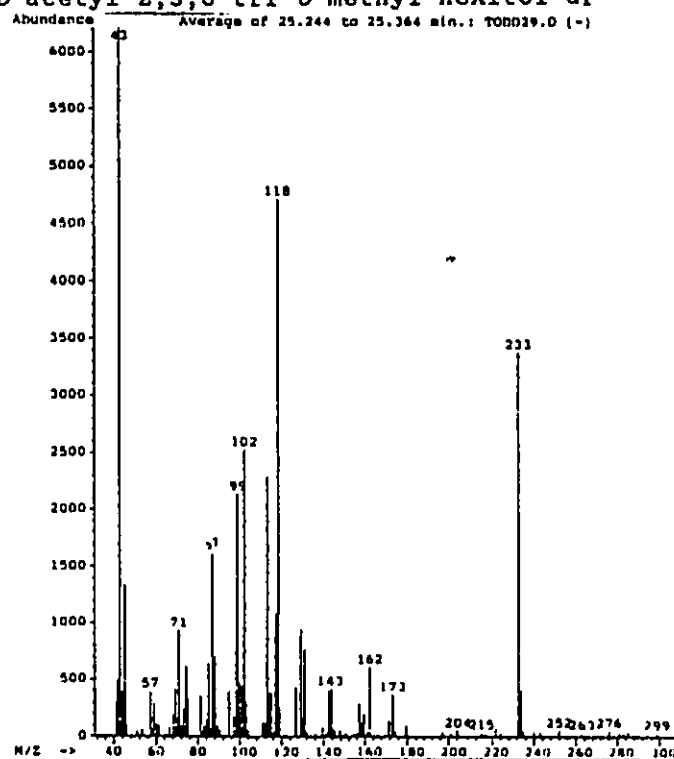
33 1,5-di-*O*-acetyl-2,3,4-tri-*O*-methyl rhamnitol-d₁

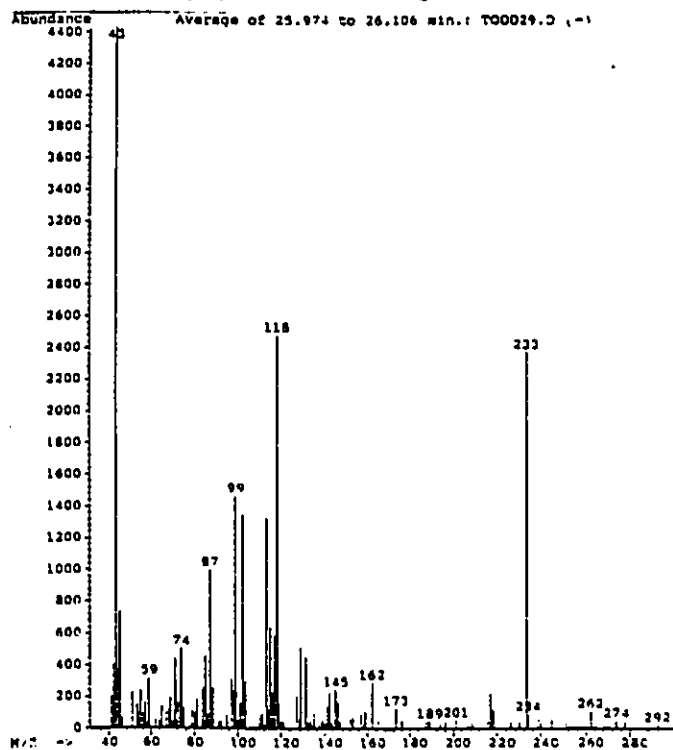
34 Unknown PMAA derivative



35 1,4,5-tri-*O*-acetyl-2,3-di-*O*-methyl rhamnitol-d₁36 1,3,5-tri-*O*-acetyl-2,4-di-*O*-methyl rhamnitol-d₁

37 1,3,4,5-tetra-*O*-acetyl-2-*O*-methyl rhamnitol-d₄38 1,2,3,5-tetra-*O*-acetyl-4-*O*-methyl rhamnitol-d₄

39 rhamnitol-d₁ pentaacetate40 1,4,5-tri-O-acetyl-2,3,6-tri-O-methyl hexitol-d₁

41 1,4,5-tri-*O*-acet, -2,3,6-tri-*O*-methyl hexitol-d₁

APPENDIX 2

NMR Spectra

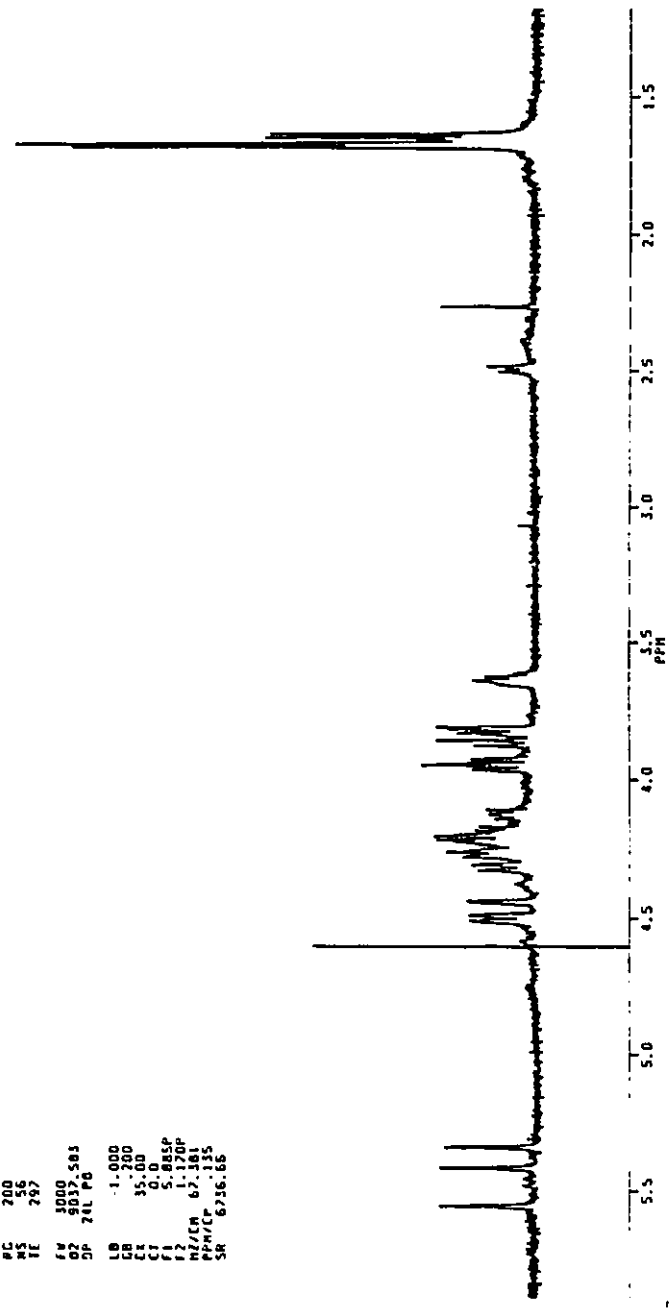
- 1 500 MHz ^1H -NMR of AK1401 A-PS in D_2O , 80°C
- 2 500 MHz ^1H -NMR of AK1401 A-PS obtained by phenol/ chloroform/
petroleum ether extraction

Nuclear Overhauser Enhancement Difference Spectra

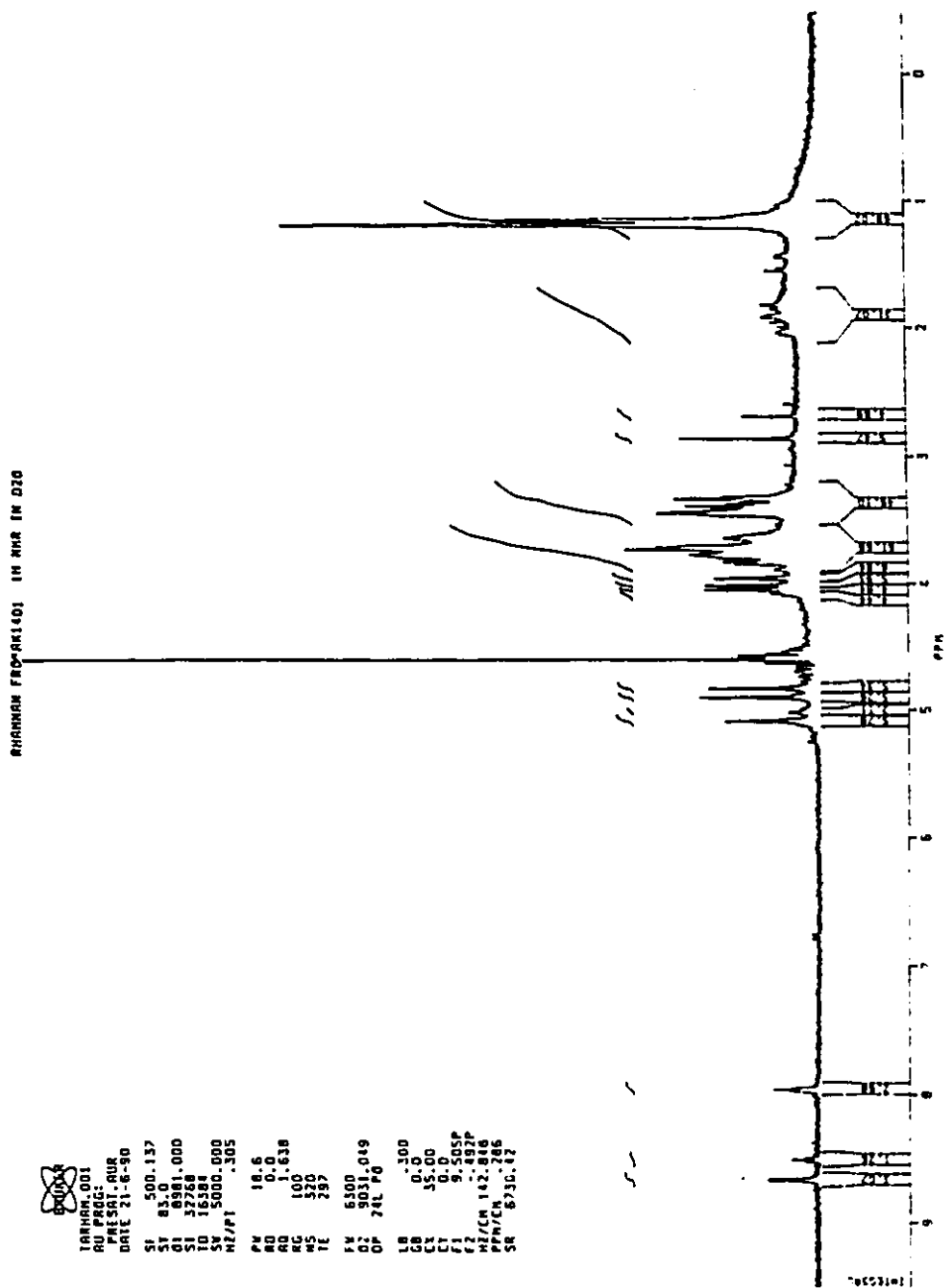
- 3 Irradiated proton: A1
- 4 Irradiated proton: B1
- 5 Irradiated proton: C1
- 6 Irradiated proton: A2
- 7 Irradiated proton: B2
- 8 Irradiated proton: C2
- 9 Irradiated proton: A3
- 10 Irradiated proton: B3-B5 multiplet
- 11 Irradiated proton: C3-A5 multiplet
- 12 Irradiated proton: C5
- 13 Irradiated proton: C6
- 14 Irradiated proton: A6-B6 multiplet

AK1401

TARK1101.003
AU PRGE:
PAE SRT: RWR
DATE 3-11-89
SF 500.137
SI 83.0
OI 6502.085
SI 32268
LD 16384
MZ/PI 2358.124
PV 19.2
AD 0.0
AO 203.473
MC 280
TE 297
FW 3000
OZ 5037.583
DP 2LL PG
LB -1.000
GB -1.200
CA 35.00
CI 0.0
FZ 5.150P
MZ/CM 67.181
PPM/C .135
SR 6736.66

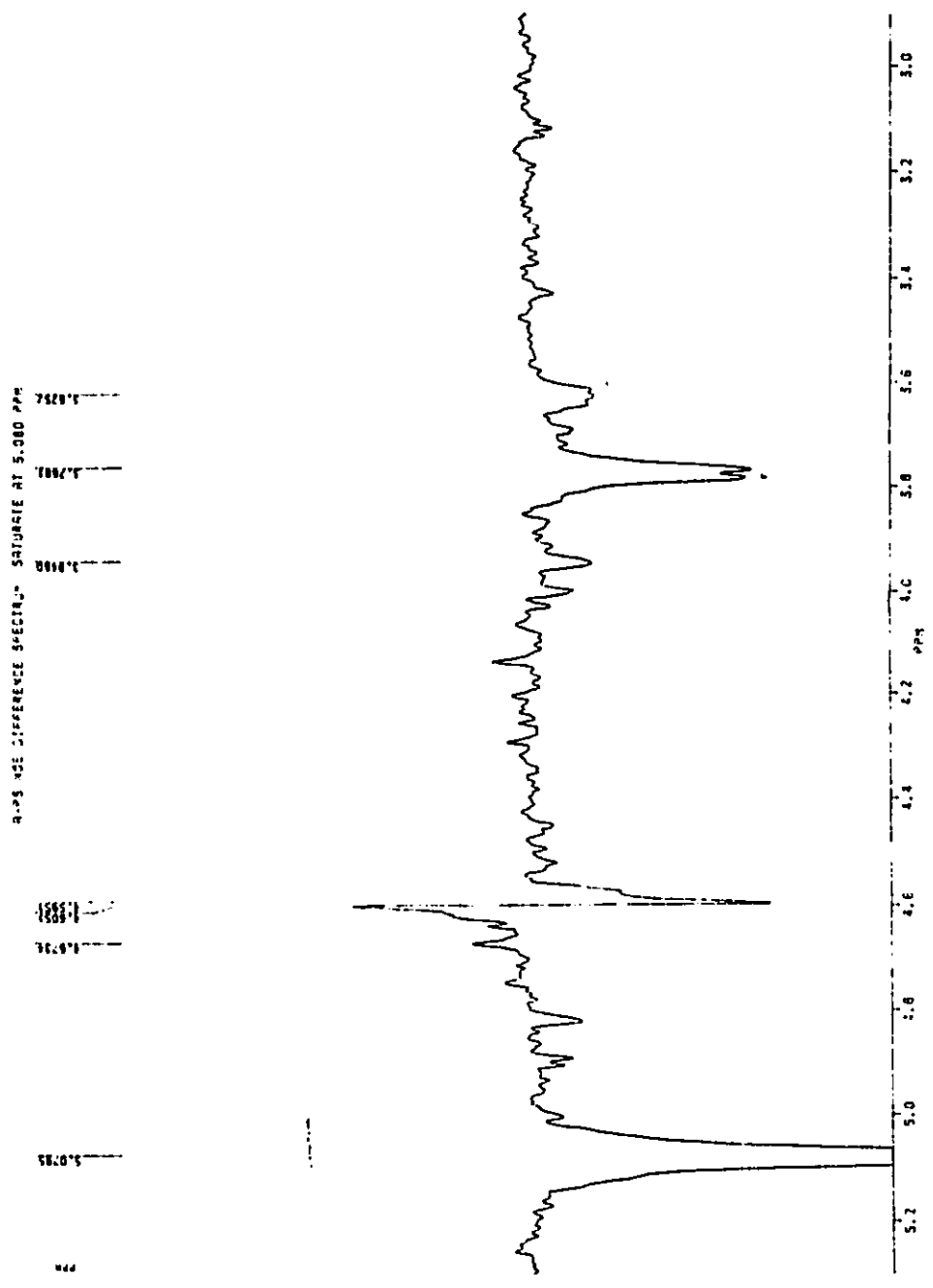


1 500 MHz ¹H-NMR of AK1401 A-PS in D₂O, 80°C

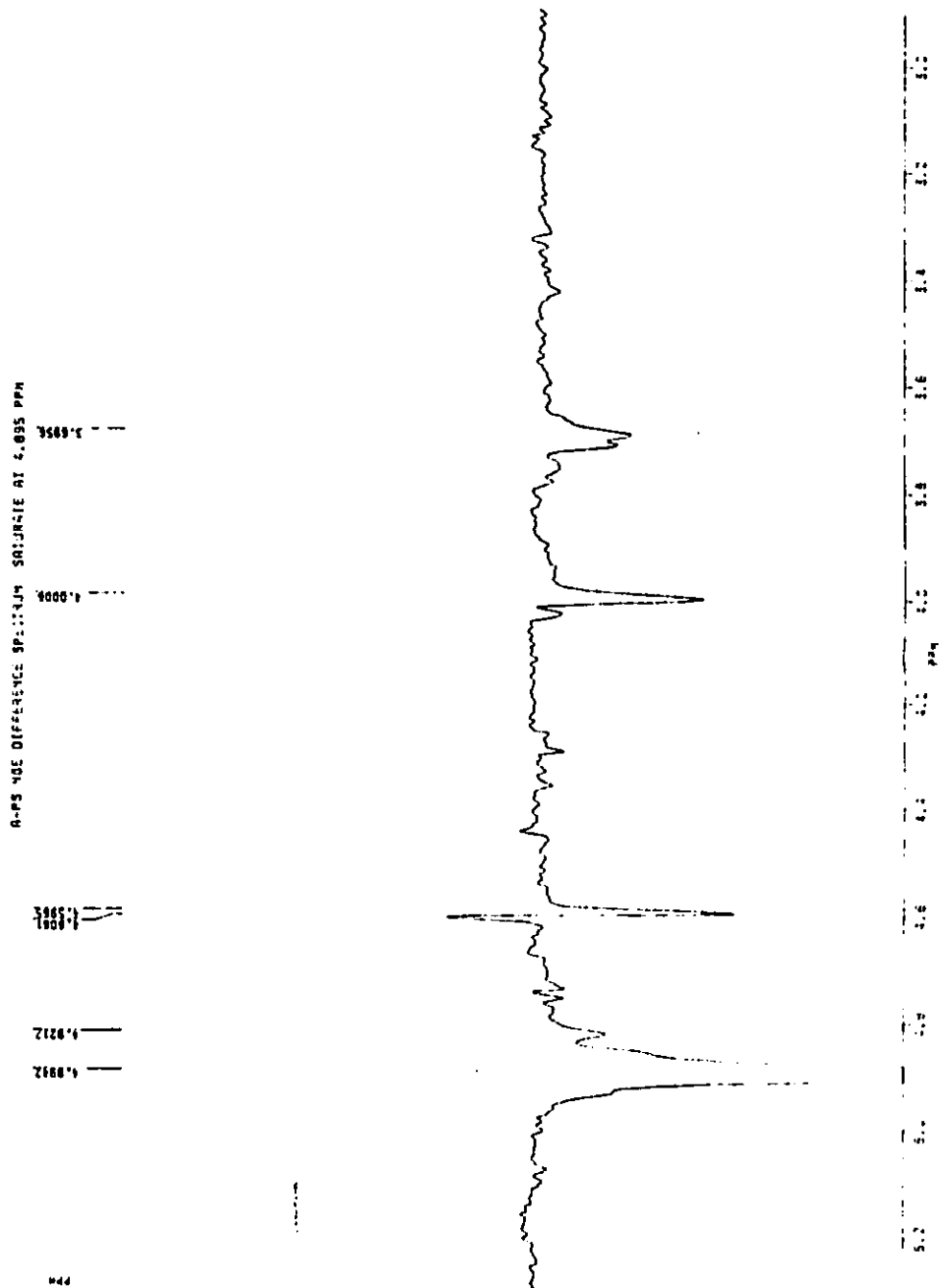


2 500 MHz ¹H-NMR of AK1401 A-PS obtained by phenol/ chloroform/

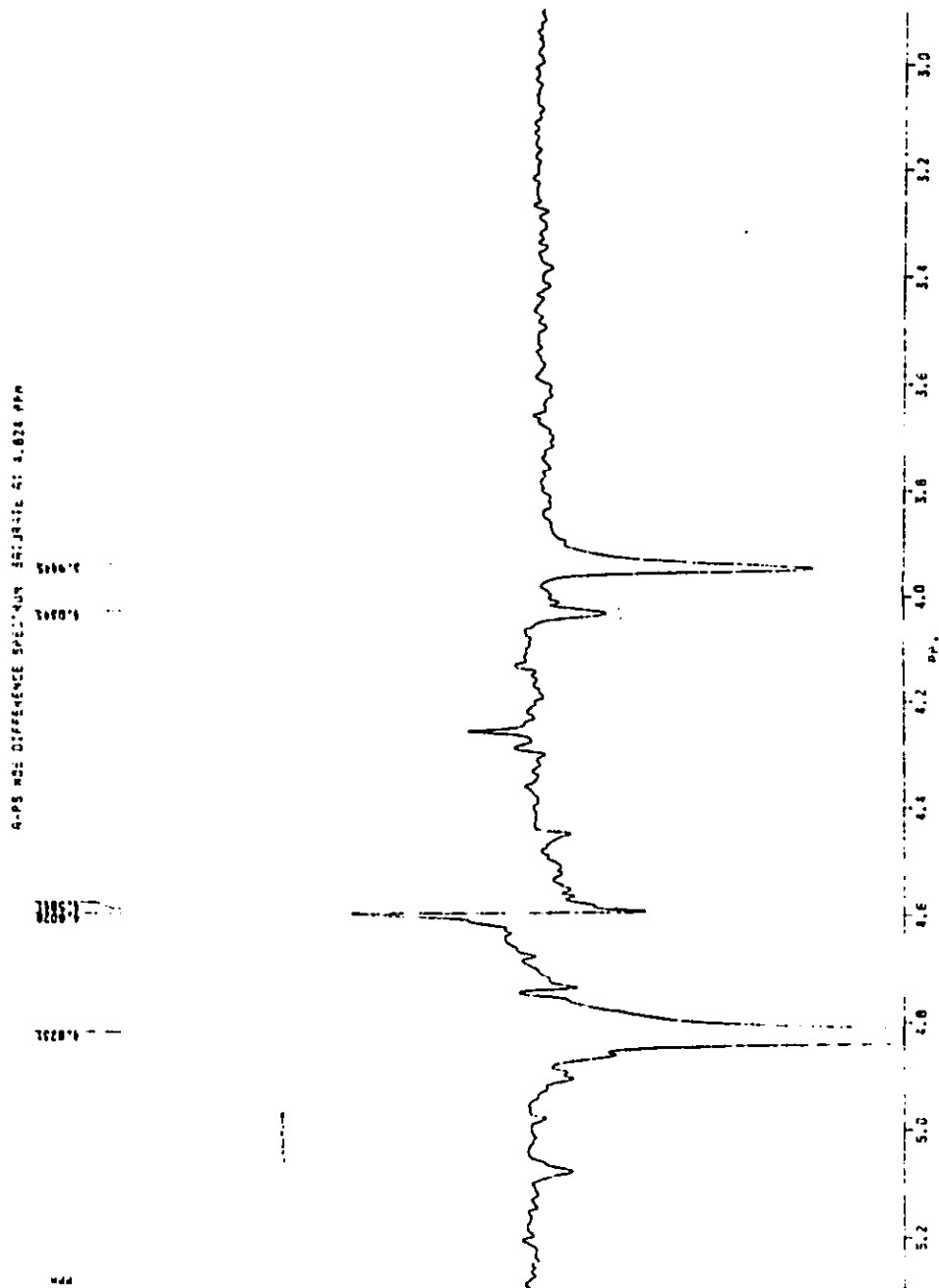
petroleum ether extraction



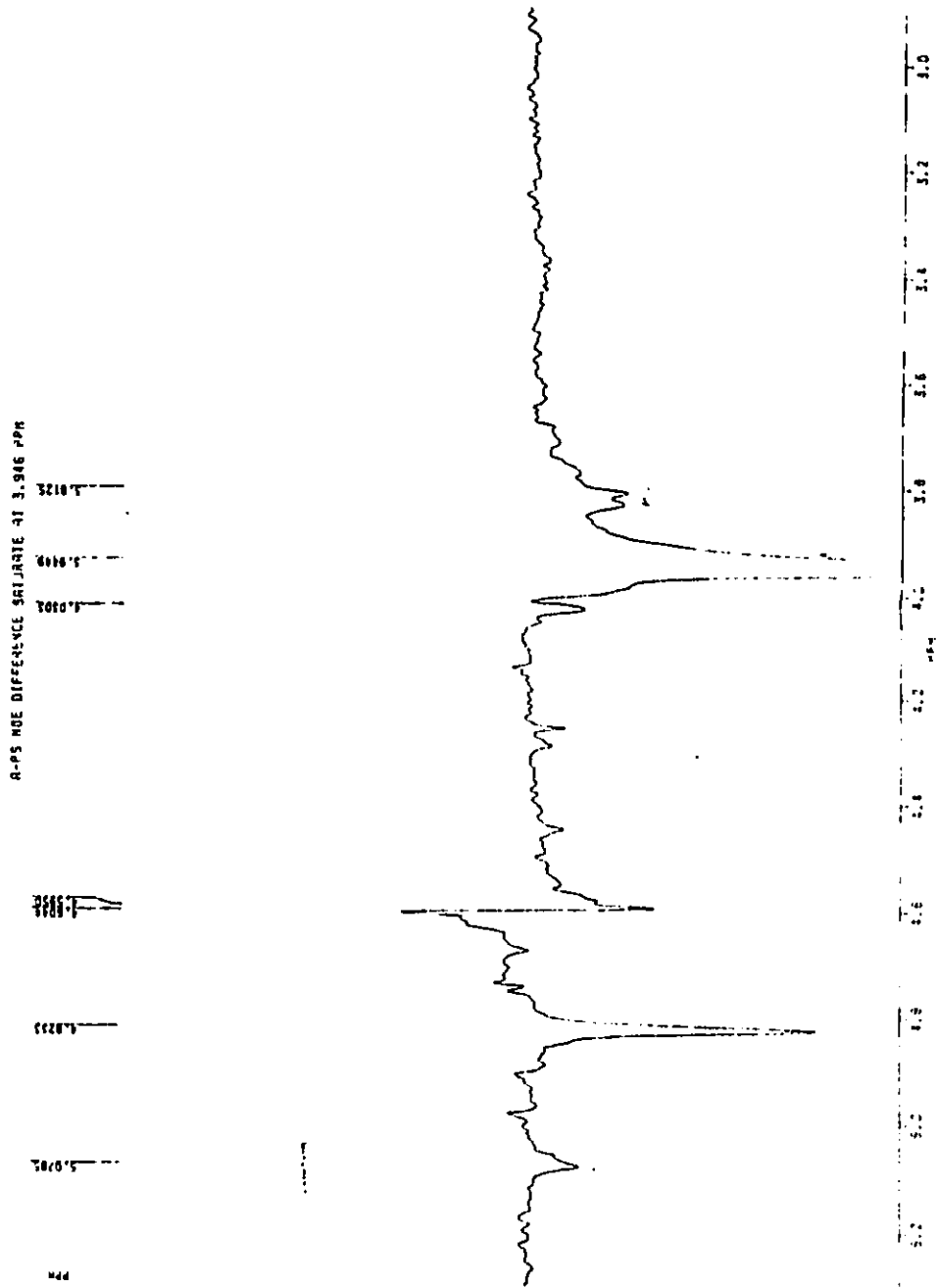
3 Irradiated proton: Al



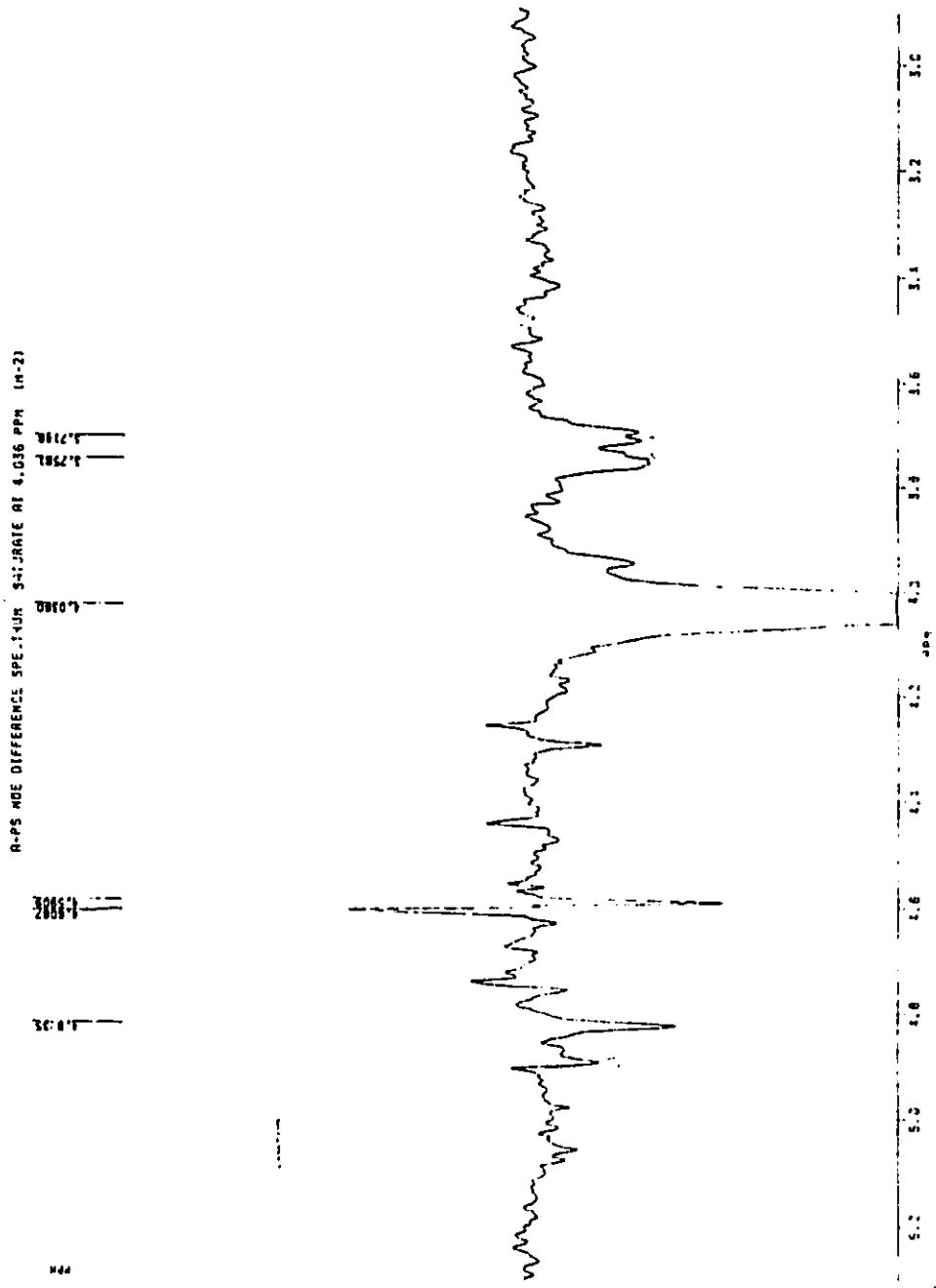
4 Irradiated proton: B1



5 Irradiated proton: Cl

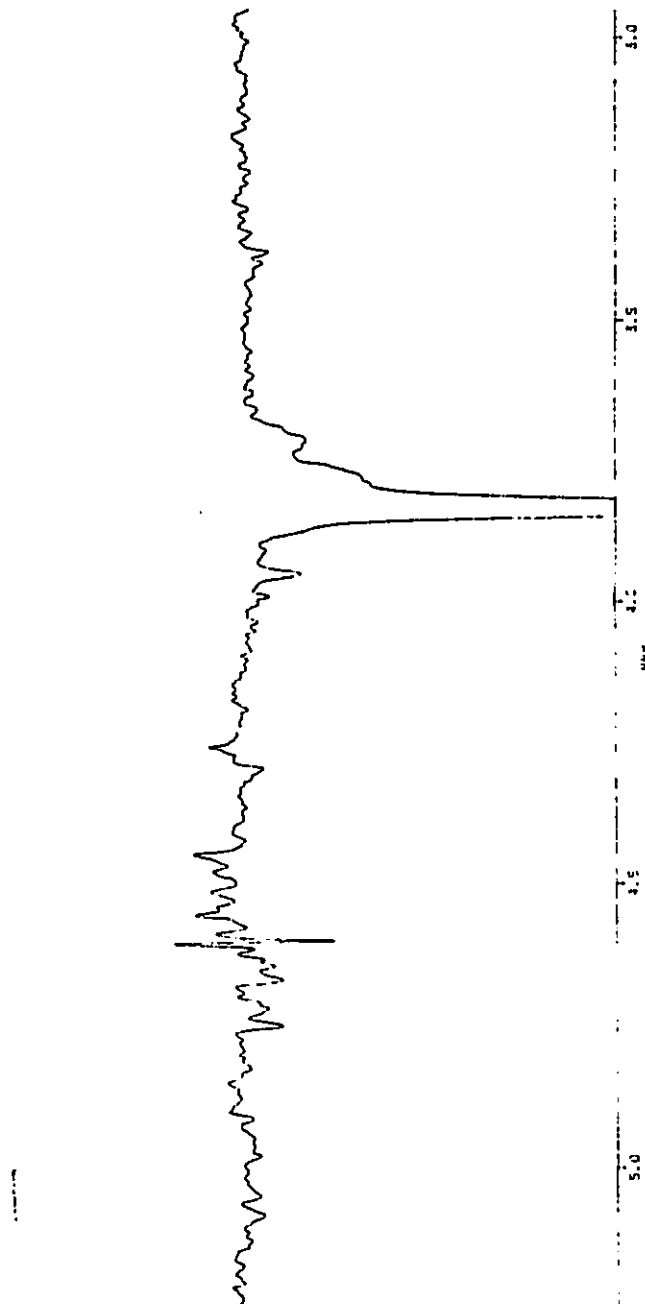


6 Irradiated proton: A2



8 Irradiated proton: C2

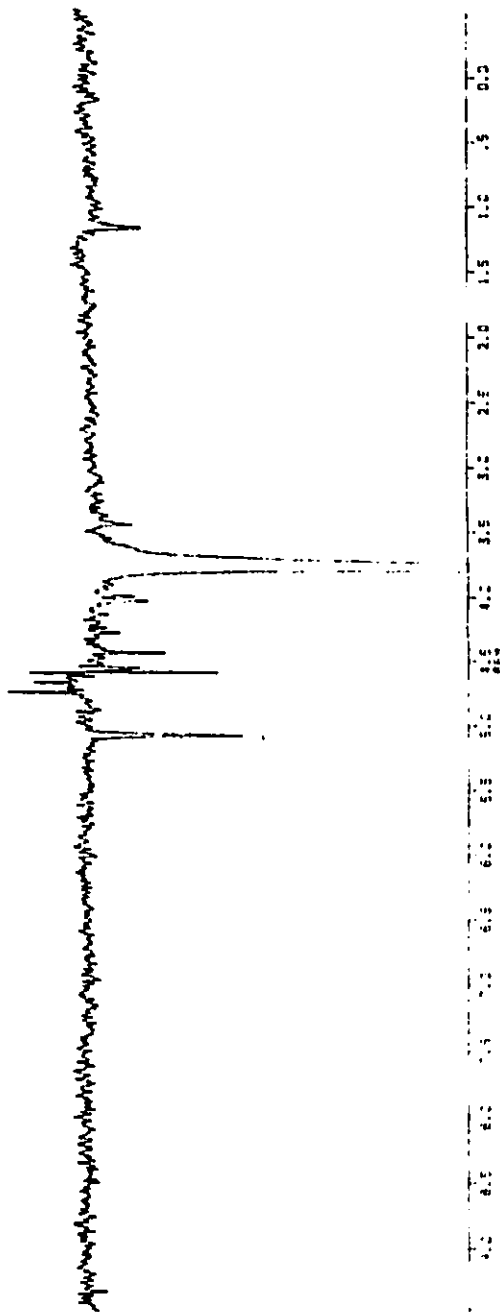
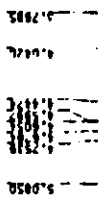
90 MHz NMR DIFFERENCE SPECTRUM AT 3.000 PPM



9 Irradiated proton: A3

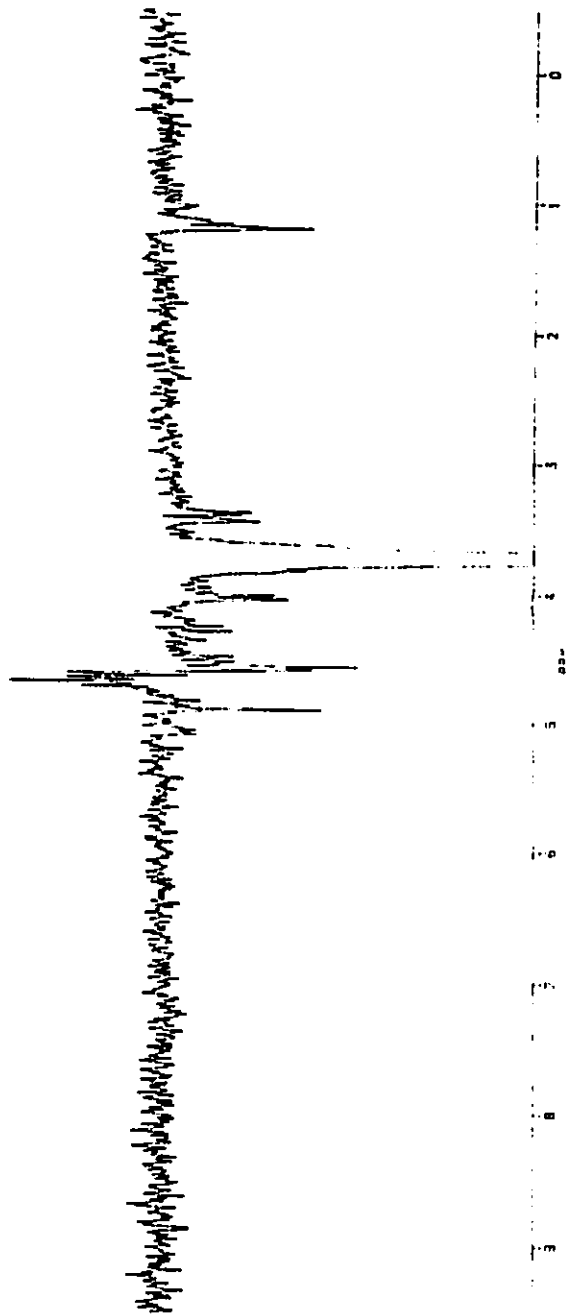
PPM

AMS NMR DIFFERENCE SPECTRUM AT 3.768 PPM

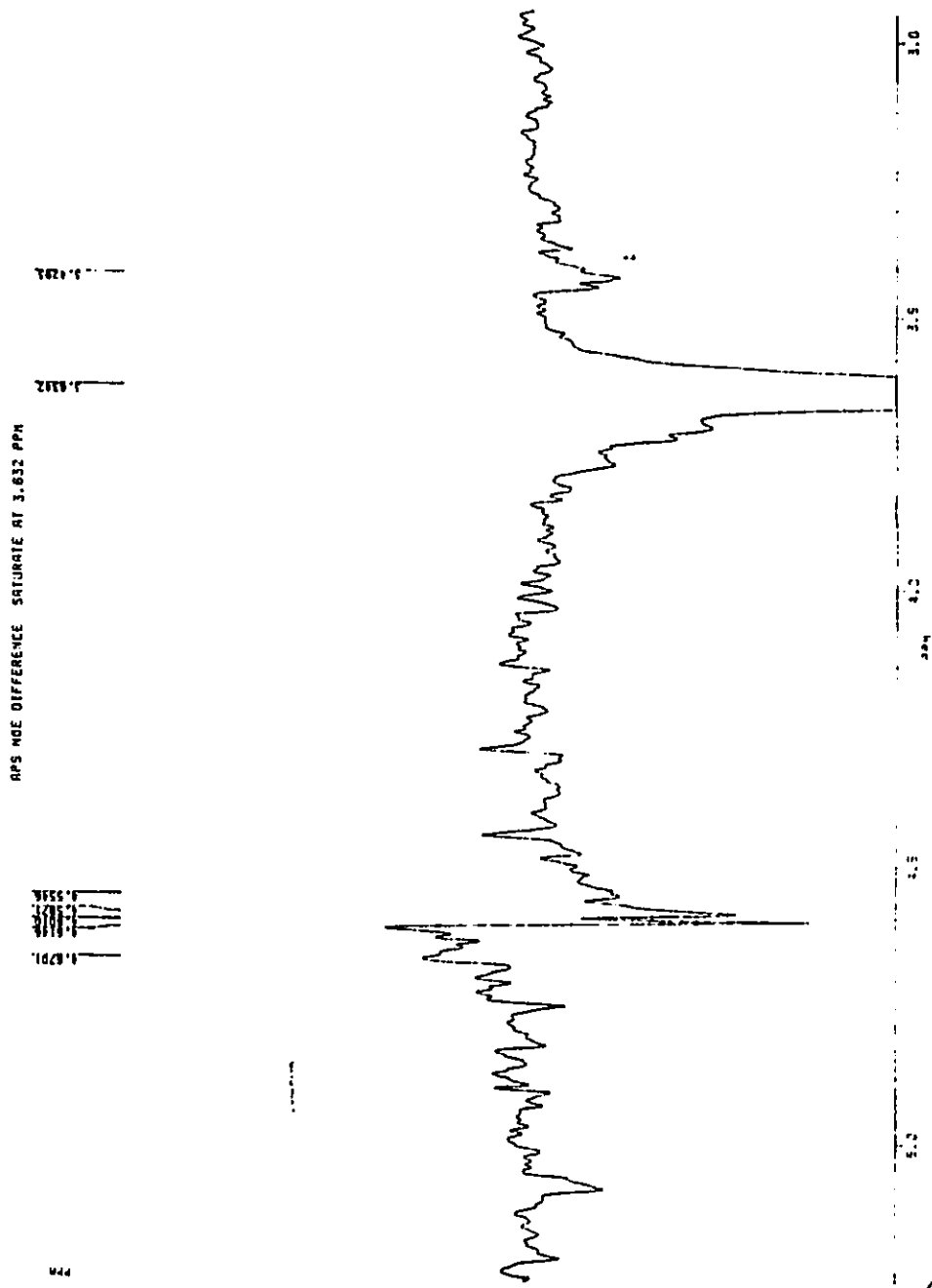


10 Irradiated proton: B3-B5 multiplet

AMS NOE 310P 101000 SR1_001E AT 1.00E 000



11 Irradiated proton: C3-A5 multiplet



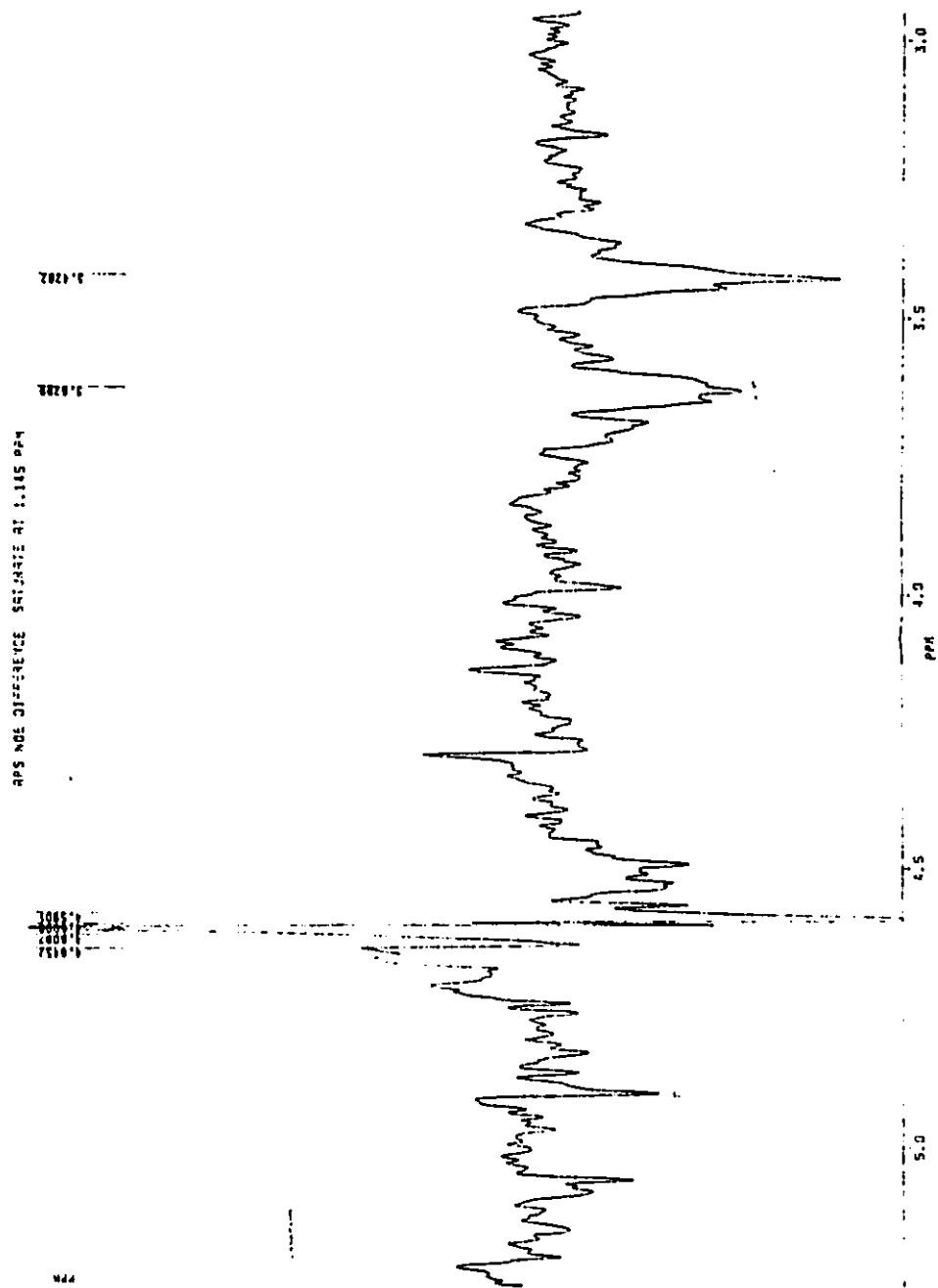
I2 Irradiated proton: C5

1.021
1.554
1.554
1.554
1.554

RPS NOE DIFFERENCE SATURATE AT 3.632 PPM

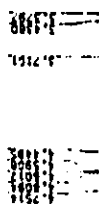
1.117
1.117

44

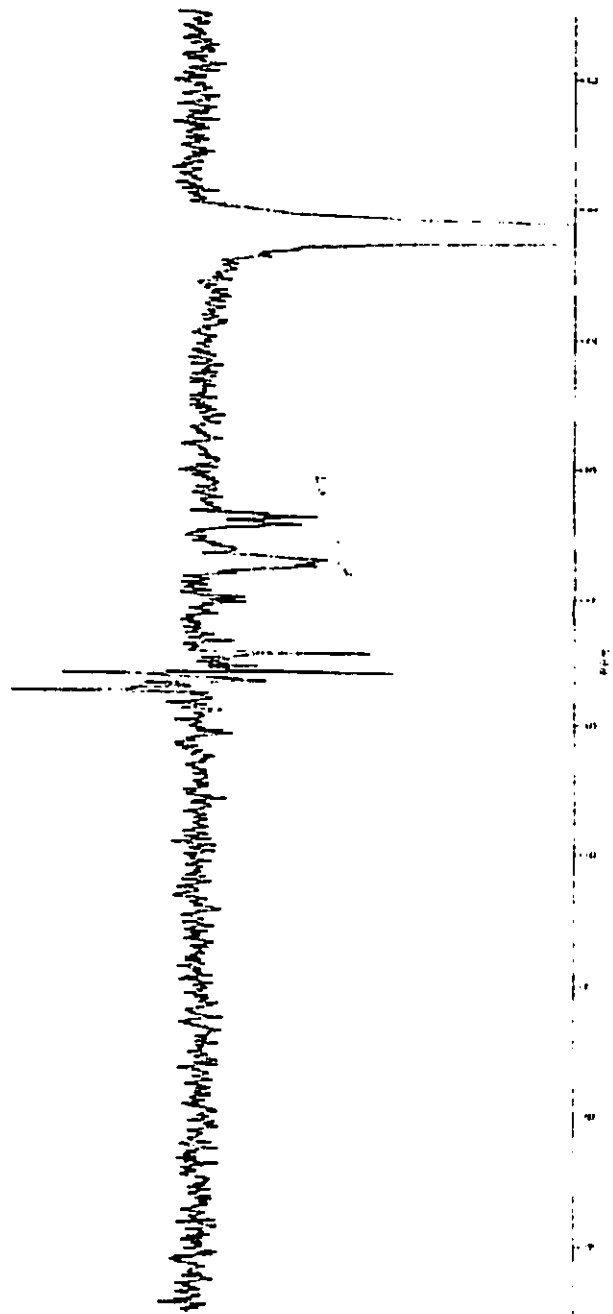


13 Irradiated proton: C6

APS NOE DIFFERENCE SPECTRUM AT 1.182 PPM



1.182 PPM



14 Irradiated proton: A6-B6 multiplet

APPENDIX 3

```

100 REM PROGRAM 1
110 PRINT "THIS PROGRAM CALCULATES POSSIBLE COMPOSITIONS FOR RESIDUAL"
120 PRINT "MASSES X AND Y IN FIGURE 26, GIVEN THAT RHAMNOSE, 3-O-METHYL"
130 PRINT "RHAMNOSE, RIBOSE AND 3-O-METHYLHEXOSE ARE THE ONLY ALDOSES"
140 PRINT "THAT SURVIVE PERIODATE OXIDATION (FROM COMPOSITION ANALYSIS"
150 PRINT "IN SECTION 3.4.4)"
160 INPUT "RESIDUAL MASS", XOH.NH4
170 FOR RHA= 0 TO 4
180 FOR OMERHA= 0 TO 4
190 FOR RIB= 0 TO 4
200 FOR OMEHEX= 0 TO 3
210 SUM= 59+230*RHA+202*OMERHA+216*RIB+260*OMEHEX+19
220 IF SUM=XOH.NH4 THEN PRINT "RHA=",RHA;"OMERHA=",OMERHA;"RIB=",RIB;"OMEHEX=",O
MEHEX
230 NEXT OMEHEX
240 NEXT RIB
250 NEXT OMERHA
260 NEXT RHA
270 END

```

```

RUN
THIS PROGRAM CALCULATES POSSIBLE COMPOSITIONS FOR RESIDUAL
MASSES X AND Y IN FIGURE 26, GIVEN THAT RHAMNOSE, 3-O-METHYL
RHAMNOSE, RIBOSE AND 3-O-METHYLHEXOSE ARE THE ONLY ALDOSES
THAT SURVIVE PERIODATE OXIDATION (FROM COMPOSITION ANALYSIS
IN SECTION 3.4.4)

```

```

RESIDUAL MASS712
RHA=          0 OMERHA=      1 RIB=          2 OMEHEX=      0
RHA=          1 OMERHA=      2 RIB=          0 OMEHEX=      0
Ok

```

```

RUN
THIS PROGRAM CALCULATES POSSIBLE COMPOSITIONS FOR RESIDUAL
MASSES X AND Y IN FIGURE 26, GIVEN THAT RHAMNOSE, 3-O-METHYL
RHAMNOSE, RIBOSE AND 3-O-METHYLHEXOSE ARE THE ONLY ALDOSES
THAT SURVIVE PERIODATE OXIDATION (FROM COMPOSITION ANALYSIS
IN SECTION 3.4.4)

```

```

RESIDUAL MASS684
RHA=          0 OMERHA=      3 RIB=          0 OMEHEX=      0
Ok

```

```

100 REM PROGRAM 2
110 PRINT "THIS PROGRAM CALCULATES POSSIBLE COMPOSITIONS FOR RESIDUAL MASSES"
120 PRINT "R1 AND R2 IN FIGURE 26, GIVEN THE SAME ALDOSE CONSTITUENTS USED IN"
130 PRINT "PROGRAM 1, AND ALLOWING THE REDUCING END GROUP TO BE GLYCEROL,"
140 PRINT "ERYTHRITOL, 1,2,3-BUTANETRIOL, OR AN UNKNOWN AGLYCONE HAVING A"
150 PRINT "FORMULA WEIGHT OF 14 AMU LESS THAN GLYCEROL DIACETATE (SEE"
160 PRINT "SECTION 3.4.3)"
170 INPUT "RESIDUAL MASS", R
180 FOR RHA= 0 TO 4
190 FOR OMERHA= 0 TO 4
200 FOR RIB= 0 TO 4
210 FOR OMEHEX= 0 TO 3
220 FOR GLY=0 TO 1
230 FOR ERY= 0 TO 1
240 FOR BUT= 0 TO 1
250 FOR UNK= 0 TO 1
260 SUM= 230*RHA+202*OMERHA+216*RIB+260*OMEHEX+159*GLY+231*ERY+173*BUT+145*UNK
270 IF SUM=R THEN PRINT "RHA=",RHA;"OMERHA=",OMERHA;"RIB=",RIB;"OMEHEX=",OMEHEX;
  "GLY=",GLY;"ERY=",ERY;"BUT=",BUT;"UNK=",UNK
280 NEXT UNK
290 NEXT BUT
300 NEXT ERY
310 NEXT GLY
320 NEXT OMEHEX
330 NEXT RIB
340 NEXT OMERHA
350 NEXT RHA
360 END

```

RUN

THIS PROGRAM CALCULATES POSSIBLE COMPOSITIONS FOR RESIDUAL MASSES
R1 AND R2 IN FIGURE 26, GIVEN THE SAME ALDOSE CONSTITUENTS USED IN
PROGRAM 1, AND ALLOWING THE REDUCING END GROUP TO BE GLYCEROL,
ERYTHRITOL, 1,2,3-BUTANETRIOL, OR AN UNKNOWN AGLYCONE HAVING A
FORMULA WEIGHT OF 14 AMU LESS THAN GLYCEROL DIACETATE (SEE
SECTION 3.4.3)

RESIDUAL MASS665

RHA=	0	OMERHA=	0	RIB=	0	OMEHEX=	2	GLY=
0	ERY=	0	BUT=	0	UNK=	1		

Ok

RESIDUAL MASS651

Ok

RESIDUAL MASS693

RHA=	0	OMERHA=	0	RIB=	0	OMEHEX=	2	GLY=
0 ERY=	0	BUT=	1	UNK=	0			
RHA=	0	OMERHA=	0	RIB=	1	OMEHEX=	0	GLY=
1 ERY=	0	BUT=	1	UNK=	1			
RHA=	0	OMERHA=	1	RIB=	0	OMEHEX=	1	GLY=
0 ERY=	1	BUT=	0	UNK=	0			

Ok

RESIDUAL MASS679

RHA=	0	OMERHA=	0	RIB=	0	OMEHEX=	2	GLY=
1 ERY=	0	BUT=	0	UNK=	0			
RHA=	0	OMERHA=	1	RIB=	0	OMEHEX=	0	GLY=
1 ERY=	0	BUT=	1	UNK=	1			

Ok

REFERENCES

1. Bergey's Manual of Systematic Bacteriology, Vol. 1, *edited by* N.R. Krieg and J.G. Holt. Williams and Wilkins, Baltimore, MD, 1984.
2. Carbohydrate Chemistry, *edited by* J.F. Kennedy. Clarendon Press, Oxford Science Publications, 1988.
3. S. Wendenbaum, P. Demange, A. Dell, J.M. Meyer, and M.A. Abdallah. *Tetrahedron Lett.* 24, 4877-4880 (1983).
4. H. Mayer, R.N. Tharanathan, and J. Weckesser. *Meth. Microbiol.* 18, 157-207 (1985).
5. L. Kenne, and B. Lindberg, in The Polysaccharides, Vol. 2, *edited by* G.O. Aspinall. Academic Press, New York, NY, 1983. pp. 287-363.
6. P.V. Liu, H. Matsumoto, H. Kusama, and T. Bergan. *Int. J. System. Bacteriol.* 33, 256-264 (1983).
7. J.Y. Homma. *Jpn. J. Exp. Med.* 46, 329-336 (1976).
8. M.W. Fisher, H.B. Devlin, and F.J. Gnabasik. *J. Bacteriol* 98, 835-836 (1969).
9. I. Habs. *Z. Hyg.* 144, 218-228 (1957).
10. B. Lanyi and T. Bergan. *Meth. Microbiol.* 10, 93-168 (1978).
11. Y.A. Knirel, E.V. Vinogradov, N.A. Kocharova, N.A. Paramonov, N.K. Kochetkov, B.A. Dmitriev, E.S. Stanislavsky, and B. Lanyi. *Acta Microbiol. Hungarica* 35, 3-24 (1988).
12. M. Rivera, L.E. Bryan, R.E.W. Hancock, and E.J. McGroarty. *J. Bacteriol.* 170, 512-521 (1988).

13. M. Rivera and E.J. McGroarty. *J. Bacteriol.* 171, 2244-2248 (1989).
14. S.-I. Yokota, S. Kaya, S. Sawada, T. Kawamura, Y. Araki, and E. Ito. *Eur. J. Biochem.* 167, 203-209 (1987).
15. N.A. Kocharova, Y.A. Knirel, N.K. Kochetkov, and E.S. Stanislavskii. *Bioorg. Khim.* 14, 701-703 (1988).
16. A.R.W. Smith, S.E. Zamze, and R.C. Hignett. *J. Gen. Microbiol.* 131, 963-974 (1985).
17. A.R.W. Smith, S.E. Zamze, S.M. Munro, K.J. Carter, and R.C. Hignett. *Eur. J. Biochem* 149, 73-78 (1985).
18. A.S. Shashkov, Y.A. Knirel, N.V. Tanatar, and N.K. Kochetkov. *Carbohydr. Res.* 146, 346-349 (1986).
19. Y.E. Tsvetkov, L.V. Backinowsky, and N.K. Kochetkov. *Carbohydr. Res.* 193, 75-90 (1989).
20. S. Sawada, T. Kawamura, Y. Masuho, and K. Tomibe. *J. Infect. Dis.* 152, 1290-1299 (1985).
21. N.A. Kocharova, K. Hatano, A.S. Shashkov, Y.A. Knirel, N.K. Kochetkov, and G.B. Pier. *J. Biol. Chem.* 264, 15569-15573 (1989).
22. J.R.W. Govan and S. Glass. *Rev. Med. Microbiol.* 1, 19-28 (1990).
23. T.L. Pitt, J. MacDougall, A.R.L. Penketh, and E.M. Cooke. *J. Med. Microbiol.* 21, 179-186 (1986).
24. R.E.W. Hancock, L.M. Mutharia, L. Chan, R.P. Darveau, D.P. Speert, and G.B. Pier. *Infect. Immun.* 42, 170-177 (1983).
25. M.Y.C. Lam, E.J. McGroarty, A.M. Kropinski, L.A. MacDonald, S.S. Pedersen, N. Hoiby, and J.S. Lam. *J. Clin. Microbiol.* 27, 962-967 (1989).

26. E.J. Hiller and D.T. Langford. 13th Ann. Meet. Eur. Working Group Cystic Fibrosis, Jerusalem, Tel Aviv, 1985. Cystic Fibrosis Found. Abstr. P-3.
27. D. Berry and A.M. Kropinski. *Can. J. Microbiol.* 32, 436-438 (1986).
28. A. Fox, S.L. Morgan, and J. Gilbert, in Analysis of Carbohydrates by GLC and MS, edited by C.J. Biermann and G.D. McGinnis. CRC Press, Boca Raton, FL, 1989. pp.87-117.
29. K. Leontein, B. Lindberg, and J. Lönngren. *Carbohydr. Res.* 62, 359-362 (1978).
30. W. Pigman and D. Horton, in The Carbohydrates: Chemistry and Biochemistry, Vol. IA, edited by W. Pigman and D. Horton. Academic Press, New York, NY, 1972. pp. 39 and 45-46.
31. Ibid., p. 40.
32. M. Karplus. *J. Am. Chem. Soc.* 85, 2870-2871 (1963).
33. C. Altona and C.A.G. Haasnoot. *Org. Magn. Res.* 13, 417-429 (1980).
34. K. Bock and C. Pedersen. *J. Chem. Soc. Perkin Trans. 2*, 293-297 (1974).
35. W.G. Overend, in The Carbohydrates: Chemistry and Biochemistry, Vol. IA, edited by W. Pigman and D. Horton. Academic Press, New York, NY, 1972. p. 306.
36. W. Pigman and D. Horton, in The Carbohydrates: Chemistry and Biochemistry, Vol. IA, edited by W. Pigman and D. Horton. Academic Press, New York, NY, 1972. pp. 35-36.
37. P.-E. Jansson, L. Kenne, H. Liedgren, B. Lindberg, and J. Lönngren.

- Univ. of Stockholm Chem. Commun., No. 8, 1976.
38. R.J. Ferrier, in The Carbohydrates: Chemistry and Biochemistry, Vol. IB, *edited by* W. Pigman and D. Horton. Academic Press, New York, NY, 1972. p. 1441.
 39. D. Rolf, J.A. Bennek, and G.R. Gray. Carbohydr. Res. 137, 183-196 (1985).
 40. I.J. Goldstein, G.W. Hay, B.A. Lewis, and F. Smith, in Methods in Carbohydrate Chemistry, Vol. V, *edited by* R.L. Whistler. Academic Press, New York, NY, 1965. pp. 361-370.
 41. J. Dabrowski, in Two-Dimensional NMR Spectroscopy: Applications for Chemists and Biochemists, Methods in Stereochemical Analysis Vol. 9, *edited by* W.R. Croasmun and R.M.K. Carlson. VCH Publishers, 1987. p. 366.
 42. K. Bock, C. Pedersen, and H. Pedersen. Adv. Carbohydr. Chem. Biochem. 42, 193-225 (1984).
 43. P.-E. Jansson, L. Kenne, and G. Widmalm. Pure Appl. Chem. 61, 1181-1192 (1989).
 44. B. Meyer, T. Hansen, D. Nute, P. Albersheim, A. Darvill, W. York, and J. Sellers. Science 251, 542-544 (1991).
 45. K. Bock and C. Pedersen. Carbohydr. Res. 71, 319-321 (1979).
 46. K. Bock and C. Pedersen. Acta Chem. Scand. B 29, 258-264 (1975).
 47. K. Bock, I. Lundt, and C. Pedersen. Tetrahedron. Lett., 1037-1040 (1973).
 48. R. Freeman and H.D.W. Hill. J. Magn. Res. 5, 278-280 (1971).
 49. L.D. Hall and G.A. Morris. Carbohydr. Res. 82, 175-184 (1980).

50. K. Bock and C. Pedersen. *Carbohydr. Res.* **145**, 135-140 (1985).
51. F.A. Bovey. *NMR Spectroscopy*, Academic Press, New York, NY, 1988.
52. H. Kessler, M. Gehrke, and C. Griesinger. *Angew. Chem. Int. Ed. Engl.* **27**, 490-536 (1988).
53. J. Dabrowski, in *Two-Dimensional NMR Spectroscopy: Applications for Chemists and Biochemists*, *Methods in Stereochemical Analysis* Vol. 9, edited by W.R. Croasmun and R.M.K. Carlson. VCH Publishers, 1987. pp. 349-386.
54. G. Eich, G. Bodenhausen, and R.R. Ernst. *J. Am. Chem. Soc.* **104**, 3731-3732 (1982).
55. D.W. Hughes, R.A. Bell, T. Neilson, and A.D. Bain. *Can. J. Chem.* **63**, 3133-3139 (1985).
56. S.W. Homans, R.A. Dwek, D.L. Fernandes, and T.W. Rademacher. *Proc. Natl. Acad. Sci. USA* **81**, 6286-6289 (1984).
57. R.P. Darveau, and R.E.W. Hancock. *J. Bacteriol.* **155**, 831-838 (1983).
58. C. Galanos, O. Luderitz, and O. Westphal. *Eur. J. Biochem.* **9**, 245-249 (1969).
59. S.-T. Chen, S.-H. Chiou, Y.-H. Chu, and K.-T. Wang. *Int. J. Peptide Protein Res.* **30**, 572-576 (1987).
60. S. Hakomori. *J. Biochem.* **55**, 205-207 (1964).
61. J. Sambrook, E.F. Fritsch, and T. Maniatis. *Molecular Cloning: A Laboratory Manual*, 2nd ed., Cold Spring Harbor Laboratory Press, 1989. (Appendix E.5).
62. C.W. Gehrke, K.C. Kuo, R.A. McCune, K.O. Gerhardt, and P.F. Agris.

- J. Chromatogr. 230, 297-308 (1982).
63. J.C. Richards, M.B. Perry, and P.J. Kniskern. *Can. J. Biochem. Cell Biol.* 63, 953-968 (1985).
64. J.E.G. van Dam, J. Breg, R. Komen, J.P. Kamerling, and J.F.G. Vliegthart. *Carbohydr. Res.* 187, 267-286 (1989).
65. A. de Bruyn, M. Anteunis, R. de Gussem, and G.G.S. Dutton. *Carbohydr. Res.* 47, 158-163 (1976).
66. A.S. Perlin, and B. Casu, in *The Polysaccharides*, Vol. 1, *edited by G.O. Aspinall*. Academic Press, New York, NY, 1983. p. 147.
67. S.-I. Yokota, S. Kaya, Y. Araki, E. Ito, T. Kawamura, and S. Sawada. *J. Bacteriol.* 172, 6162-6164 (1990).
68. G.G.S. Dutton, J.L. Di Fabio, D.M. Leek, E.H. Merrifield, J.R. Nunn, and A.M. Stephen. *Carbohydr. Res.* 97, 127-138 (1981).
69. K. Biemann, D.C. DeJongh, and H.K. Schnoes. *J. Am. Chem. Soc.* 85, 1763-1770 (1963).
70. J.M. Peltier, D.B. Maclean, and W.A. Szarek. *Rapid Commun. Mass Spectrom.* 5, 446-449 (1991).
71. O.S. Chizhov, N.K. Kochetkov, N.N. Malysheva, A.I. Shiyonok, and V.L. Chashchin. *Org. Mass Spectrom.* 5, 1157-1167 (1971).
72. K.G. Das and B. Thayumanavan. *Org. Mass Spectrom.* 10, 455-468 (1975).
73. C. Bosso, F. Taravel, J. Ulrich, and M. Vignon. *Org. Mass Spectrom.* 13, 477-482 (1978).
74. O.S. Chizhov, L.A. Polyakova, and N.K. Kochetkov. *Doklady Acad. Nauk SSSR* 158, 685-688 (1964).

75. T. Radford and D.C. DeJongh, in Biochemical Applications of Mass Spectrometry, edited by G.R. Waller. Wiley- Interscience, New York, NY, 1972. pp. 313-350.
76. R.J. Cotter. Anal. Chem. 52, 1589A-1606A (1980).
77. V.N. Reinhold. Meth. Enzymol. 138, 59-84 (1987).
78. J.M. Peltier, R.W. Smith, D.B. MacLean, and W.A. Szarek. Org. Mass Spectrom. 27, 31-36 (1992).
79. T.L. Arsenault, D.W. Hughes, D.B. MacLean, W.A. Szarek, A.M.B. Kropinski, and J.S. Lam. Can. J. Chem. 69, 1273-1280 (1991).